INFLUENCE OF COIL CHARACTERISTICS ON HEAT TRANSFER TO NEWTONIAN FLUIDS

A Thesis submitted to
The Faculty of Graduate Studies and Research of
McGill University

by

Devanahalli G. Prabhanjan

In partial fulfillment of the
requirements for the Degree of

Doctor of Philosophy

Department of Agricultural and Biosystems Engineering
Faculty of Agricultural and Environmental Sciences, McGill University
Ste Anne de-Bellevue, H9X 3V9
Quebec, Canada

0-612-70003-8

ABSTRACT

Devanahalli G.Prabhanjan Ph.D. (Agric. & Biosystems Engineering)

INFLUENCE OF COIL CHARACTERISTICS ON HEAT TRANSFER TO NEWTONIAN FLUIDS

A water bath thermal Processor was designed and built to study the influence of helical coil characteristics on heat transfer to Newtonian fluids like water and base oil with three different viscosities. The system consisted of a thermally insulated water bath, an electric heater, pump to re-circulate water in the bath and for pumping the processing fluid through the coil, copper helical coils and a storage tank for the processing fluid.

Comparative study has shown that the outer and total heat transfer coefficients were significantly lower in natural than in forced convection water bath. However, inner heat transfer coefficient was not significantly affected. Flow rate as low as 0.001 $m.s^{-1}$ in the water bath improved the outer and total heat transfer coefficients by 35 and 22% respectively. One could expect a higher rate with an increase in water re-circulation rate inside the water bath. Percent rise in heat transfer was limited to seven with respect to inner heat transfer. With the Pearson correlation, it was possible to express total heat transfer rate directly in terms of outer and inner rates. Significant interactions were observed between variables and constants.

Experiments with 2 pitch cases were conducted with water to water heat transfer using coils to determine the Nusselt number correlation for natural convection. Characteristic lengths were changed in the models. The Nusselt number was under-predicted by 25 to 37% for water bath temperatures of 75° and 95 ° C respectively. Flow rate inside the coil had slight effect on Nusselt number due to change in the temperature gradient along the length of the coil.

Studies conducted with three base oils have shown significant difference in viscosity after heating the oil for several turns. Each fluid was heated in a distinct flow regime. The observed Nusselt number inside the coil for low

Reynolds number was as high as an order of magnitude than the predicted values calculated by Seider-Tate relation for laminar flow. Vorticies formed associated with the eddy structure could very well be the cause for this kind of rise in the value.

Preliminary study conducted has shown a higher rise in temperature of processing fluid in case of helical coil compared to that of a straight tube. Larger the diameter of the tube better was the heat transfer. An elevated bath temperature had higher heat transfer.

RESUME

Devanahalli G.Prabhanjan Ph.D. (Genie Agricloe et des Biosystemes)

EFFETS DES CARACTÉRISTIQUES DES ÉCHANGEURS EN SPIRALE SUR LE TRANSFERT DE CHALEUR DANS DES LIQUIDES NEWTONIENS

Un processeur thermique a été conçu pour étudier les effets des caractéristiques des échangeurs en spirale sur le transfert de chaleur lors d'essais sur des fluides newtoniens. Les fluides utilisés pour les essais étaient : l'eau et des huiles avec trois viscosités différentes. Le système consistait en un réservoir d'eau isolé à température contrôlée, de différents échangeurs en spirale, d'éléments chauffants, d'une pompe pour circuler les fluides à l'intérieur des échangeurs en spirale, et d'un réservoir pour le fluide étudié. Les essais comparatifs ont démontré que les coefficients de transfert de chaleur externes et totaux mesurés lors des essais effectués en convection forcée étaient significativement supérieurs à ceux enregistrés lors des essais en convection naturelle. Toutefois, les coefficients de transfert de chaleur internes n'étaient pas affectés par les caractéristiques de l'échangeur en spirale. Il a été démontré que des débits aussi faible que 0,001 $m \cdot s^{-1}$ dans le bain d'eau avait pour effet d'augmenter les taux de transfert de chaleur externes et totaux de 35% et de 22% respectivement. On pouvait s'attendre à des taux plus élevés lorsqu'on augmentait le taux de circulation de l'eau dans le bain d'eau. L'augmentation du taux de transfert de chaleur interne a été limitée à sept pourcent. Il a été possible d'établir la relation entre les taux de transfert de chaleur internes et externes aux taux de transfert de chaleur totaux en utilisant le modèle de Pearson. Des interactions significatives ont été observées entre les variables et les constantes.

Les expériences avec deux inclinaisons ont été effectuées avec des échangeurs en spirale eau-eau pour établir la corrélation du nombre de Nusselt en mode de convection naturel. Les longueurs caractéristiques ont été changées dans les modèles. Les nombres de Nusselt ont été sous-

estimés de 25 à 37% pour des températures du réservoir d'eau allant de 75 à 95°C, respectivement. Le débit du fluide à l'intérieur de l'échangeur en spirale n'a eu qu'un effet marginal sur le nombre de Nusselt à cause du changement du gradient de température le long de l'échangeur.

Les essais effectués avec les huiles de viscosités différentes ont indiqué que leur viscosité changeait de façon significative après avoir été chauffé sur plusieurs tours. Chaque fluide a été chauffé sous un régime fluidique distinct. Les nombres de Nusselt associés à l'écoulement à l'intérieur du serpentin, sous des débits caractérisés par de faibles valeurs du nombre de Reynolds, étaient supérieurs d'un ordre de grandeur aux valeurs calculées à partir des relations de Seider-Tate développées pour les écoulements laminaires. La formation de vortex associée aux structures de Eddy pourrait très bien expliquer ce phénomène.

Des essais préliminaires ont indiqué une plus grande augmentation du fluide traité dans les échangeurs hélicoïdaux que dans les échangeurs en tubes droits. Plus le diamètre du tube était grand et meilleur était le transfert de chaleur. De plus, de meilleurs taux de transfert de chaleur ont été obtenus lorsque la température du bain était élevée.

This work is dedicated to my parents,

Gopalakrishna and Anasuya

who even with low income kept priority

to support their children for education.

ACKNOWLEDGEMENT

My immense gratitude to Professor G.S. Vijaya Raghavan for the support and encouragement he provided during the course of my extended study. His constant guidance and nurturing provided me enthusiasm to cherish my teen-age ambition.

This study would not have been possible without Sam Sotocinal, Yvan Gariepy, and Ray Cassidy who made their time in-spite of busy schedule to provide technical advice and assisted while building the equipment. Also, thanks to Peter Alvo and Tim Rennie who contributed in many ways.

I sincerely thank Professor Ramaswamy and Dr. Srikanth for their inexhaustible wealth of information on different aspect of the study. The contributions of Valerie Orsat, Venkatesh Sosle and Venkatesh Meda in various phases of this study are greatly appreciated.

It was Dr. Raghavan's and Dr. Ramaswamy family who provided home away from home environment, without which life would have been more miserable during my stay in Canada.

To the Office Staff of the Department of Agricultural and Biosystems Engineering who facilitated most of my paper work, I express my sincere thanks. This study would not have been possible but for the financial support received from CORPAQ, NSERC, the Faculty of Graduate Studies and Research, McGill University and Hydro-Quebec fellowship.

I acknowledge moral support given by my brother-in-laws Veenu, Balaji and co-brother Lakshman and their family members during course of my study.

I fail in my duty if I don't acknowledge the support given by my wife Suguna, son Pavan, brother Badarinath, sister-in-law Bharathi, nephew Prithvi and niece Prathima, who always wondered when I graduate. I greatly appreciate their patience and understanding.

TABLE OF CONTENTS

LIST OF FIGURES

LIST OF TABLES

NOMENCLATURE

A	cross sectional area of heat flow, m^2
a	radius of the tube, mm
C_p	specific heat, $kJ.kg^{-1}\cdot{}^{\circ}C^{-1}$
d	distance traveled, mm
D	diameter of the helix, mm
De	Dean number
De'	modified Dean number
F	Weisbach friction factor
h	the convective heat transfer coefficient, $W.m^{-2}\cdot{}^{\circ}C^{-1}$
h_t	overall heat transfer coefficient, $W.m^{-2}\cdot{}^{\circ}C^{-1}$
h_{ti}	overall heat transfer coefficient based on inside of the tube, $W.m^{-2}\cdot{}^{\circ}C^{-1}$
h	height , m
K	Deans number
K	power factor
k	thermal conductivity, $W.m^{-2}\cdot{}^{\circ}C^{-1}$
k_c	thermal conductivity of the boundary material, $W.m^{-2}\cdot{}^{\circ}C^{-1}$
m	mass, kg
m	mass flow rate, $L.min^{-1}$
p	pressure, Pa
P	pitch, mm
PID	proportional integral derivative
q	heat input, kJ
Q	heat absorbed, kJ
R	radius of helix , mm
R	fouling coefficient
T	temperature, °C
U_m	mean velocity, $m.s^{-1}$
W_0	mean velocity in axial perpendicular to central line, $m.s^{-1}$

$Nu = h.D.k^{-1}$, Nusselt number

$Re = \frac{\rho V d}{\mu}$, Reynolds number

$De = Re\sqrt{\frac{a}{R}}$, Dean number

$Pr = \frac{c_p \mu}{k}$, Prandtl number

x	thickness of boundary layer, mm
cosα	angle of inclination to the tube axis
λ	torsion factor
ν	kinematic viscosity, $m^2.s^{-1}$
μ	dynamic viscosity, $N.s.m^{-2}$
ρ	density, $kg.m^{-3}$
π	Bernoulli constant
ε	parameter

Subscripts

crit	critical
turb	turbulent condition
viscous	viscous force
b	bulk
ba	bath
bo	buoyancy force
c	coil
cf	centrifugal force
f	flow
o	outer
i	inner
s	surface
st	straight
t	overall

w	wall
in	inlet
out	outlet
∞	infinite distance
0	associated with Poiseuille flow

I. INTRODUCTION

1.0 Background

The widespread use of helical tubes in heat exchangers, condensers, and evaporators in food processing, pharmaceuticals, chemical engineering, refrigeration, air conditioning and nuclear power engineering is due to several consequences of the unique flow patterns resulting from tube curvature, as well as to the advantage of volume compactness. The flow patterns are substantially more complex than in straight tubes because curvature induces a centrifugal force that distorts the cross-sectional velocity profile compared to that in a straight tube, and is manifested as what is usually termed a 'secondary flow pattern'. The secondary flow pattern influences the transport of all quantities associated with the fluid (ie. heat, mass, momentum).

The influence of the secondary flow pattern on mixing, wall stresses, scouring, particle deposition, dispersion and other phenomena has elicited interest from a variety of fields other than heat transfer (Berger et al., 1983). The most widely applied and studied practical consequence of tube curvature is nevertheless greater heat transfer inside the coil than in a straight tube under comparable conditions. The heat transfer rates are usually a few percent to several-fold higher in a helical coil, the amount depending on type of flow regime (laminar or turbulent), fluid properties and helix configuration, although there are situations in which curvature may become a disadvantage (Prusa and Yao, 1982). It should also be noted that the effect on the overall exchanger heat transfer coefficient, h_t, may or may not be significant, since the relative advantage of using a coiled tube rather than a straight tube depends on the relative magnitudes of the inner and outer heat transfer coefficients. This latter assertion stems from the resistance relationship:

$$h_n = \frac{1}{\frac{1}{h_i} + \frac{A_i \ln\left(r_o/r_i\right)}{2\pi kL} + \frac{A_i 1}{A_o h_o}} \tag{1.1}$$

where,

h_o is the heat transfer coefficient outside the exchanger surface,

h_i is that inside the exchanger surface,

h_{ti} is the overall heat transfer coefficient based on inside of the tube,

d_i is the inner diameter of the cylinder ,

d_o is the outer diameter of the cylinder,

k_c is the thermal conductivity of boundary material,

which implies that h_t cannot be larger than the smaller of h_i and h_o (the resistances associated with the other terms are negligible in comparison). The degree to which h_t can be improved by increasing h_i therefore depends on the relative values h_i and h_o. This is rarely explicitly stated in the literature on heat transfer in helical coils even though it is of fundamental importance in assessing the net advantage of implementing a helical coil for heat exchange in a thermal processing application. Increasing h_i is far more important when h_i is limiting, but can also yield substantial improvement when h_o is limiting, if the alternative h_i is within an order of magnitude of h_o.

The literature relevant to the design of helical coil heat exchangers is largely oriented towards heating a fluid moving through the coil, which is the application of interest in this thesis. Far less attention has been paid to the characteristics of heat loss from a coil, although this application is important in many engineering areas (Ali, 1994). Most of the information available for designing heat exchange equipment involving helical coils is the result of theoretical and experimental work on predicting the inner heat transfer based on one of the following sets of boundary conditions (Shah and Joshi, 1987):

(a) constant wall temperature (axial and peripheral);

(b) constant axial wall heat flux with peripherally constant wall temperature;

(c) constant axial and peripheral heat flux at the wall.

Note: axial refers to the direction of mean flow (ie. in the direction of the pressure gradient), whereas peripheral refers to the circumference of the tube at a given axial distance from the entry to the tube.

Although (a) can arise in practice if steam is supplied to the outer surface of the coil, (b) and (c) are difficult to achieve due to the asymmetrical temperature distribution resulting from the secondary flow pattern (Shah and Joshi, 1987). Sandeep and Palazoglu (1999) recently cautioned that many of the existing correlations between the Nusselt number and other dimensionless numbers that characterize the flow, the fluid and the coil, cannot be used without special consideration of the conditions under which they were obtained. This thought underlies their affirmation that the design of processes involving helical coil heat exchangers is still dominated by the trial and error approach, and reflects the fact that many real situations do not correspond to the boundary conditions under which the correlations were developed. In effect, there is little or no information pertaining to helical exchangers for variable boundary conditions, even though these may arise in many situations of possible practical interest.

The research to be presented in this thesis is concerned with such a situation. It represents the first step in a research thrust aimed at determining the potential advantages of using helical coils in fluid-to-fluid exchangers with low-grade heat sources for the thermal treatment of foodstuffs, or for thermal treatment of such materials by electromagnetic energy transfer (dielectric heating) and induction heating. To our knowledge, there have been no experimental studies of the interaction between external and internal flow conditions, and how such interactions might influence the overall, inner and outer heat exchange coefficients.

The main purpose of this thesis was to conduct experiments permitting evaluation of the pertinence of existing correlations for the heat transfer in coils in terms of flow characteristics, fluid properties and helix geometry, in application to fluid-to-fluid heat exchange.

1.1 OBJECTIVES

The main objective of the research presented in this thesis was to study the relationships between tube geometry, operating parameters (heat carrier temperature and flow rate), target fluid viscosity, and dimensionless numbers describing the flow field in the tube and the heat transfer across the surface of the coil.

The specific objectives were:

1) To design and build equipment in which to study heat transfer across a helical coil with various internal and external conditions (flow rates, bath temperatures, coil dimensions and coil pitch).
2) To compare heat transfer across a straight tube with that across a helical tube of the same diameter at various pitches.
3) To compare heat transfer across a helical tube in conditions of natural convection of the carrier fluid with that in conditions of forced convection of the carrier fluid.
4) To compare the heat transfer at the inner periphery of the coil with that at the outer periphery.
5) To evaluate heat transfer along the length of the coil in order to determine the point at which the transfer efficiency might be highest for different ratios of radius of curvature to tube inner diameter (D/d ratio).
6) To evaluate the influence of fluid viscosity on the heat transfer characteristics of the coil.
7) To determine whether thermal inputs cause irreversible change in the viscosity of the target fluids used.
8) To evaluate the existing models with present data.

1.2 SCOPE

The following limitations apply to the research presented herein:

1) The target fluids were all Newtonian without particulate matter: water and three poly-alkaline glycol base oils of different viscosity.

2) The coils used were all made of 1.2 mm thick copper tube, regardless of their other dimensions.
3) Only one condition of forced convection of the carrier fluid was used.
4) There was no attempt to characterize the flow conditions of the carrier fluid.
5) Natural convection experiments were not conducted on the base oils.
6) The coil was positioned vertically with the fluid flow in the tube being from top of the bath to the bottom through the coil.

II. REVIEW OF LITERATURE

2.0 Introduction

The purpose of this literature review is to outline in some detail the literature relevant to fluid flow and heat transfer in helical coils. Existing correlations for the Nusselt number and friction factor, perhaps the two most important considerations in design, will be introduced.

The most important references in this area are without a doubt the original papers of W.R. Dean (1927, 1928) on streamline flow in curved tubes. Together, these papers provide the conceptual and mathematical framework on which subsequent work was based. The reader may then refer to three fairly recent review papers. The review by Berger et al. (1983) provides a broad picture of the main research topics in which helical coils are of interest, but includes only a brief section on heat transfer per se. Most of the paper is concerned with steady flow in rigid coils, but the authors include sections on different wall characteristics (variable curvature, flexible walls, porous tubes), mixing and transport, and unsteady flows. Flexible walls, variable curvature and pulsating flows are of particular interest in medicine.

The chapter by Shah and Joshi (1987) is an excellent summary of heat transfer in helical coils (constant radius of curvature) and includes some results for spiral coils (increasing radius of curvature). They provide equations for heat transfer in laminar and turbulent flows for Newtonian and non-Newtonian fluids, discuss friction factors, entry lengths and introduce results for coils of non-circular cross-section. The authors have expressly organized their material to ensure that the reader be aware of the boundary conditions relevant to the theoretical and empirical equations that they present. Finally, Sandeep and Palazoglu (1999) provide what may be considered a brief update of secondary flow and heat transfer in coils, relative to corresponding sections in the two papers mentioned above.

2.1 Brief History

The review by Berger et al. (1983) states that J. Thomson reported the first *observations of the striking effects of curvature on open-channel flow* in 1876. After the turn of the century, J. Eustice (1911) observed the trajectories of ink injected into water flowing in tubes wound around pipes of different diameter. W.R. Dean (1927) began to develop a mathematical framework to explain the streamlines observed by Prof. Eustice, and later (Dean, 1928) turned his attention to a mathematical explanation of the reduction in flow rate due to tube curvature, earlier observed experimentally by Eustice (1910). By writing the equations of fluid motion in terms of a toroidal coordinate system, and accounting for the centrifugal force due to curvature, Dean was able to reproduce many of the qualitative features of the streamlines observed by Eustice.

In attempting to explain the reduction in flow in a curved tube compared to that in a straight tube at the same axial pressure gradient, Dean (1928) introduced the variable K, defined as $2n^2a/R$, where n is the Reynolds number. K is the precursor of the Dean number (De), which is now expressed as $Re(a/R)^{1/2}$ by many authors, although Berger et al. (1983) suggest that it should be expressed as $2Re(a/R)^{1/2}$.

Note: Berger et al. (1983) discuss the various forms of the Dean number that have been used in the literature and caution the reader to note the equivalences in interpreting data, since much confusion has arisen.

The experimental work of Eustice and the mathematical formulations of Dean set the foundations for, essentially, all subsequent work in this area. Although Dean's approach was limited to the lower range of laminar flow in a torus of small curvature, he clearly expressed these limitations and suggested approaches to extend the results to turbulent flow. Even at this early stage, Dean and Eustice had recognized several of the consequences of tube curvature on fluid flow that received more detailed attention in the following decades. Among these were the facts that there is no clear critical Reynolds number at which the demarcation between laminar and turbulent flow arises and that the onset of turbulence occurs at a substantially higher Reynolds number than in a straight pipe (see section 2.2.3). The problem of entry flow was discerned, and the effects of curvature on the friction factor and the relationship between pressure gradient and mass flux were analyzed in terms of analytical solutions to the governing equations. More recent references on these matters will be discussed in succeeding sections.

Early work regarding the heat transfer in coiled tubes also dates back to this era, beginning perhaps with Jeschke's (1925) study of heat transfer to air flowing in a coil. Jeschke showed that the heat transfer was greater in the coil than in a straight tube, and his limited results fit the equation:

$$Nu_c = Nu_s\,(1+3.5\,a/R) \tag{2.1}$$

where the subscript 'c' is for the coil and the subscript 's' is for a straight tube of the same diameter, length and wall thickness. This was probably the first attempt to express the improvement in heat transfer due to curvature in terms of helix geometry. Much of the work on heat transfer in helical coils has been oriented towards developing this type of relationship, since an accurate correlation would certainly simplify design given that the straight-tube situation is extremely well-defined. According to Shah and Joshi (1987), there are about 15 experimental and theoretical correlations to calculate the Nusselt number in a helical coil, some of which are quite similar to Jeschke's relation.

At this point, it should be noted that the subject of heat transfer in a coil is substantially more complex than that of fluid flow with no heat exchange. One reason for this added complexity is that buoyancy forces induced by heating can dominate the flow pattern (Prusa and Yao, 1982). Another is that the heat input along the coil may be distributed in various fashions (ie. according to one of the three boundary conditions given in the introduction, or to some other pattern). The temperature-dependence of properties such as viscosity also complicates estimation of the heat transfer along the length of the coil. Finally, the transfer of interest in cooling applications is that from a warm fluid inside the coil to a cooler environment, and this represents a different problem altogether than transfer to the inner fluid.

2.2 Flow in Curved Tubes: the Dean Vortices

It is worthwhile visualizing the flow pattern observed by Eustice and described by Dean. Dean (1927) used the toroidal coordinate system shown in Figure 2.1 to set up the governing equations, although strictly speaking, Eustice's observations were in helical coils. As shown in Figure 2.2, Dean's solutions indicated that there exists a secondary flow in the form of a pair of vortices rotating in opposite directions. The lines in this figure

> *"represent what may loosely be called the projections of the paths of fluid elements on the cross-section of the pipe"* (Dean, 1927, p.218),

although this is not evident without clarification from Figure 2.3, also from Dean (1927). Figure 2.3 represents a top view of a torus (ie. the tube itself occupies the region between the concentric lines, the central circle being the 'hole in the doughnut'), with one trajectory of a fluid element. Here, a fluid element is projected from the inner periphery of the tube to its outer periphery. If the fluid element lies on the central plane (ie. the extension in the direction of the mean flow of the horizontal line at the middle of the circular cross-section), Dean's solution suggests that it never leaves this central plane. Rather, it moves in a curved trajectory from the inner periphery to the outer periphery and back again as it continues in the direction of the pressure gradient (ie. downstream).

(Note: This is but a theoretical result applicable to an imaginary fluid element with no volume. Dean notes that when Eustice injected ink at the central plane, the coloured line split into two bands when it reached the outer wall. Also, even though the mathematical formulation implies that the central plane acts as a solid boundary preventing exchange of fluid between the top and bottom halves of the cross-section, this condition is unlikely to be strictly satisfied in the case in a real flow).

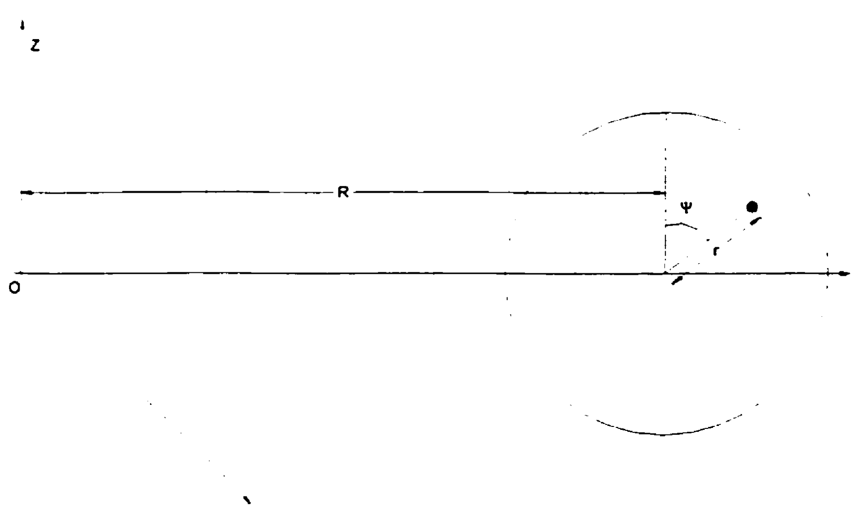

Figure 2.1 The toroidal coordinate system.

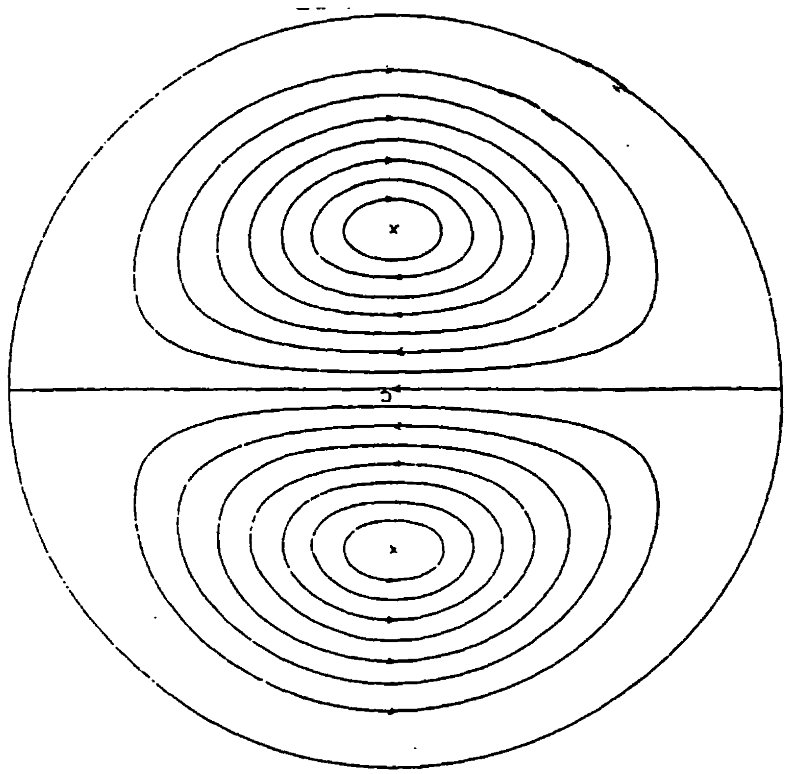

Figure 2.2 Secondary flow in the form of a pair of vortices rotating in opposite directions (Dean 1927).

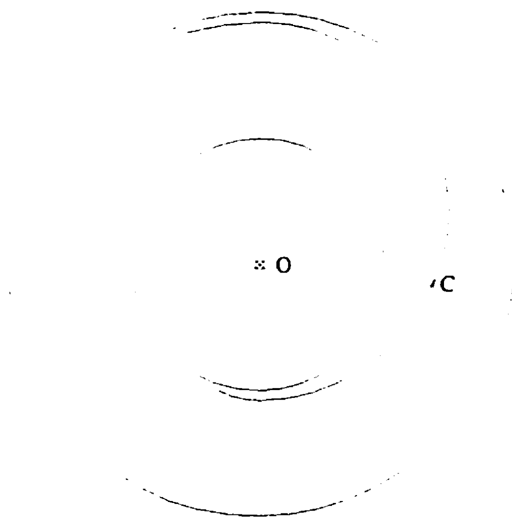

Figure 2.3 Top view of a torus with path of one fluid element C (Dean 1927).

Fluid elements off the central plane are also projected towards the outer periphery and away from the central plane when they are outside the central line (ie. on the outer peripheral side). The motion is towards the central plane when the element is inside the central line. One consequence of these considerations is that a fluid element that is above the central plane stays above it, and conversely, one that is below stays below. Except in the case of an imaginary element starting on the central plane, the horizontal distance of any other fluid element from the central plane increases and decreases as the element moves downstream, as does its radial distance from the center line of the tube.

The distinct circulations above and below the central plane have been referred to as 'Dean vortices' in the literature. Figure 2.4a,b further clarifies the nature of the flow. Here, the Dean vortices are shown as dashed lines, and the contours of constant axial velocity are shown as solid lines. Besides the presence of the secondary flow, the mean radial velocity distribution also differs from straight-tube Poiseuille flow in that the maximum downstream velocity is displaced towards the outer edge of the tube cross-section. This results in a *greater velocity gradient (and shear stress) on the outer periphery. For a given* diameter tube, the contours of constant axial velocity are compressed and shifted to the outer periphery as the velocity increases (compare Fig. 2.4a with 2.4b).

Subsequent work, performed primarily since 1950 (Janssen and Hoogendoorn, 1978), has substantially clarified the nature of flow in helical coils over a much wider range of conditions than those to which Dean's formulation applies (and as seen for example in Figure 2.4b). Dean himself specified that his approach is limited to small curvature ($a/R<<1$), low velocities and a circular cross-section. The maximum Dean number (according to $K=2Re^2a/R$) to which his results apply is 576 (or 34 according $De=2Re(a/R)^{1/2}$)), which does not cover the full range of laminar flow. Furthermore, the torus he considered analytically is but an approximation of the helix, in the sense that it approximates the shape of one turn of a helix. The helix as such, has a further dimension perpendicular to the central plane of the torus, which gives rise to a twisting or torsion force. It is interesting to note that even though Eustice worked with *helically coiled tubes, the true helical configuration was not considered* analytically for almost 50 years (Berger et al., 1983).

Another configuration of curved tubes that has received some attention in the literature (for which results are summarized by Shah and Joshi, 1987) is that of a spiral. Here, the added dimension is in the same plane as that of the central plane of the torus, such that the radius increases continuously. Other cross-sectional forms have also been considered.

What arises from the early work in this field is that the flow in a curved tube is substantially different than that in a straight tube. It is of consequence that even under laminar conditions, each fluid element approaches the tube walls one or more times as it is carried downstream, since this cannot but alter the temperature distribution over the tube cross-section. In laminar flow

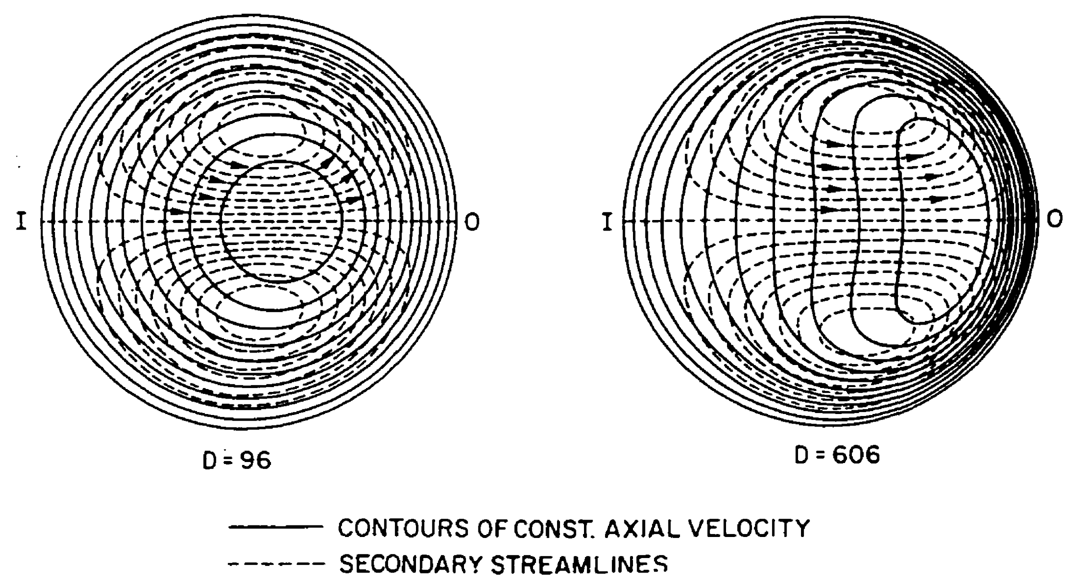

Figure 2.4 a,b. Secondary streamlines and axial-velocity contours at low and Intermediate Dean nos. at inner bend (I) and outer bend (O) (Berger, Talbot and Yao, 1983).

in a straight tube, the temperature is essentially conducted from the wall to the center (heating case) such that it requires a substantial residence time to affect the fluid at the center. This residence time required to achieve a mean bulk temperature can be expected to be shorter in a curved tube because of the mixing induced by the secondary flow pattern described above. This is analogous to the enhanced heat and mass transfers associated with turbulence, which are due to the spatial exchange of fluid elements relative to a source or sink.

Finally, it is interesting to consider the consequences of the onset of turbulence in a curved tube. One might expect that as turbulent perturbations alter or break down the secondary flow pattern, the flow in a curved tube should resemble that in a straight tube to an increasing extent. At the same time, the heat and mass transfer advantages of curvature diminish. It is worth citing Shah and Joshi (1987: p.5-25) regarding the heat transfer in curved tubes under turbulent conditions:

> *"...other than space saving, a coiled tube does not offer any significant advantages over a straight tube for turbulent flow."*

2.2.1 Flow in a Helical Coil – the Influence of Pitch

As mentioned in the previous section, a helical coil has one more dimension than does a curved tube. The helical coil has several turns and can be stretched to different pitches, which introduces an additional torsion force. This complicates the mathematical representation of the flow. A number of papers have dealt with this issue, one of the most recent being that of Germano (1989).

Germano (1989) extended Dean's equations to suit the geometry of a helix with circular or elliptical cross-section. He adopted an orthogonal coordinate system used in the field of hydromagnetic equilibria, and showed how his results corresponded to those of previous workers (Wang, 1981; Murata et al., 1981; Kao, 1987) *once the differences in coordinate systems* and notation were taken into account. He introduced a new parameter λ/Re, where λ is defined as the ratio of torsion to the curvature. Germano concluded that the effect of torsion is most noticeable at low Re. Tuttle's (1990) analysis indicates that the effect of torsion at low Re is to rotate the secondary flow. Yang and Ebadian (1996) describe the effect of torsion as a developing asymmetry between the counter-rotating vortices, such that the top vortex becomes larger than the other one. Since increasing the pitch means stretching the helix, it eventually becomes a straight tube. Thus, one *can imagine that at some larger pitch, the secondary flow structure* disappears altogether and the flow resumes a Poiseuille character if Re_{crit} has not been exceeded.

The most recent analysis of flow in a helical pipe may be that of Zabielski and Mestel (1998). The authors claim that their approach is completely general and is not limited to laminar flows. They introduce the correlation $Re=h_bGa^3/v^2$, which is related to the Dean number by:

$$Re=Deh_b(R/a)^{1/2} \tag{2.2}$$

Here, a is the tube radius, R is the helix radius, and $h_b=(1+\varepsilon^2b^2)^{1/2}$, and ε is a parameter relating the distance travelled along the helix central axis to the rotation angle about this axis. The distance travelled, d, is expressed as $d=2\pi/\varepsilon$. Thus ε is a function of the inverse of the non-dimensional pitch, since as the pitch tends to 0, $2\pi/\varepsilon$ also tends to 0 (the case for a torus).

Note: The paper wrongly states that ε, is the pitch, whereas the authors take d to be the pitch (J. Mestel, pers. comm.).

Re thus appears to be a Reynolds number generalized for curvature *(embodied in De) and pitch.*

The authors' numerical solutions indicate that, contrary to Webster and Humphrey's (1973) statement that the Dean vortices are present at all velocities, only a single vortex is present at very small Re. As Re increases, a second vortex appears in the bottom of the cross-section and grows until symmetry is reached. At much higher Re, the secondary flow bears little resemblance to the twin vortices of Dean. Zabielski and Mestel (1998) describe the situation at large Re as "an asymptotic structure with inviscid core and viscous boundary layers" that separate at the inner periphery (Figure 2.5). It seems then that the secondary flow pattern associated with laminar flows fades away at higher velocities.

In order to describe the influence of pitch on the flow at a given Re, the authors fall on a geometrical interpretation of flow in a helix – ie. it is a rotation about the axis during translation along the axis. Translation is favored as pitch increases while rotation is favored as pitch tends to 0 (torus). The influence of pitch is therefore to alter the relative dominance of translation and rotation (at a given set of conditions of curvature, flow rate and fluid properties). The more dominant is the translation, the less one can expect symmetry of the vortices (at conditions at which two vortices exist). As pitch increases, the velocity at which the two vortices are symmetrical is greater (in the limit of infinite pitch, there are never two vortices).

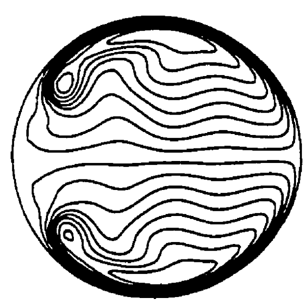

Figure 2.5. Flow at very large Re=50^3. An asymptotic structure emerging . with R=$^{-1/3}$ boundary layers which separate before the inside of . the bend (Zabielski and Mestel, 1998).

2.2.2 Pressure Drop and Friction Factor

One of the important consequences of tube curvature from the point of view of process design, is a lower volume flux for the same pressure gradient as in a straight tube (or greater pressure drop for the same volume flux). Pressure drop is usually calculated on the basis of the friction factor, for which many relationships have been developed (Ito, 1959). The phenomenon had been recognized by Dean and others near the turn of the 20th century. Dean (1928) explained the phenomenon with clear simplicity as follows:

> *"The reason why the pressure required to maintain a given rate of flow is greater in a curved pipe than in a straight one is mainly that in a curved pipe part of the fluid is continually oscillating between the central part of the pipe, where the velocity is high, and the neighbourhood of the boundary, where the velocity is low. This movement is due to the centrifugal tendency of the fluid, and implies a loss of energy which has no counterpart in stream-line motion in a straight pipe."*

It was in attempting to quantify the reduction in flow rate that explain this phenomenon that Dean (1928) revised his formulation and introduced the original Dean number, K=2Re(a/R). He deduced that the ratio between the flux in a curved pipe and that in a straight pipe could be written to a first approximation as:

$$^{1}F_{c}/F_{st} = f_1(K) = 1 - (K/576)^2(0.03058) \qquad (2.3)$$

and to a second approximation as:

$$^{2}F_{c}/F_{s} = f_2(K) = f_1(K) + (K/576)^4(0.01195) \qquad (2.4)$$

Dean obtained equations 2.3 and 2.4 by expanding the solution to the governing equations in powers of K and dividing by the straight-tube flux $\pi W_0 a^2/2$. Here, W_0 is the mean velocity in the axis perpendicular to the central line (ie. along the line joining the centers of the two vortices).

Unfortunately, the range of application of equation (2.4) is very small. This is because equation 2.4 describes a function that decreases from 1 (when K=0) to about 0.98 at K=650, and increases thereafter. Dean notes that the lower limit for K is 350, since at this value, the decrease in flux due to curvature is only 1%, barely large enough to be measurable. For values of a/R less than about 0.3, the Reynolds numbers associated with K are of the order of 10^2 making equation 2.4 applicable only to laminar flows.

Dean (1928) saw no practical advantage in extending the number of terms in the series to extend the limits of application due to the manipulations required, even though the function with additional terms might have a minimum at larger values of K. In fact, it was due to the development of computers that Van Dyke (1978) was able to extend the series to 24 terms and show that it converges for K<576, thus proving the limitation of Dean's formulation.

The problem of flux decrease due to curvature was later studied in terms of the friction factor and extended to the turbulent range. Ito (1959) presented data for isothermal flow of water through five straight-drawn copper pipes with one turn. The radius ratios (R/a) ranged from 16.4 to 648, and the flows covered both laminar and turbulent ranges ($10^3 < Re < 10^5$). The observed friction factors, f_c, conformed to (based on the notation of Rogers and Mayhew, 1964):

$$f_c = 0.076\ Re^{-0.25} + 0.00725\ (a/R)^{0.5} \tag{2.5}$$

where, a and R are the tube and coil radius, respectively. Equation 2.5 is applicable to $0.034 < Re(a/R)^2 < 300$. Given that Ito's data extend to Re = $3x10^5$, the expression does not apply to a/R ratios greater than 1/31 at the higher Re limit.

Ito (1959) also noted that for $Re(a/R)^2 < 0.034$, the friction factor is the same as that for a straight pipe. Interpreted in light of Dean's results (equation 2.4), this means rather that at very low Re or for a very loose coil, the difference in friction factor relative to a straight pipe is too small to be easily measured.

No less than 21 correlations for the friction factor in curved tubes have appeared in the literature (Sandeep and Palazoglu, 1999). The most recent is perhaps that of Yang and Chang (1994), which is given as a function of De, Pr, Ra and δ (=a/R) as follows:

$$f_c/f_s = 0.689\ De^{0.0817} Pr^{0.0081} Ra^{0.0068} \delta^{0.0084} \tag{2.6}$$

with, $10 < De < 25{,}000$, $0.7 < Pr < 100$, $0 < Ra < 320$, $0.01 < \delta < 0.8$.

It should be noted that only one of the relationships account for the influence of coil pitch. That is the correlation developed by Mishra and Gupta (1979) for laminar flow:

$$f_c/f_s = 1 + 0.033\ (\log De')^4 \tag{2.7}$$

Here, De' is a modified Dean number based on the following expression for the coil radius:

$$R_c = R\ (1+(P/2\pi R)^2) \tag{2.8}$$

where, R is the usual coil radius, and P is the pitch (m). The equation applies to $1 < De' < 3000$, $0.00289 < a/R < 0.155$, $0 < P/D < 25.4$.

2.2.3 Transition from Laminar to Turbulent Flow in Curved Pipes

Dean and others had recognized that there is no clear transition from laminar to turbulent flow in a curved pipe, and that the transition occurs at higher Re than in a straight pipe. Based on experimental work, Ito (1959) concluded that the critical Reynolds number at which the transition to turbulent flow occurs in a curved pipe could be expressed in terms of curvature as:

$$Re_{crit} = 2 \times 10^4 \, (a/R)^{0.32} \qquad (2.9)$$

and that the equation was suitable for a/R in the range 0.0012 to 0.067. At the lower value, Re_{crit} is estimated to be 2325 and is 8421 at the upper value. For a/R<0.0012, the straight-tube value should be used (Ito, 1959). Sandeep and Palazoglu (1999) cite three other equations for Re_{crit} that were developed in the 1960's, one of which differs slightly from Ito's in the constant and exponent, while the other two increase from the straight tube value as fractional exponential functions of a/R. The critical Reynolds number is presumably also influenced by pitch, based on the previously described influence on vortex structure; however, there does not appear to have been a specific effort made towards including pitch in any of the expressions for Re_{crit}.

2.2.4 Entry Length

Although it was not explicitly stated earlier, the descriptions of flow patterns and their influence on certain characteristics of pipe flow have assumed that the flow is fully developed. A fully developed flow is understood to mean a flow whose characteristics are independent of the distance from the pipe entrance. Over the length in which the flow is not fully developed, the flow pattern, heat transfer and other characteristics are not as predicted, and may have to be taken into account in design if the pipe length is relatively small. For a straight pipe, the entry length for laminar flow is often given as:

$$l_s = 0.25aRe \qquad (2.10)$$

where, a is the pipe radius, and Re is based on the uniform axial velocity at the pipe entry. Berger et al. (1983) reviewed a number of results for curved tubes. For large Dean numbers, the entrance length for a curved tube is predicted by:

$$l_c = l_s\, 8e_l K^{-1/2} \tag{2.11}$$

where $2<e_l<4$ (being weakly dependent on a/R), and K is the Dean number according to $2Re(a/R)^{1/2}$. The authors add that although there is an implication that $l_c/l_s<<1$, the ratio can be much closer to 1 for practical situations (eg. for a/R=0.05 and Re=2000, then l_c/l_s=0.584). Shah and Joshi (1987) note that since the entrance length for curved tubes is 20 to 50% shorter than for a straight tube for most engineering applications for which De>200, design can be based on the fully developed flow without significant error. For turbulent flows, the entry length has been shown experimentally to have a magnitude of 50 to 100 tube diameters (Daily and Harleman, 1966).

2.3 Heat Exchange Involving Curved Ducts

The study of heat exchange in curved tubes and coils dates back to the same era as the description of isothermal flow in a torus by Dean. Jeschke, White, and Adler were among the early contributors. The contributions of these authors have been summarized in some of the works that will be reviewed in this section (see for example Seban and McLaughlin, 1963; Rogers and Mayhew, 1964) and will not be included here. Most of the research in this area has focused on heat transfer from the tube outer surface to a fluid circulating inside it. In most cases, experimental setups have been devised to approximate the boundary conditions mentioned in the introduction.

Several aspects of heat transfer in curved ducts have been investigated. These include: the variation of the Nusselt number in the axial direction, peripheral variations of Nu at a given axial position, thermal entry length, influence of a/R, influence of De, influence of pitch, significance of fluid viscosity and buoyancy, and interactions betweens these factors. Since most of the earlier literature does not consider the influence of pitch, the first section is devoted to precisely that literature. The second section will discuss the few recent studies that have considered the true helical geometry. Much less literature is available concerning the problem of heat transfer from a coiled tube to the environment, but will be covered in Chapter VI.

2.3.1 Heat Exchange in Coils – Pitch not Considered

Seban and McLaughlin (1963) noted that, at that time, it was difficult to describe the phenomenon of heat transfer in coils analytically because of "the difficulty in assessing the effects of the distortion of the mean velocity profile and because of the quantitatively unknown nature of the secondary flow, while added to the basic problem is the marked asymmetry of the flow that is demonstrated by Adler's results." They saw the need for additional experimental data, which they obtained under conditions of constant heat flux to fluids using electrical dissipation to heat coils in an insulated box.

They used two Type 321 stainless steel tubes of 7.4 mm inside diameter and 0.3 mm wall thickness. One tube was formed into a coil with 6.5 turns and 125.2 mm diameter, the other was formed into 1.5 turns with 764.5 mm diameter. Freezene oil was used to study heat transfer in laminar flow, whereas water was used to study the turbulent range. Heat input and flow rate were varied in each case. For the oil, the Prandtl number ranged from 100 to 657, and the Reynolds number ranged from 12 to 5600. For water, the Prandtl range was 2.9 to 5.7 and the Reynolds range was 6000 to 65600. Pressure taps were inserted near the entry and exit of each coil to determine the friction factor. Thermocouples were inserted into the tubes to determine temperatures at various axial positions, and additional thermocouples were positioned so as to determine the peripheral distributions at given axial positions along each coil.

For the laminar flow, the authors found that the heat transfer coefficients on the outer and inner peripheries were substantially higher than in a straight tube under the same conditions, and that the coefficients for the outer periphery were higher than those on the inner periphery. They determined that the ratio between the outer and inner coefficients was 4:1 (positions 0 and 180°). They found little effect of coil diameter. One of the interesting results of this study was that although the local heat transfer coefficients dropped from inlet towards outlet, there was a tendency for them to rise at the last measurement position (near the outlet). This was attributed to a buoyancy effect because the increase appeared to be relatively greater at higher heat flux input. They proposed the following equation:

$$(hd/k)(\nu/\alpha)^{-1/3} = A[f/8(U_m d/\nu)^2]^{1/3} \qquad (2.12)$$

where, h is the heat transfer coefficient, d is the diameter, k is the thermal conductivity, ν is the kinematic viscosity, α is the thermal diffusivity, f is the Weisbach friction factor, U_m is the mean velocity. A is a constant suggested to be 0.13 for the small coil, and 0.74 for the larger coil. This equation defines the minimum peripheral average heat transfer coefficient for coil to diameter ratios of 17 to 104 in the Prandtl range of their experiments.

For turbulent flows, the authors found that the ratio of heat transfer coefficients (outer to inner periphery) was of the order of 2. This was attributed to the absence of a pronounced minimum at the inner periphery. Moreover, there was little axial variation. For the large coil, it was found that the average circumferential heat transfer was well represented by:

$$(hd/k)(\nu/\alpha)^{-0.4} = f/8(U_m d/\nu) \qquad (2.13)$$

Results on the smaller coil were quite variable. The authors also note that measurements of the outside wall temperatures were erratic. Nevertheless, it appeared that Jeschke's equation underestimated the heat transfer coefficient by about 8% on the average.

$$(Nu)_b = 0.023\,(Re)_b^{0.85}\,(Pr)_b^{0.4}(a/R)^{0.1} \tag{2.14}$$

where the subscript indicates that fluid properties are evaluated at the bulk temperature rather than the film temperature. At the film temperature, the same equation applies wherein the exponent is 0.021 rather than 0.023. Nevertheless, the authors did not seem particularly satisfied with their data. Rogers and Mayhew (1964) attempted to consolidate the results of Seban and McLaughlin (1963) and others using steam-heated coils to transfer energy to water in turbulent flow ($Re>10^4$). Three coils were used, all with a pitch of 38.1 mm. The coil to tube diameter ratios were 10.8, 13.3 and 20.12, and the coils had 8.5, 6.5 and 4.5 turns, respectively. Entry lengths of 180 tube diameters were provided to ensure flow development. The overall heat transfer coefficients, U, were based on the log-mean temperature difference between inlet and outlet. Their heat transfer results were best described by the relationship that available in the literature, noting that "it is essential that a better experimental technique be devised".

Mori and Nakayama (1965, 1967), Dravid et al. (1971), and Patankar et al. (1974) modelled the temperature distribution in curved pipes assuming the geometry of a torus. Mori and Nakayama (1965) analyzed the problem for high Dean number laminar flows (De>100) and turbulent flows (Mori and Nakayama, 1967) in terms of a boundary layer and core region, assuming peripherally constant temperature and axially constant heat flux. These assumptions were due to their interpretation of measurements for heat transfer involving water and oils by Seban and McLaughlin (1963). Their analyses were restricted to the case of fully developed flows. They present equations for the ratio of the peripherally-averaged Nusselt number in a curved tube to one in a straight tube for the laminar and turbulent regions (note: since these equations involve a number of coefficients that arise from the authors' complete theoretical development, the equations are not included here).

Several conclusions can be drawn from their work. First, the increase in heat transfer due to curvature is much less marked in turbulent flow than in laminar flow. In both laminar and turbulent flow, the temperature profile is markedly different from that in a straight pipe (coolest at the center, increasing symmetrically towards the wall as an inverted parabola). The temperature distribution along the horizontal axis of the tube cross-section is skewed to the left, the peak temperature being shifted towards the inner wall. The temperature distribution along the vertical axis of the cross-section is essentially flat, indicating full mixing, although there is some evidence of local minima near the top and bottom of this axis, corresponding to the centers of the flow vortices. Finally, at high Dean number, the heat transfer in the curved tube exceeds that in a straight tube by a factor that is proportional to the square root of the Dean number.

Dravid et al. (1971) then focused on the determination of heat transfer coefficients for the thermal entrance region in laminar flows with De>100, and on the oscillations in heat transfer coefficient with distance from the coil entrance. They developed an analytical solution for the thermal entrance region and a numerical solution for the fully developed region that is based on the equation of heat transport with the assumptions of constant fluid properties and negligible viscous dissipation of energy. Figures 2.6a,b shows the dimensionless wall temperature at 3 peripheral positions, the peripherally-averaged wall temperature and the bulk temperature as a function of the dimensionless axial distance for water (Pr=5) and a fluid with Pr=15, respectively, in laminar flow (Re=1000). These figures indicate an oscillatory behavior for some distance from the entrance.

The authors explain the first oscillation as the propagation of a step-change in temperature at the thermal boundary layer some distance from the entrance, which is due to the rapid transport of heat from the wall near the entrance, energy which is driven around the tube periphery then back through the center to meet the thermal boundary layer at the same peripheral position further downstream. The meeting of warmer fluid with the wall causes a drop in thermal gradient and consequently, a decrease in the flux as shown in Figure 2.7 (peripherally-averaged wall heat flux as a function of dimensionless axial distance for Prandtl number of 0.5, 5 and 15). The subsequent oscillations are considered to be resonances of the first, and, as seen in Figures 2.6a,b, and 2.7, damp out as the fully-developed condition is approached. Figures 2.8a-e show how the cross-sectional view evolves with axial distance. Figure 2.8 a shows the entrance conditions, where the inner periphery is warmer due to slower heat transport, and Figure 2.8 e shows the fully developed condition with two cool regions corresponding to the faster-moving vortex centers.

The authors brought up the following points from their analysis. In the entry region, there is little or no effect of the secondary flow field on the thermal boundary layer, and the ratio of Nu_c to Nu_{st} varies as $De^{1/6}$. In the fully-developed region the ratio depends on $De^{1/2}$. The initial oscillations are due to the fact that the core region is not well-mixed. They proposed the following equation for the asymptotic Nusselt number, indicating that the thermal entry length dependence can be neglected since the entry length is short, making the estimate only slightly conservative:

$$Nu_c = (0.76 + 0.65De^{0.5})\, Pr^{0.175} \qquad (2.15)$$

Tarbell and Samuels (1973) and Patankar et al. (1974) also considered the approximate evolution of velocity and temperature profiles in helical coils under laminar conditions. The temperature profiles both these authors present correspond well with those of Dravid et al. (1971). Although the magnitudes of predictions vary to some extent from one author to another, the general picture seems fairly clear. Recognizing the variability of results of previous workers, Janssen and Hoogendoorn (1978) measured the heat transfer in several coils under a wide range of conditions and with liquids of different viscosities. Their data exhibit oscillations similar to those predicted by early workers. The authors comment on the Dean and Prandtl dependencies of the heat transfer.

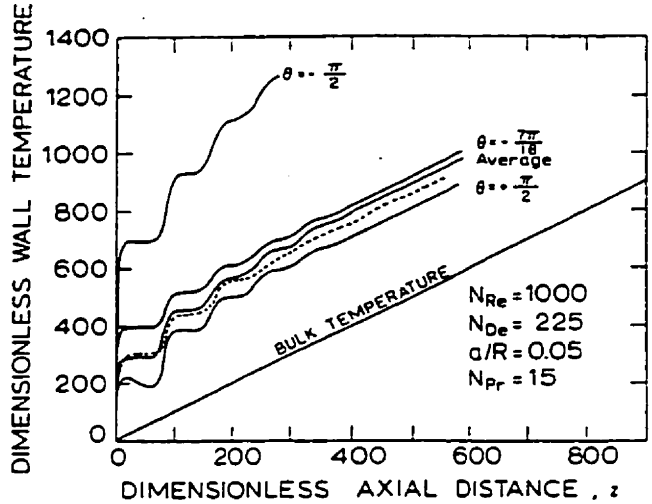

Figure 2.6 a Axial profiles of wall temperature at Pr=15, computed numerically. The wave length of the first oscillation has been schematically defined (Dravid et al., 1971).

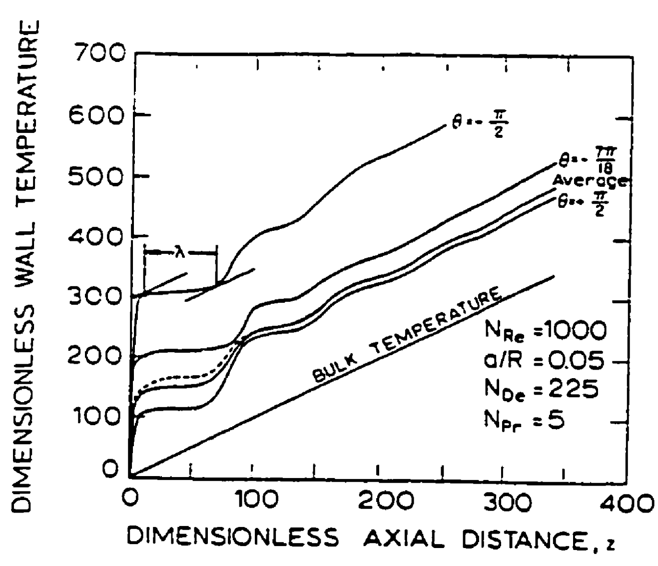

Figure 2.6 b Axial profiles of wall temperature at Pr=5, computed numerically. The wave length of the first oscillation has been schematically defined (Dravid et al., 1971).

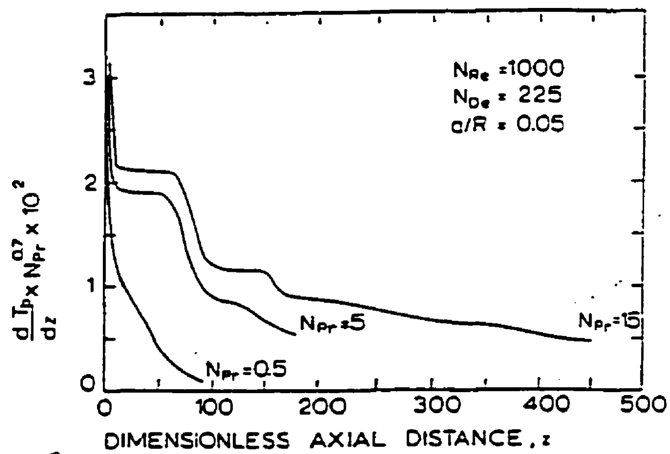

Figure 2.7. Axial profile of the θ-averaged wall heat flux at several values of Prandtl no. computed numerically. The term dT_b/dz is proportional to the θ-averaged wall heat flux (Dravid et al., 1971).

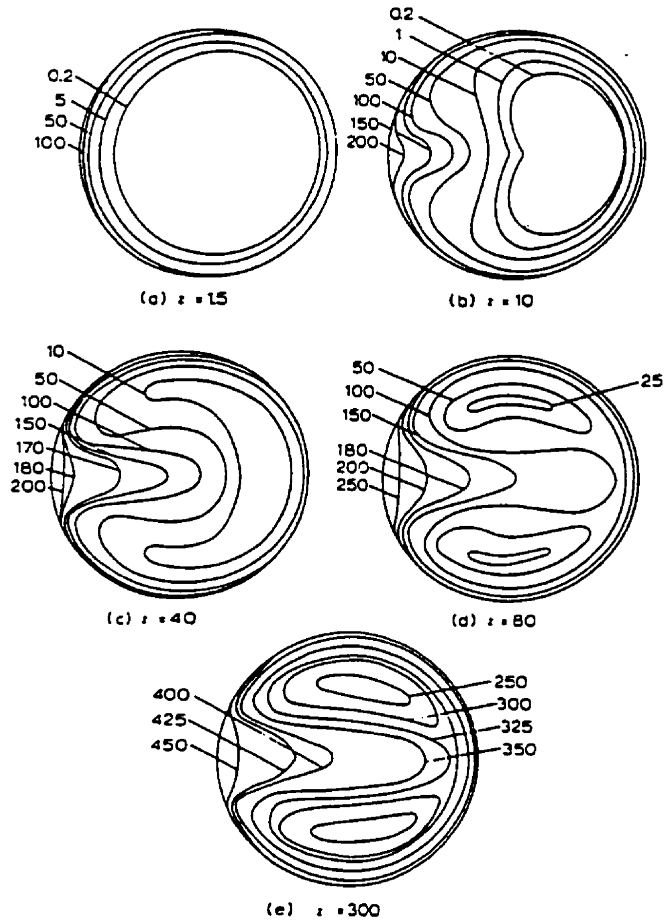

Figure 2.8 a-e. Development of the temperature field for the constant wall heat flux case, computed numerically. First cross section at five axial positions are shown. Each contour represents an isothermal the indicated dimensionless temperature. Other parameters are Re=1000, Pr=5, De= 225 and a/R = 0.05 (Dravid et al., 1971)

2.3.1.1 Study of Buoyancy Effects

The paper by Prusa and Yao (1982) revisits the question of buoyancy effect mentioned earlier by Seban and McLaughlin (1963). The authors refer to a demonstration by Morton (1959) that a secondary flow composed of two vertical vortices can be generated in a straight tube by strong heating, and use a finite-difference method to investigate the relative dominance of centrifugal and buoyant forces on the secondary flow in curved tubes. Essentially, they showed that buoyancy forces can dominate the centrifugal forces and vice versa, resulting in a flow regime map with three sectors (Figure 2.9). In region I, the centrifugal force is dominant and the analysis of flow is treated as if the momentum and energy equations are uncoupled. In region II, the forces are of

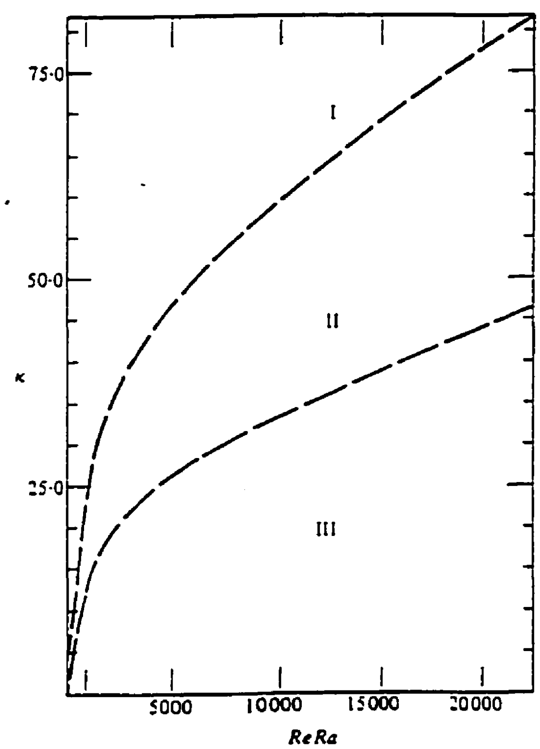

Fgure 2.9. Region of fully developed flow in heated curved tube (Prusa and Yao, 1982).

similar importance and a general solution is used. In region III, the centrifugal forces are much smaller than the buoyancy forces and the straight-tube analysis with buoyancy is appropriate. Thus, region III represents a situation with a large axial temperature gradient and small curvature.

Futagami and Aoyama (1988) further pursued these questions, extending the analysis to high Prandtl number fluids. The particularity of their work was that they investigated the influence of the tilt angle of the helix on the relationship between buoyant and centrifugal forces, following earlier work on inclination of angle of straight tubes by the first author. They proposed an approximate expression for the peripherally-averaged Nusselt number inside the coil for the region where buoyant and centrifugal forces are both significant:

$$Nu/Nu_{0f} = 1 + [(Nu_c/Nu_0 - 1)^4 + (Nu_b/Nu_0 - 1)^4]^{1/4} \qquad (2.16)$$

where,

$$(Nu_{cf}/Nu_0)^6 = 1 + \{0.195(DePr^{0.54}\cos\alpha)^{0.5}\}^6 \qquad (2.17)$$

$$(Nu_b/Nu_0)^{4.5} = 1 + \{0.19(DeRaPr\cos\alpha)^{0.2}\}^{4.5} \qquad (2.18)$$

Here, Nu_0 is the Nusselt number for Poiseuille flow, Nu_c is the Nusselt number associated with the condition of centrifugal force acting alone (ie. Ra=0), Nu_b is that associated with the condition of buoyancy force acting alone (De=0), and α is the angle of inclination of the tube axis. These authors also performed experiments to verify their equations. The fluid used was water, and the coil was a 9.9 mm copper tube with 1.2 mm wall thickness, arranged into a 1 m coil diameter with 1.5 turns, and angle of inclination of 7°. The coil was heated by nichrome wires and insulated with asbestos. The experimental results were within 30% of the predicted values.

2.3.1.2 Summary

Although a number of equations for the Nusselt number or Nusselt number ratio for curved to straight tube have been presented, experimental results agree only approximately with predictions. Moreover, several authors have expressed difficulties associated with experimental technique. It appears that only Futagami and Aoyama (1988) have taken the trouble to include a deaerator in the experimental setup, yet their results do not correspond to predicted values to a better extent than the experimental results of others (ie. about 30% error).

Up to this point, none of the research has considered the influence of pitch on the heat transfer, even though the work done on buoyancy effects implies that pitch could have a significant influence on the heat transfer.

2.3.2 Heat Transfer In Helical Coils considering Pitch

The full helical geometry (ie. including pitch) had been considered by Germano (1982) and others for isothermal flow. Compared to the analysis for a torus, the analysis for a helical coil with non-negligible pitch involves consideration of the torsion force that arises as the coil is stretched. Gong et al. (1994) and Yang and Ebadian (1996) investigated the influence of the torsion on the Nusselt number.

Gong et al. (1994) used a perturbation solution to the governing equations written in a helicoidal coordinate system with torsion in terms of the pitch as:

$$\lambda = R/\pi D \tag{2.19}$$

where R is the pitch in meters and D is the diameter of the helix. Their numerical solution led to the conclusion that torsion affects the temperature profile by rotating the contours and destroying their symmetry. The effect is greater at higher Pr, Re and a/R. However, the influence on the Nusselt number remains small (about 1% reduction for an increae in λ form 0 to 0.3, with Pr=5, Re=30 and ε=0.3). (Note: ε is the dimensionless curvature)

Yang and Ebadian (1996) studied forced convection heat transfer in coils with substantial pitch and turbulent flow conditions. This work was based on numerical solutions to the governing equations written in helicoidal coordinates. Figures 2.10 show how torsion (λ) due to increasing pitch twists the temperature profiles for air (Pr=0.7) and water (Pr=5). The authors present Tables 2.1 and 2.2, which indicate how torsion can influence the Nusselt number for these two fluids, as well as indicate the Re dependence. The behaviour is different for the two fluids but the torsion effect does not appear to be terribly important in light of the magnitude of errors that have been observed experimentally in previous works.

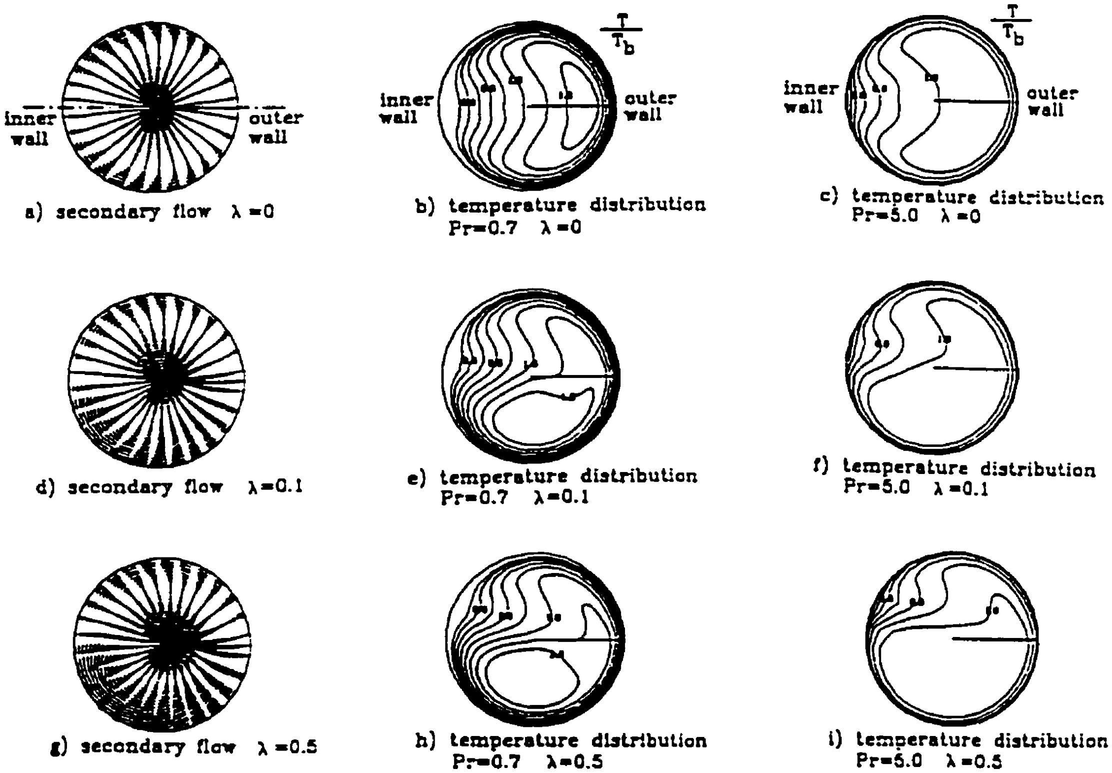

Figure 2.10. The secondary flow and the temperature distribution in a cross-section oh helicoidal pipe (Yang and Ebadin, 1996).

Table 2.1 Effect of torsion on the heat transfer rate for Re=3x10^{6}.

		Pr=0.7		Pr=5.0	
λ	°	Nu	$Nu/Nu_{\lambda=0}$	Nu	$Nu/Nu_{\lambda=0}$
0	0	114.1	1.0	190.6	1.0
0.1	17.8°	117.8	1.032	194.1	1.018
0.2	34.9°	120.1	1.053	197.0	1.034
0.3	50.4°	121.1	1.061	197.7	1.037
0.5	76.3°	122.0	1.069	197.5	1.036
0.7	95.4°	122.5	1.074	196.2	1.029
1.0	115°	123.4	1.082	192.8	1.012

Note: ° here is the inclination angle of the turns created by increasing the pitch.

Table 2.2 Effect of torsion on the heat transfer behaviour at different flow rates.

	Pr=0.7			Pr=5.0		
Re	λ=0	λ=0.3	λ=1.0	λ=0	λ=0.3	λ=1.0
2x10^{4}	88.0	90.1	90.8	133.3	135.5	132.0
3x10^{4}	114.1	121.1	123.4	190.6	197.7	192.8
5x10^{4}	151.6	175.4	180.3	285.6	314.8	305.2

Both tables indicate that the effect of increasing the pitch is to increase the heat transfer at first. In the case of air, Nu continues to increase, at least up to λ=1.0. One would expect a decrease at still higher λ, since the straight-tube condition would be approached. For water, there seems to be a maximum Nu somewhere near λ=0.3. The λ at which Nu is a maximum might be expected to be smaller for higher Pr fluids. Table 2.2 seems to indicate that the λ maximum of Nu shifts towards higher values at higher Re, presumably to some limiting value.

2.3.3 Current Approach to Design of Helical Exchangers

Jeschke's equation (eq. 2.1) has elicited substantial controversy. On the one hand, Patil et al. (1982), Perry's Handbook of Chemical Engineering (1984) and Haraburda (1995) all suggest that the tube-side heat transfer coefficient (h_i) be computed according to equation 2.1, using the Seider-Tate relationships to obtain h_{st} for the corresponding straight-tube case. The Seider-Tate relationship that applies to Re>10,000 (fully-developed turbulent flow), 0.7<Pr<700, and L/D>60 is:

$$Nu_{st} = 0.023\ Re_{st}^{0.8} Pr_{st}^{1/3} (\mu_b/\mu_W)^{0.14} \qquad (2.20)$$

where, μ_b and μ_W are the bulk fluid viscosity and the viscosity at the wall, respectively, L is the length of the straight tube and D is its inner diameter. For laminar flow and ($Re_{st}PrD/L$)>10, the straight tube Seider-Tate expression is:

$$Nu_{st} = 1.86\ (Re_{st}Pr_{st})^{1/3}(D/L_{st})^{0.33} (\mu_b/\mu_W)^{0.14} \qquad (2.21)$$

Jeschke's correction factor was put in doubt by Seban and McLaughlin's (1963) experimental work, and then severely criticized by Rogers and Mayhew (1964). Interestingly enough, eleven years earlier, the Handbook of Heat Transfer (Roshenow and Hartnett, 1973) made no mention of Jeschke's equation. Rather, it suggested equations for laminar flow developed by Mori and Nakayama (1965), and equations for turbulent flow based on the works of Ito (1959), Seban and McLaughlin (1963) and Rogers and Mayhew (1964).

Shah and Joshi (1987) noted that there are about 15 different experimental and theoretical correlations for the ratio of the Nusselt number for heat transfer inside a coil to that inside a straight tube. They also calculated them for various combinations of Re and a/R, concluding that the Nusselt numbers for coils with a/R in the range of 0.01 to 0.1, are 10-30%

higher than for a straight tube, and that the various correlations give results within ±10% when $Re>10^4$. The authors recommend the following correlations for the specified conditions:

a) Schmidt's correlation valid for $2x10^4<Re<1.5x10^5$ and $5<a/R<84$ developed from data on air and water with the assumption of axially constant heat flux and peripherally constant wall temperature:

$$Nu_c/Nu_s = 1.0 + 3.6\{1-(a/R)\}(a/R)^{0.8} \qquad (2.22)$$

b) Pratt's correlation valid for $1.5x10^3<Re<2x10^4$, based on water and isopropyl alcohol:

$$Nu_c/Nu_s = 1 + 3.4(a/R) \qquad (2.23)$$

c) Mikheev's correlation for $a/R<0.167$ is recommended to account for the temperature-dependence of fluid properties:

$$Nu_c/Nu_s = \{1 + 3.54(a/R)\}(Pr_m/Pr_w) \qquad (2.24)$$

where, 'm' refers to properties at bulk mean fluid temperature, and 'w' refers to properties evaluated at the wall temperature.

III. PRELIMINARY STUDY

3.0 Introduction:

Many experimental and theoretical papers have reported on convective heat transfer in a circularly curved tube, and have shown that secondary flow resulting from the centrifugal force causes the heat transfer coefficient to be significantly higher.

Understanding the flow phenomena through helical coil tubes and its influence on heat transfer aspects and comparing the results with that of a similar straight tube setup are the objectives of the preliminary work:

To achieve the above objectives the following were done:

1) a helical and straight tube heat exchanger was built to study the flow behavior of liquid.
2) the heat transfer rate in a helical tube was studies to quantify its enhancement compared to that of a straight tube setup operating under similar conditions.

The key issue in the design of the processor is the computation of the heat transfer coefficient, as some data, parameters and factors which are essential for calculating the heat transfer coefficients as they are unknown. Experiments were conducted to have an understanding of the subject for further research on the determination of heat transfer coefficients in a helical tube and of similar dimension straight tube setup with similar process parameters. The effect of

I) shape of the tube as coil parameter and

II) flow rate of the target fluid through the coil on overall heat transfer coefficient were examined.

III) influence of temperature of water in the bath on overall heat transfer coefficient was also examined.

3.1 Materials and Methods:

Experimental setup for the study was fabricated at the Agricultural & Biosystems Engineering department workshop, McGill University.

3.1.1 Helical heat exchanger:

The setup consisted of a helical coil with 10 turns. Coils were manufactured in India. The tube had 15.7 mm internal diameter (i.d), with a wall thickness of 1.2 mm. When stretched, the tube was 6.38 m long. The helical diameter of the coil was 203 mm. The coil was formed from initially straight tubing of copper. Fine sand filled the tube before bending, to preserve the smoothness of the inner surface and this was washed with hot water after the process. Care was taken to see that no ellipticity of the coil was there during the bending process. The length of the coil is calculated using the formula $L = \pi DN$. Required pitch of the coil was obtained using plexi glass spacers with a length equal to the pitch of the coil required. Coil used for the experiment was mounted to a rectangular mild steel plate with the help of swage lock fitting. The inner diameter of the fitting was equal to the inner diameter of the coil. This prevented any disturbance to the flow pattern. Rubber gasket was glued on both side of the mounting plate and also on to the water bath container coil holder. This prevented leak of water from the water bath while running the experiment. Teflon coating was removed from top of the thermocouple. The tip of the thermocouple was soldered and was inserted into the predrilled hole on surface of the coil. Five minute epoxy was used to glue the thermocouple to the coil which prevented any leak of the processing fluid from the heat exchanger into the water bath and vice versa.

3.1.2 Straight tube heat exchanger:

The system consists of a copper tube of i.d 17 mm of length equivalent to that of the stretched length of the helical coil of helix diameter 203 mm with 10 turns. As the coils were manufactured in India, similar i.d tube was not available in Canada hence this difference in i.d of the straight to coil tube. The conditions in this setup are faithful to those of the helical system.

3.1.3. Constant Temperature Water Bath for Straight Tube Heat Exchanger:

Consists of a smooth mild steel pipe of 1287 mm diameter and 6 mm thick and the length being equal to the stretched length of the helical coil of similar diameter and of helix diameter 203 mm. Two electrical heating coils of capacity 2,400 W each mounted at the bottom of the water bath supplied energy to heat the water in the bath. A CN9000A model PID miniature auto-tune temperature controller (Omega Engineering Corporation, Stamford, CT) maintained temperature of the water in the bath. Insulation to the water bath was provided by fiber glass wool and was surrounded by galvanized steel sheet.

3.1.4. Constant Temperature Water Bath used for Helical Heat Exchanger for preliminary study:

A cylindrical mild steel container of dimension 450 mm dia and 600 mm length was used as the constant temperature water bath. Opening was provided on one side of the cylinder through which the coil could be inserted into and out of the water bath. A 4,800 W electrical heating coil mounted at the bottom of the water bath supplied energy for heating the water in the bath. A CN9000A model PID miniature auto-tune temperature controller (Omega Engineering Corporation, Stamford, CT) maintained temperature of the water in the bath. Insulation to the water bath was provided by fiber glass wool and was surrounded by mild steel sheet.

3.2 Experimental Design:

The experimental design used for running the experiment is presented in Table 3.1 below. One coil was used for the experiment. One radius of curvature of helix with no pitch was used to find the influence of variables on heat transfer for this preliminary study.

Table 3.1. Experimental design

FACTOR	LEVELS	DESCRIPTION
Diameter of the tube	1	15.7 mm
Diameter of the helix	1	203 mm
Pitch if helix	1	No pitch
Bath temperature	1	40 C
	2	50 C
Flow rate	1	5 l/min
	2	15 l/min
	3	25 l/min
Model liquid	1	Water stored in a reservoir from tap

3.3. Heat Transfer Experiments:

The helical and straight tube heat exchangers described above were used for conducting the experiment. Target fluid from mains stored in a feed tank was pumped into the heat exchanger placed inside the constant temperature water bath using positive displacement pumps of three different capacities.

3.3.1. Heat transfer coefficient calculation:

The energy balance for the convection heating of a liquid being heated by the medium of constant temperature water bath can be derived by equating the rate of heat that is being transferred to the liquid to the rate of accumulation of heat within the liquid.

$$\dot{m} * C_p * (T_{out} - T_{in}) = A * h_t * \{(T_{ba} - T_{in}) - (T_{ba} - T_{out})\} \qquad (3.1)$$

where, T_{ba}= temperature of water in the bath,

T_{in}= temperature of inlet water,

A = inside area of the pipe,

Transient temperature of the processing fluid was monitored during the experiment and the overall heat transfer coefficient 'h_t' was determined using equation 3.1 with the following assumptions:

1) The flow field is fully developed before heat transfer starts. In what follows, the expression tube inlet will imply the initiation of heat transfer with velocities already developed.
2) Temperature distribution along the length of the coil is constant in time.
3) Free convective heat transfer from water bath to the coil.
4) The fluid properties are constant.
5) Viscous dissipation of energy is negligible.

3.4 Results and discussion

3.4.1 Temperature profile of the processing fluid inside the coil:

Figure 3.1 below shows the temperature profile of the target fluid observed over a period of about 18 minutes. Experiments were run for a very long period to assert that the system had achieved steady state. It is shown that the gain in temperature by the target fluid remained almost constant over experimental period. This explains that the temperature of water inside the bath was constant and hence the surface temperature of the coil remained constant through out the experiment. Also the surface temperature of the coil measured at the beginning of first turn and at the end of the tenth turn has remained constant exhibiting that the setup had attained a steady state through out the experimental period.

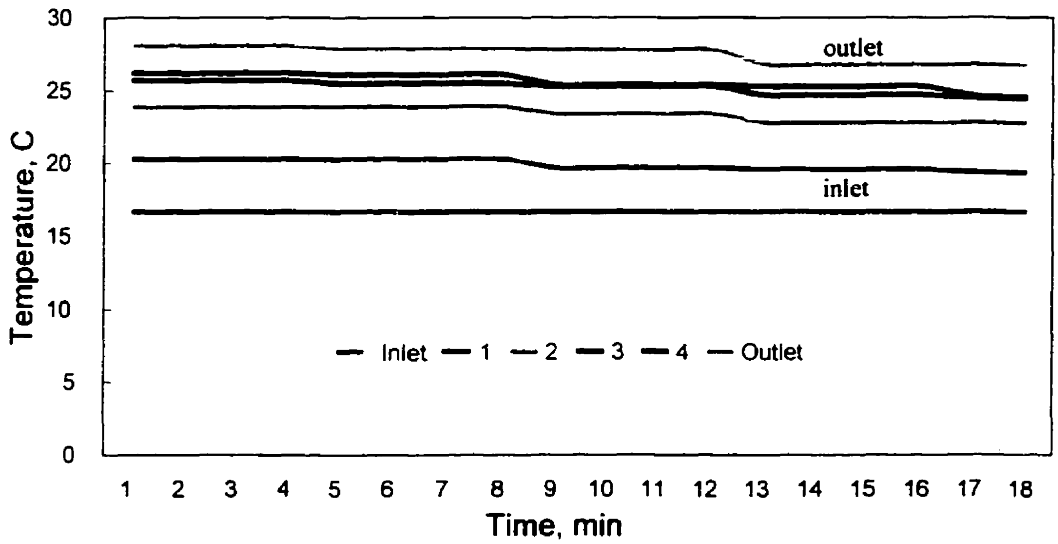

Figure 3.1 Time-temperature profile of the target fluid .

Numbers 1, 2, 3 and 4 in figure 3.1 indicate the thermocouple position on turn no. 1, 4, 7 and 10 of the coil.

3.4.2. Rise in temperature of the target fluid:

Rise in temperature of the target fluid was greater for bath temperature of 50 °C both in case of helical and straight tubes. Difference in temperature of the target fluid between the inlet to outlet was dependent on the residence time of the fluid inside the heat exchanger. At highest flow rate of 25 l/min as the residence time of the liquid was shortest, rise in temperature was very low (Figure 3.2). With the present setup a higher water bath temperature could not be obtained because of the limited heat input to the system. Additional heat input was necessary to study the effect of bath temperature on heat transfer. Since water was taken as a model fluid, the efficacy of the heating medium used could be compared with respect to the overall heat transfer coefficient. An increase in flow rate from 5 to 15 l/min resulted in an increase in h_t of the tube for both helical

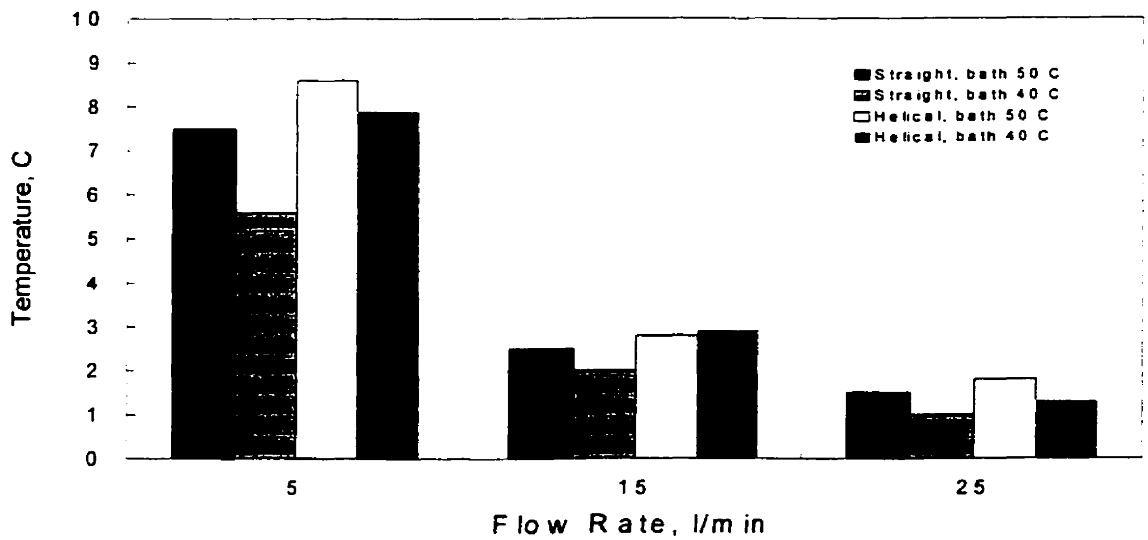

Figure 3.2 Rise in temperature of target fluid under different conditions.

and straight tubes. A decrease in overall heat transfer coefficient was observed at flow rate of 25 l/min in both helical and straight tube for a bath temperature of 40 C (Figure 3.3). This flow rate is too high for the length of tube used, resulting in a very short residence time. Hence, very small rise in temperature was gained by the target fluid. Lower h_t at very high flow rate may also be attributed to experimental uncertinities because of the limitation of the precision with the data acquisition system used.

Statistical analysis of the data showed that the heat transfer coefficient was influenced by the flow rate of the target fluid inside the coil ($p \leq 0.05$) and also the shape of the coil i.e curvature of helix or the straight tube at $p \leq 0.05$ level. Data gathered from experiments were used to calculate overall heat transfer coefficient in terms of dimensionless Nusselt number. A nonlinear regression was performed using the data gathered with helical coil at two temperatures and three flow rates which yielded the following Nusselt correlation equation for water as processing fluid. Slope and constant was obtained by the regression equation.

$$Nu = 0.7058 * Re^{0.2032} * Pr^{0.33} \quad (3.3)$$

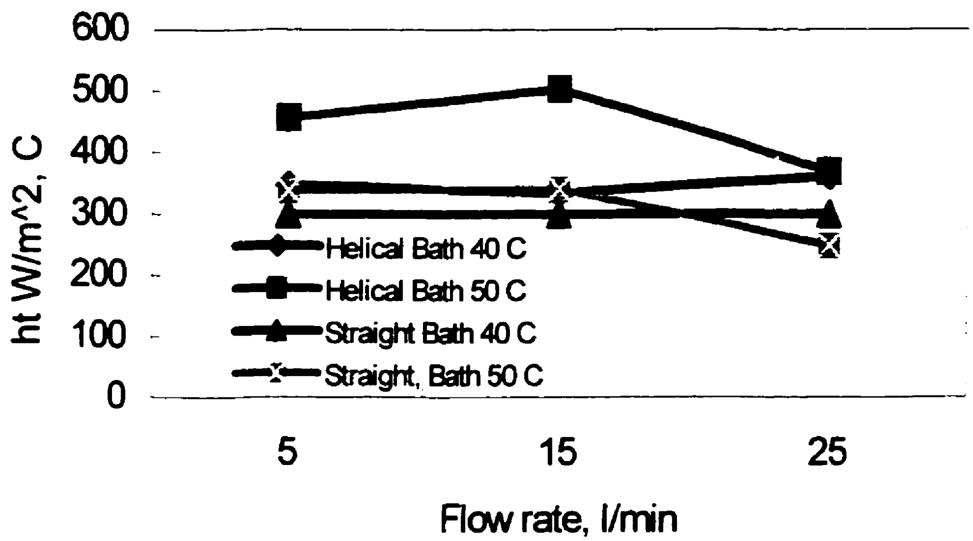

Figure 3.3 "h_t" as influenced by the flow rate and shape of the tube at different bath temperatures.

This correlation (R^2 = 0.93) developed for preliminary results has its own limitation since only one tube dia, one helix dia, and one pitch at three different flow rates were used to get the dimensionless relationship. Experiments were not replicated as each set was run for a very long period of time of about 18 min. This represents that each experiment was run as a continuous process and hence replications were not necessary.

3.5 Conclusion :

This study indicated that:

- Shape of the tube and the temperature of water in the bath influenced the heat transfer coefficient.
- Temperature rise of the target fluid was almost constant through out the study period showing that the system had attained steadystate and hence replication of experiment was not necessary.

Based on the preliminary study it was felt necessary to improve the hot water bath and to have different combinations of variables by :

- Having additional heat input to the system to get elevated temperature of water in the bath.
- Helical-coil tubes of different diameter, helix radius and pitch are to be tried to better understand the influence of coil parameters on heat transfer.
- As the flow rate selected for the experiment was high it was decided to have lower flow rates of 4, 8 and 12 L min^{-1}.
- To circulate the water in the bath and see its effect on heat transfer.

To understand the process phenomena better it was necessary to analyze the data gathered in terms of outer, inner and total heat transfer coefficient.

I V MATERIALS AND METHODS

4.0 INTRODUCTION

The experimental setup used for this research underwent certain modifications after the preliminary set of experiments (Chapter III). They will be pointed out during the descriptions presented in this chapter.

4.1 Heat exchange and pumping setups

In the preliminary study, heat exchange in a helical coil was compared with that in a straight tube of the same length. The straight tube setup is shown schematically in Figure 4.1, while that for the helical coils is shown in Figure 4.2 and Figure 4.3 a-f shows the set up used for the equipment.

4.1.1 Straight Tube Heat Exchanger:

Schematic of the setup is given in Figure 4.1 and the description of the straight tube heat exchanger is given in the chapter III.

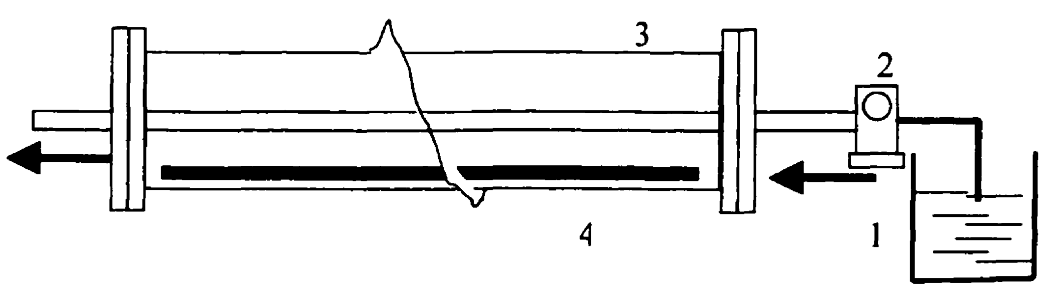

(1) Constant head reservoir to hold processing fluid, (2) Positive displacement pump, (3) Constant temperature water bath, (4) Heating element

Figure4.1 Schematic of Straight tube heat exchanger setup

4.1.2 The Helical Coil Heat Exchangers:

Four helical coils were ordered from a manufacturer of curved tubes in Bombay, India. Two were made from 13.5 mm i.d. copper tubing, 1.2 mm in thickness, while two others were made from 15.7 mm i.d. copper tubing, also 1.2 mm in thickness. All coils had 10 turns. Two of the coils (one of each i.d.) were of 203 mm helix diameter and a stretched length of 5.15 m. The two others were of helix diameter 305 mm and a stretched length of 6.9 m. All in all, this gave four different D:d

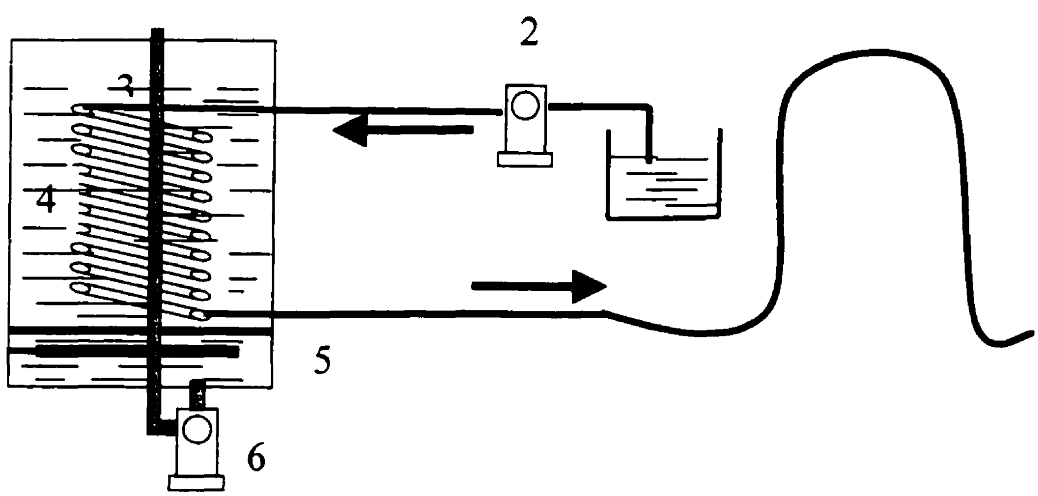

(1)Constant head reservoir to hold processing fluid, (2) Positive displacement/submercible pump for processing fluid, (3) Constant temperature water bath, (4) Helical heat exchanger, (5) Heating element, (6) Positive displacemant pump for recirculating water from bath.

Figure 4.2 Schematic of Helical coil heat exchanger setup.

ratios – 13:1, 15:1, 19.5:1 and 22.5:1.The slanted outer diameter D_s (Fig. 4.3) was measured for each turn using a vernier caliper and the helix coil diameter was calculated using the equation (Ali, 1994)

$$D = \frac{\sum_{i=1}^{N} \sqrt{D_s^2 - \left(\frac{p}{2}\right)^2}}{N} \qquad (4.1)$$

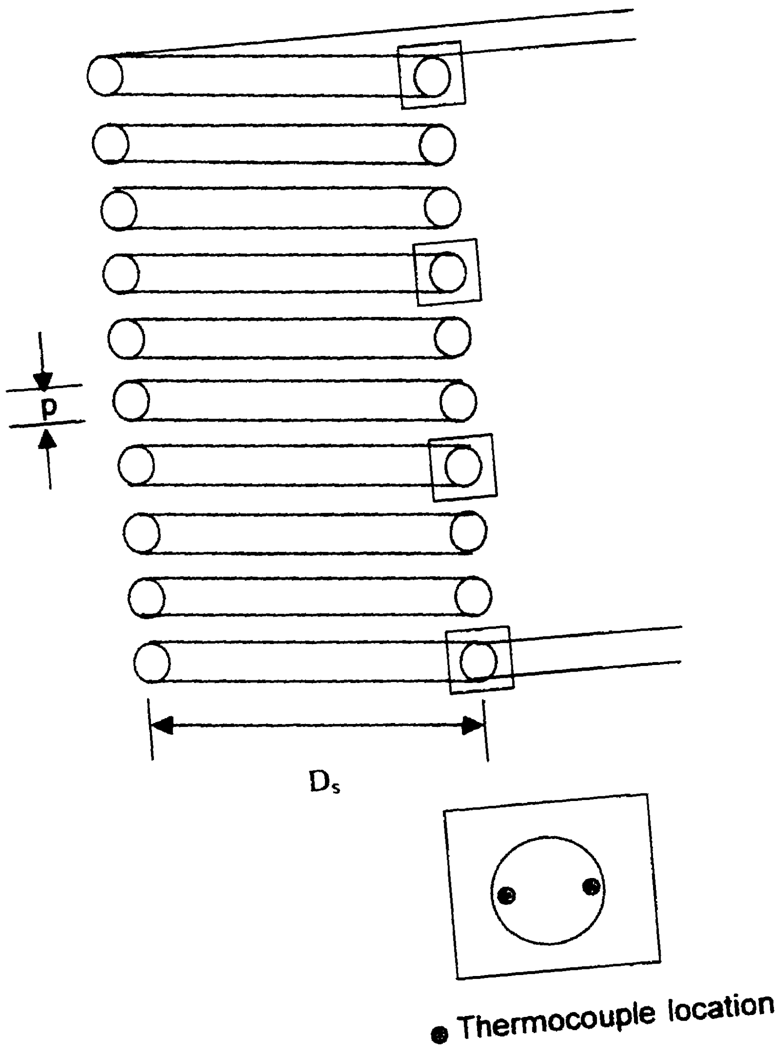

Fig. 4.3 Schematic of Helical coil

Figure 4.4 a Mounting of the coil inside the water bath

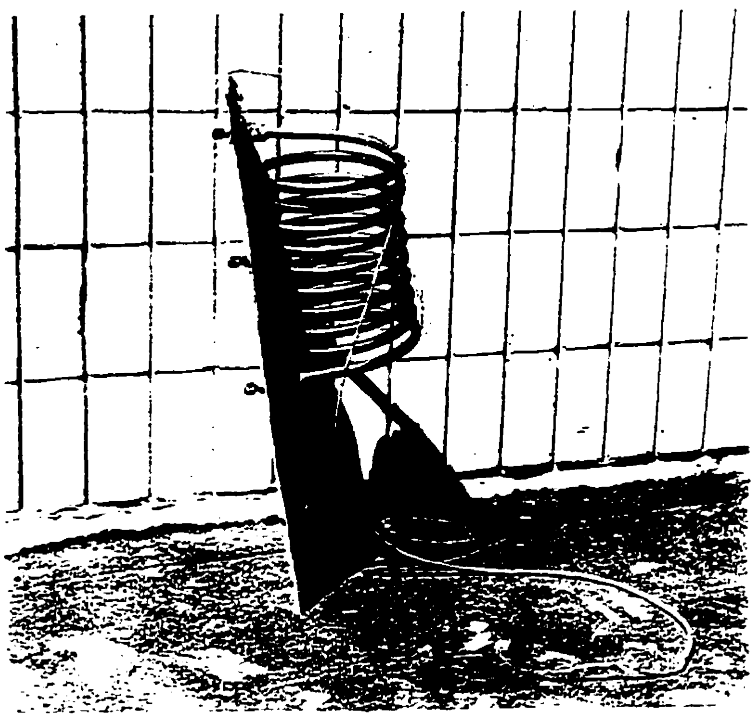

Figure 4.4 b Swage lock fitting to the coil and the coil holder

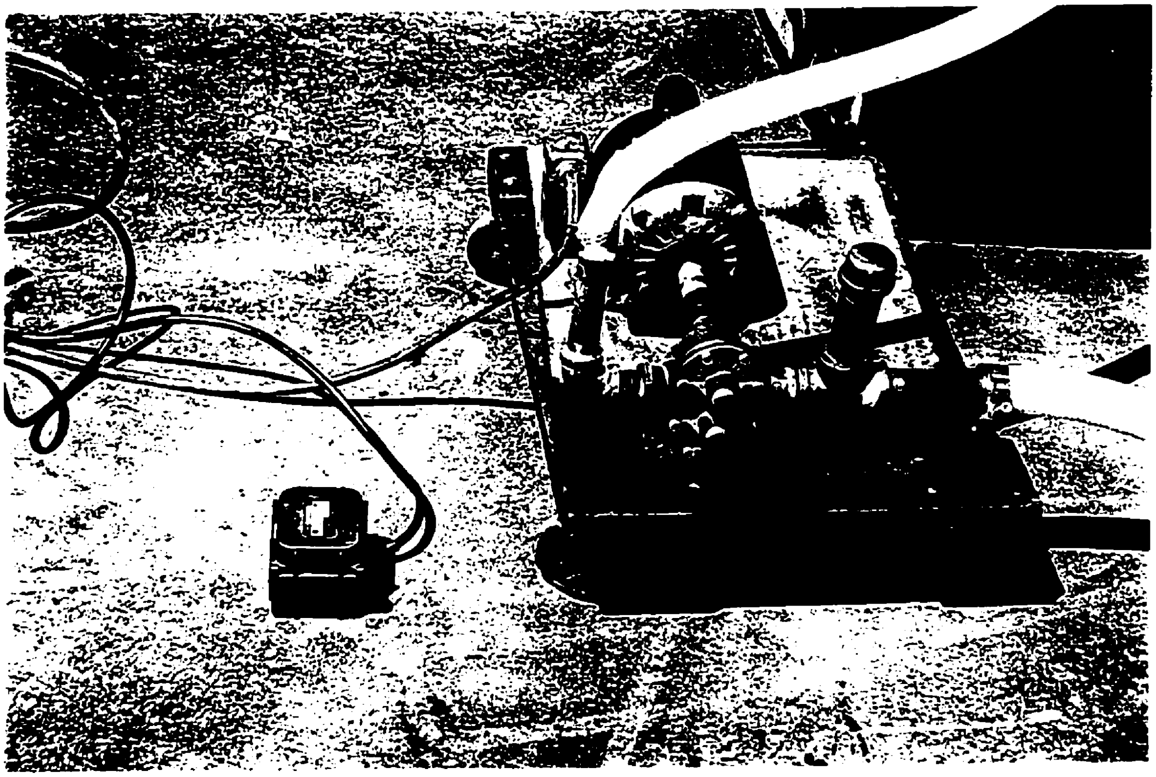

Figure 4.4 c Positive displacement pump used to recirculate water in the bath

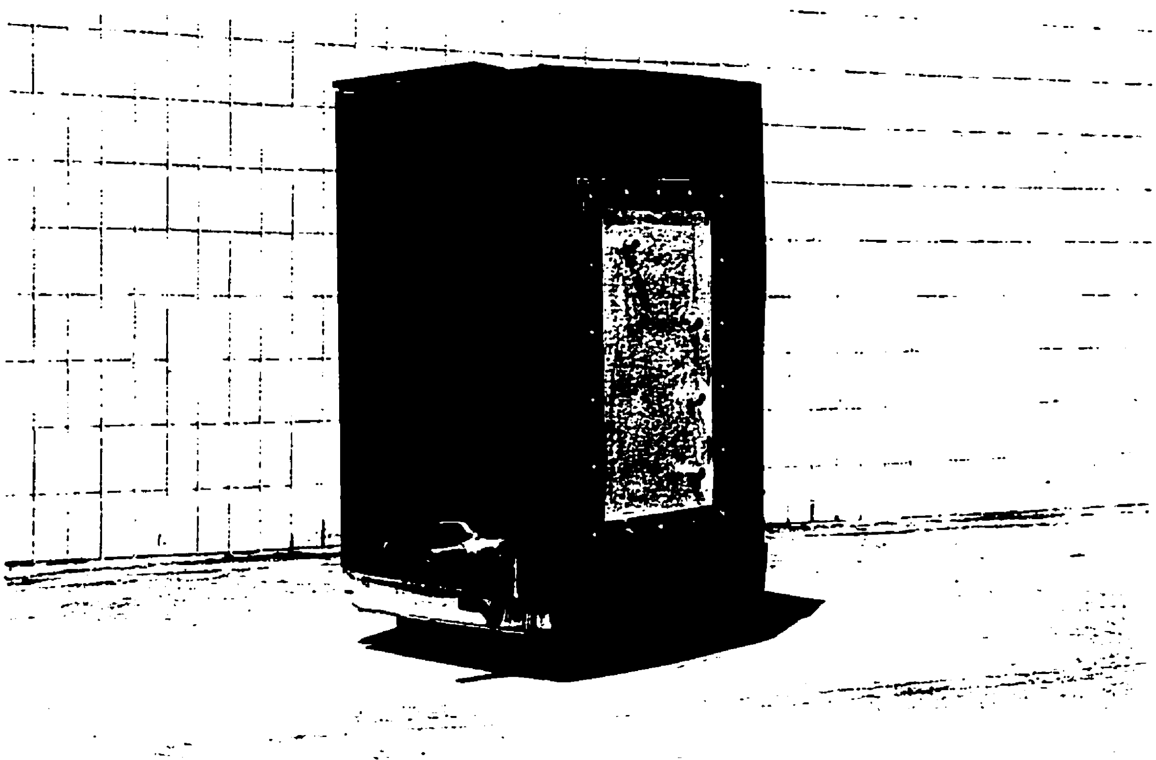

Figure 4.4 d Water bath with front cover

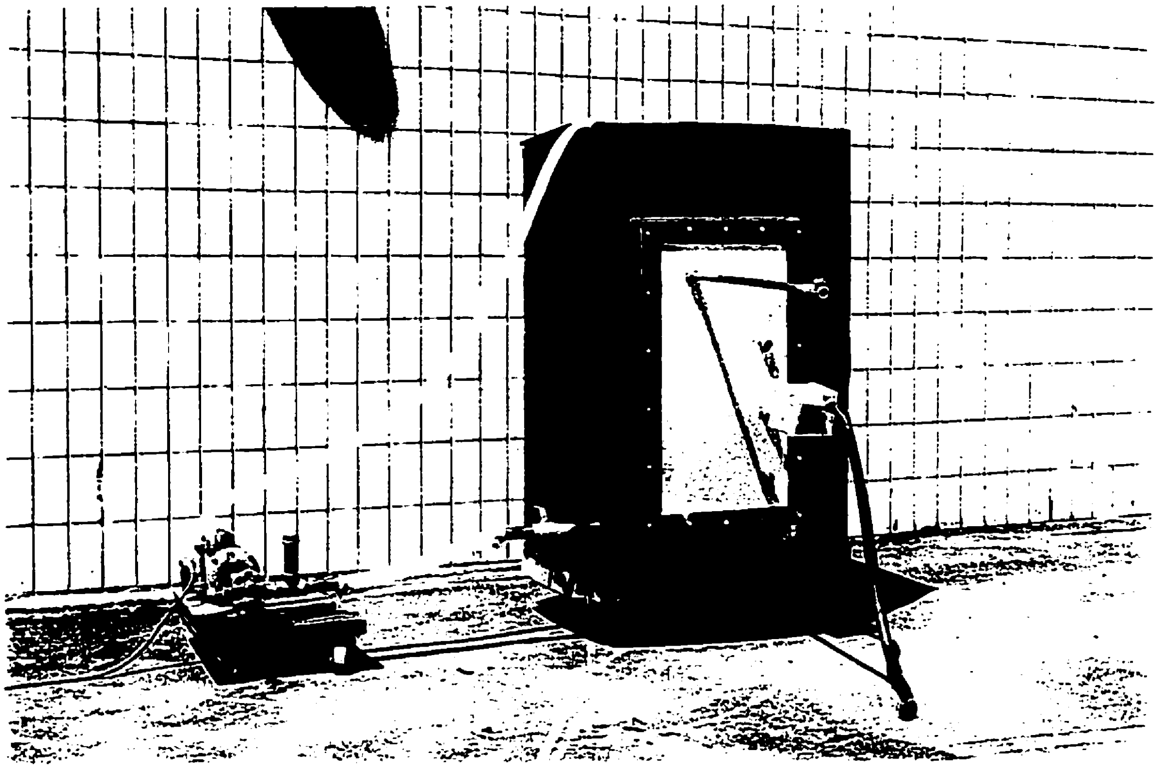

Figure 4.4 e The setup for Forced circulation system

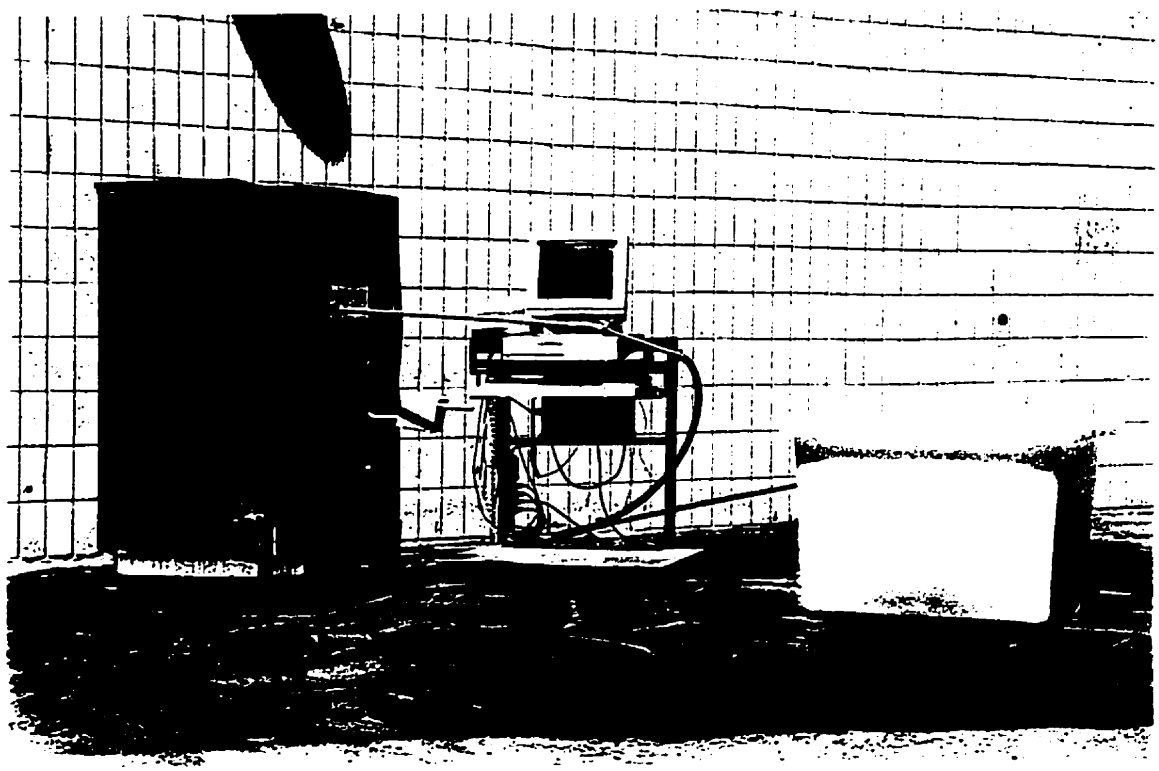

Figure 4.4 f The setup for Forced circulation system

The coil length may be calculated using the formula $L = \pi DN$. The pitch of the coils was adjusted as needed using plexiglass spacers. In this study, no pitch or 0-pitch refers to the condition in which turns are separated by a millimeter. One-pitch indicates that the spacing between turns is equal to one tube outer diameter (o.d.) and two-pitch refers to a spacing of two o.d.'s.

4.1.2.1 Mounting of the coil to the holder:

For each experiment, the required coil was mounted on a rectangular mild steel plate with swage lock fittings. The inner diameter of the fitting was equal to the inner diameter of the coil. This prevented any disturbance to the flow pattern of the fluid in question. Rubber gaskets were glued on both side of the mounting plate and also on to the surface of the water bath container holding the coil. This kept water from leaking out of the bath during test runs.

Chromium-aluminum thermocouples were used for temperature measurements. For all experiments, temperatures were measured at turns 1, 4, 7 and 10 (from inlet to outlet) at two points on the surface of the tube, one on the inner periphery and the other on the outer periphery (cross-sectional view – Figure 4.3). This was done by drilling small holes in the tube in which the thermocouples could be inserted. The incoming fluid temperature was measured 20 mm from the point at which the copper tube meets the water bath wall. The temperature of the processed fluid was measured 20 mm after the outlet (Figure 4.2). Coil surface temperatures were taken inside the bath at the mid-points of the first and last turns. The temperature distribution in the bath was also monitored with three other thermocouples located at different depths in the water bath (1/4, 1/2, 3/4th depths), 10 cm from the coil.

4.1.3 Constant Temperature Water Bath for Helical Heat Exchanger:

For the experiments described in Chapters V, Vi and VII, a larger water bath was used. It was rectangular and made of 20 gauge galvanized iron sheet. The dimensions were 600x600x1200mm. Four electrical heaters of 5000 W each were fixed at the bottom. Two were on all the time and two others were controlled by the PID as needed to maintain constant temperature. The insulation was a 50mm thick polyurethane foam (R-10), covered with galvanized iron sheet.

This water bath was also equipped with a positive-displacement gear pump driven by a 1/3 hp electric motor. The motor was switched "OFF" for natural convection experiments and was "ON" for forced convention studies.

4.1.4. Pumps used for helical coil exchangers:

For the preliminary study, the three positive displacement pumps of capacity 4, 8 and 12 l/min were used to pump water through the helical coil exchangers. For the experiments described in Chapter VI, submersible pumps were used since the processing fluid is water. For the experiments described in Chapter VII, oil was used as the processing fluid. A positive displacement pump driven by a variable speed motor was used for pumping the oil to the exchanger.

4.1.4.1 Pump discharge verification and variable-speed calibration

The discharges for the positive-displacement and submersible pumps used for water as the processing fluid were checked as follows. The processing fluid was kept in a constant-head reservoir. Pumps were operated at full capacity for a known period of time. The time of discharge was measured using a stop-watch with 1/100 s accuracy. The discharged fluid was collected in a container and its mass was determined using a balance. This gave real time discharge of fluid from the pump.

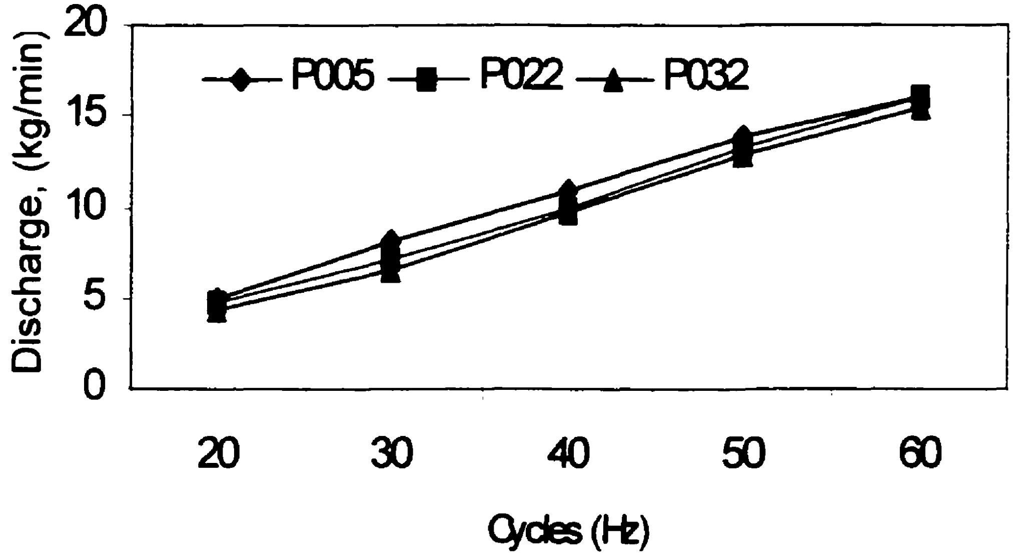

Figure 4.4 Calibration of Variable speed motor driven pump.

The pump operated by the variable speed motor used in the experiments with oils was calibrated in a similar fashion, except that the motor speed was adjusted to 5 cycles (20, 30, 40, 50, 60 Hz) and calibration curves drawn for each of the oils (Figure 4.4).

4.2 Data Acquisition System

A 12-channel Scan-log (Cole-Parmer) data acquisition system was used to record the thermocouple outputs. Readings were captured every 15s. Data were transferred to a Packard Bell personal computer. All data were saved in delimited ASCII files.

4.3 Test Materials

The heat carrier in the bath was water in all the experiments. The fluids flowing through the tube to be processed through the exchangers were water and the three different base oils supplied by MS Petro Canada. The properties of the oils were given by the supplier and are listed in Table 4.1. Since the information on viscosity was incomplete, viscosities were determined in the laboratory for different temperatures (section 4.3.1) and used in the calculations. The relevant physical properties of water (density, thermal conductivity, viscosity) over the range of temperatures encountered in this research were taken from tables in (Ozisik, 1985) and interpolated linearly to correspond to expectations at intermediate temperatures.

Table4.1 Physical Properties of Base Oil

Base Oil	Property	ASTM Test Method	Typical Values
	Density,lbs/USG at 59 F	D1298	7.08
	Appearance		
	Colour, ASTM	Visual	clear, bright
P005	Flash point(F)	D1500	<0.5
	Bio degradability	D92	284
	%CEC,L33-A-93		88.4
	Density, lbs/USG at 59 F	D1298	6.91
	Appearance		
P022	Colour, ASTM	Visual	cloudy
	Flash point (F)	D1500	<0.5
	Bio degradability	D92	284
	%CEC L33-A-93		NA
	Density, lbs/USG at 59 F	D1298	7.18
	Appearance		
	Colour, ASTM	Visual	dark cloudy
P032	Flash point (F)	D1500	<0.5
	Bio degradability	D92	374
	%CEC L33-A-93		68.0

Source:Petro Canada Base Oil Sales information sheet

4.3.1 Viscosity Measurements on Oils

Three petroleum base oils of different viscosity were heated in this setup. The oils were purchased from Thermal Lube Inc. (Pte. Claire, Quebec, Canada), and were items P005, P022 and P032. These oils are used in the cosmetic industry and could also be used as lubricants in the food processing industry. Dynamic Viscometric studies for the mineral oil were made using a Haake RV20 rotational viscometer (Haake Mess-Technik GmbHu. Co., Karlsruhe, Federal Rep. Germany) equipment. The measuring head was an M5 OSC, the rotor was MV1 (20.04 mm OD and 60 mm height) and the concentric cylindrical cup assembly was of 21.00 mm ID. Controlled temperature water was circulated through the jacketed assembly to maintain constant temperature. The assembly was interfaced to a microcomputer for control and data acquisition. The test procedure is described below.

A sample was placed into the annular space between the two concentric cylinders of the system. The sample was then subjected to a simple harmonic (dynamic) shear from 0 to 500 s^{-1} in 5 minutes at a linearly increasing rate of 100 s^{-1}/min, followed by a decrease to 0 s^{-1} at the same rate. The torque (shear stress) was measured while the inner cylinder was rotating at a defined speed (shear rate). This cycle was repeated a few more times to see if there would be any structural breakdown resulting from up and down shear-cycles. Temperature effects on flow curves were evaluated from 20 to 80° C in increments of 10 ° C. All tests were replicated three times. The flow curves were evaluated by using the Newtonian model. The results of these tests are presented in Chapter VII.

It was found that the viscosities were substantially different (Figures 4.5 a,b), P005 having a viscosity at 20°C that is over an order of magnitude less than the others. The viscosity of the oils was also determined after they had been used in the experimental runs, and also in a heating/cooling experiment.

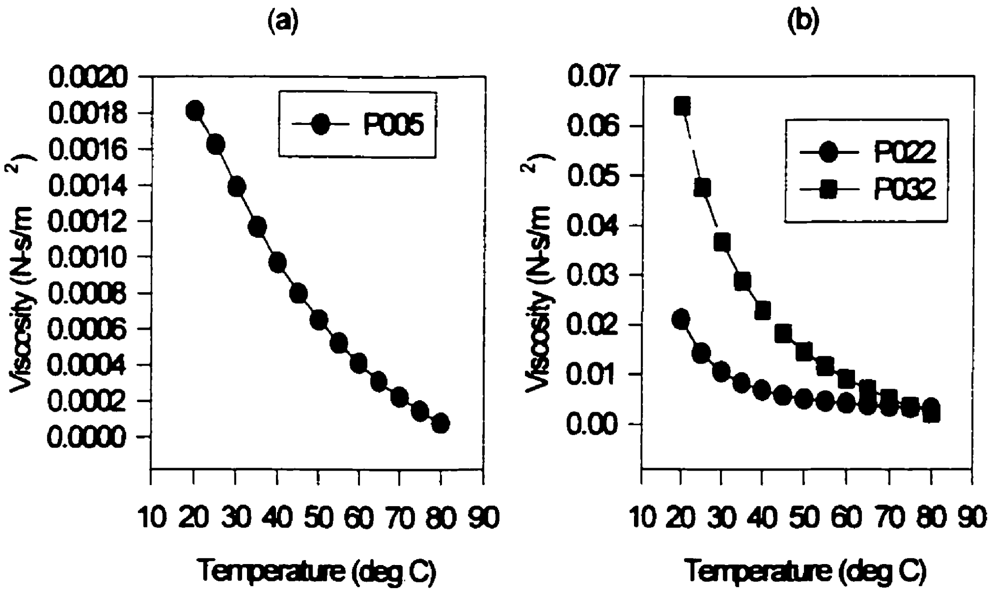

Figure 4.5 a, b. Visscosities of three different types of oil

4.3.2 Specific heat Measurements of Oils

The specific heat of the fluids was estimated in the laboratory using the thermal flask method. This involved mixing a known mass of the fluid, m_f, at a given temperature, T_f, with a known mass of water, m_w, at another temperature, T_w, and following the temperature change of the mixture until an equilibrium temperature, T_{eq}, is reached. The operation is carried out in a well-insulated flask, or thermos. The equilibrium temperature is then used to estimate the unknown c_{pf} through the equation:

$$m_w c_{pw} (T_{eq}-T_{w}) = m_f c_{pf} (T_f-T_{eq}) \qquad (4.2)$$

It was found that all three oils had c_p in the range of 1.7-1.8 kJ/(kg-°K). Unfortunately, it was not possible to carry out detailed study of the specific heat prior to running experiments, and it was necessary to assume that it was constant in the range of mean temperatures of the fluids (27-48°C). This likely introduced an error of 5-8% in the calculated heat transfer coefficients and Prandtl numbers.

4.4 Experimental Designs and Data Analysis

4.4.1 Experimental Designs

In the experiment involving water-to-water heat exchange in a natural convection water bath (no stirring or recirculation of bath water), the influence of coil geometry was studied at two bath temperatures (75 and 95°C) and three flow rates through the coils (4, 8, 12 L min^{-1}). The factors were: tube inner diameter (13.5 or 15.7 mm), helix diameter (203 or 305 mm), and pitch (none, 1 or 2). A full factorial with one replicate was conducted in this case.

The same design and factor levels were used in the study reported in forced-convection case (water recirculated in the water bath using a 1/3 hp-driven positive displacement pump). No attempt was made to characterize the flow conditions inside the water bath.

The experiment involving oils (Chapter VII) was an L_{27} orthogonal design to reduce the number of runs needed to study the relevant factors independently. This design was replicated once. As will be explained later, certain conditions regarding the parameter space were not met, which made the statistical analysis impossible. The possible analysis here was limited due to the large number of factors involved. The three fluids were heated in the coil under various conditions of water bath temperature, and fluid flow rate through the coil. The pitch of each coil was adjusted from minimal to 1 and 2 pitch. A total of 27 runs were conduced and the conditions are summarized in Table 4.2,. The design was an L_{27} orthogonal design in principle.

Table 4.2. Summary of heat transfer coefficients of oil experimental runs.

Tube Dia (mm)	Pitch (mm)	Helix Diameter (mm)	Temperature °C	Flow Rate (L/min)	Oil Type	Re (oil)	Pr (oil)
13.5	1	203	60	6	P005	7430	13
13.5	1	305	75	8	P005	8775	14.7
13.5	1	305	95	10	P005	18675	8.6
15.7	15.7	305	62	10	P005	6516	18.3
15.7	15.7	305	78	6	P005	6725	10.6
15.7	15.7	203	95	8	P005	5840	16.3
15.7	31.4	305	60	8	P005	5599	17
15.7	31.4	203	75	10	P005	6977	17
15.7	31.4	305	95	6	P005	7017	10.2
15.7	1	203	60	8	P022	634	146
15.7	1	305	75	10	P022	1070	108
15.7	1	305	95	6	P022	1022	67.6
13.5	13.5	305	60	6	P022	1220	76.6
13.5	13.5	305	75	8	P022	1405	88.8
13.5	13.5	203	95	10	P022	947	165
15.7	31.4	305	60	10	P022	855	135
15.7	31.4	203	75	6	P022	560	124
15.7	31.4	305	95	8	P022	1355	68
15.7	1	203	60	10	P032	244	464
15.7	1	305	75	6	P032	196	346
15.7	1	305	95	8	P032	423	213
15.7	15.7	305	65	8	P032	240	377
15.7	15.7	305	78	10	P032	436	258
15.7	15.7	203	95	6	P032	321	210
13.5	27	305	60	6	P032	347	263
13.5	27	203	75	8	P032	354	344
13.5	27	305	95	10	P032	811	187

4.4.2 Data Analyses

Statistical analyses were performed using Statistical Analysis System Software (SAS). Procedure GLM (General Linear Models) was used for all experiments except that on oils, for which procedure RSREG (Response Surface Regression) was used (SAS, 1988). Procedure NLIN (Non-Linear Regression) was used to estimate coefficients in power equations relating the various dimensionless numbers (Re, Nu, Pr, Dn). Further details on data analysis are provided in the appropriate chapters.

V EXPERIMENTS WITH WATER INSIDE COIL AND IN WATER BATH

5.0 Introduction

Two factorial experiments were conducted to study the heat transfer characteristics of helical coils with water as the target fluid and as the heat carrier in the bath. One of the experiments was performed with no circulation of the carrier fluid other than that caused by buoyancy due to heating from the bottom (heretofore referred to as natural convection water bath). The other was performed with circulation of the bath water through a hose that drew water from one bottom corner (near heaters) and deposited it at the opposite top corner (forced convection water bath). The flow rate through the recirculating hose was 20 L min^{-1}, resulting in an estimated free stream velocity in the water bath of the order of 0.001. Water discharged from pump was collected in a bucket for a known period of time. The mass of discharged water was taken to calculate the flow rate. Thermocouple locations were as described in Chapter IV.

The parameter space for both experiments involved all combinations of: a) two water bath temperatures (75 and 95°C); b) two tube diameters (0.0135 and 0.0158 m); c) two helix diameters (0.203 and 0.305 m); d) three pitch levels (0, 1 and 2); and e) 3 flow rates inside the coil (4, 8, 12 L min^{-1}). Thus, a total of 72 runs were made under each water bath regime (natural and forced).

The results and discussion are presented in four major sections. The first section consists of a comparison of heat transfer under the natural and forced convection water bath regimes and the relationships between the inner, outer and overall heat transfer coefficients. The influence of the control parameters on the inner and outer heat transfer coefficients is then discussed. The helical coil data are then placed in the light of presently used non-dimensional relationships (Nu=f(Re,Pr)) to estimate heat transfer in helical coils. Finally, the estimated heat transfer coefficients for three sections of the coils are presented and discussed. These involved estimates for the section from Turn 1 to Turn 4, Turn 4 to Turn 7, and Turn 7 to Turn 10. It was necessary to interpolate the coil surface temperatures at Turns 4 and 7, since there were not enough channels available for additional thermocouples.

5.1 Comparison of heat transfer under natural and forced convection water bath.

The comparisons presented here are based on the length of the coils from the inlet Turn one to the point of measurement at Turn 10. The inner heat transfer coefficients, h_i, were calculated on the basis of Log Mean Temperature Differences (LMTD) involving the temperatures at the outer surfaces of the coils, the inlet temperature and the average of the inner and outer peripheral temperatures at Turn 10 of water flowing through the coil. The overall heat transfer coefficients, h_t's, were based on the LMTD's involving the water bath temperature (control setting), the inlet temperature of the water flowing through the coil and the average inner temperature at Turn 10. The outer heat transfer coefficients, h_o's, were based on the LMTD's involving the water bath temperature (control setting) and the two temperatures on the outer surface of the coil.

5.1.1 Data reduction

The first step in the analysis was data verification. The raw data files from each run were viewed graphically with standard software (Microsoft Excel) and checked for spikes and other possible anomalies. All calculations were done on spreadsheets and the following checks were used:

a) LMTD's and their components (ie. ΔT_0, ΔT_L, ΔT_0-ΔT_L, $\Delta T_0/\Delta T_L$), were calculated and checked for inconsistencies such as negative temperature differences, differences at inlet ends being smaller than differences at outlet ends, and the ratio being equal to 1 or less.

b) The h_o's were back-calculated using the resistance relationship (eq. 1.1), not considering the fouling factors, to ensure the physical consistency of the data (a correspondence of near 1:1 would be expected between the back-calculated and observed h_o's if the temperature measurements were not flawed).

When inconsistencies did occur, they were usually caused by the thermocouples measuring the surface temperatures on the outside of the coil at turns 1 and 10. The readings at these locations were very close to, equal to, or higher than the set bath temperature on several runs. This could have been caused by poor contact between the thermocouples and the coil surface and leakage of bath water under the tape that was to insulate the thermocouple from the bath. Problematic runs were repeated.

The relationship between the measured and back-calculated h_o's is shown in Figure 5.1. The correspondence is excellent, although the observed values exceed the back-calculated values by about 5%. In performing this analysis, it was necessary to assume that the heat transfer coefficients were independent of the inlet water temperatures, which were not identical from run to run. The inlet water temperatures ranged from 13 to 22°C over the period needed to perform the full set of experiments.

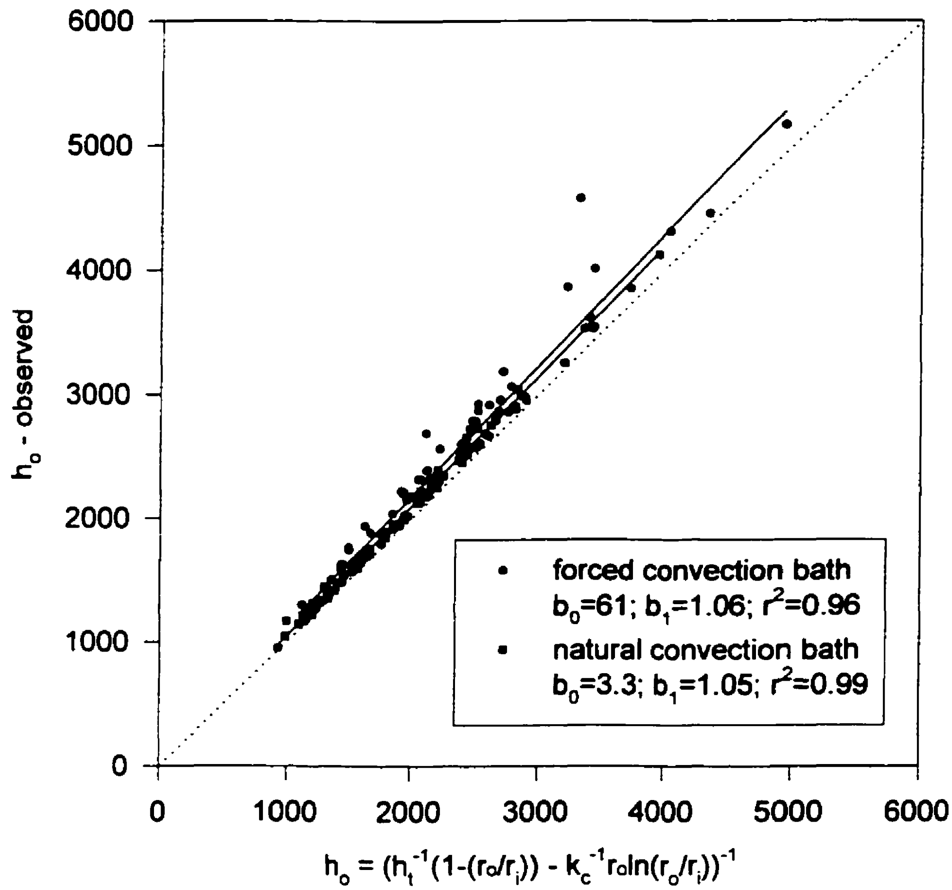

Figure 5.1 Correspondence between back-calculated and observed outside heat transfer coefficients for forced and natural convection water baths.

5.1.2 Influence of circulation in water bath on heat transfer

The heat transfer coefficients obtained in the water bath with natural convection are plotted against those obtained with the forced convection water bath in Fig. 5.2 to 5.4. The overall and outer heat transfer coefficients are clearly significantly lower in the case of the natural convection water bath (slopes are small and most points are below the 1:1 correspondence line in Figures 5.2 and 5.3). In the case of h_i (Figure 5.4), the points are more

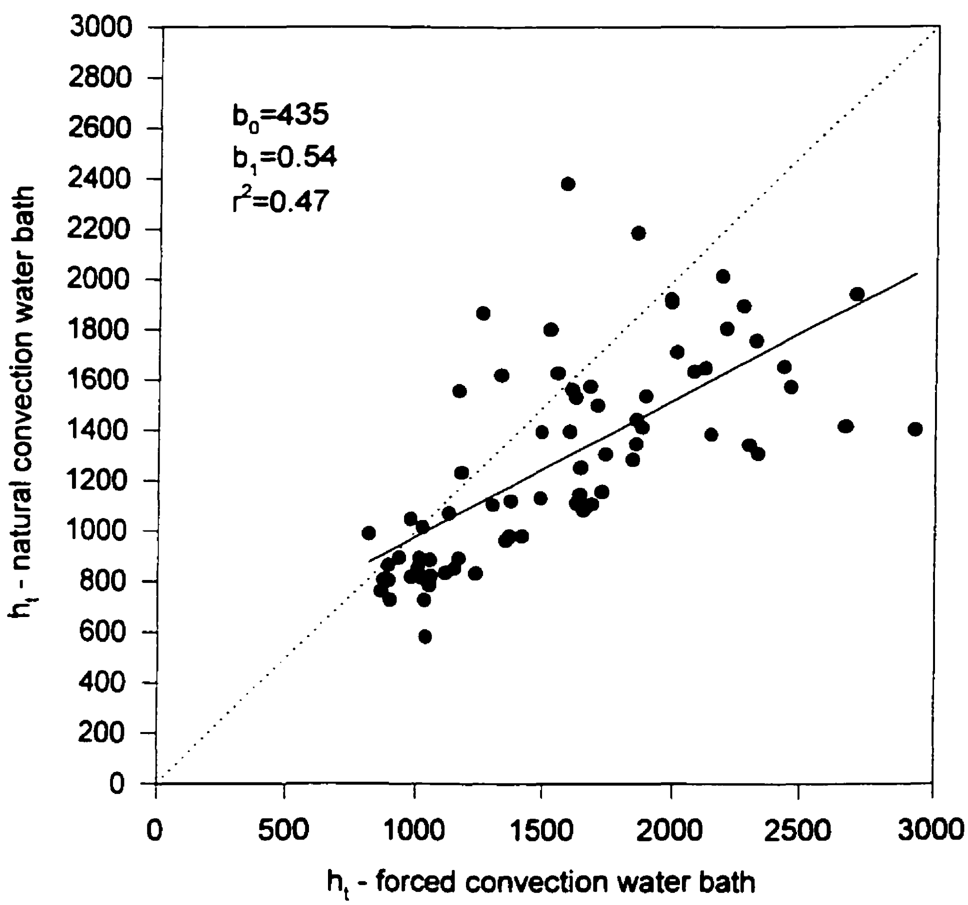

Figure 5.2. Comparison of overall heat transfer coefficients (h_t) obtained in natural and forced convection water bath.

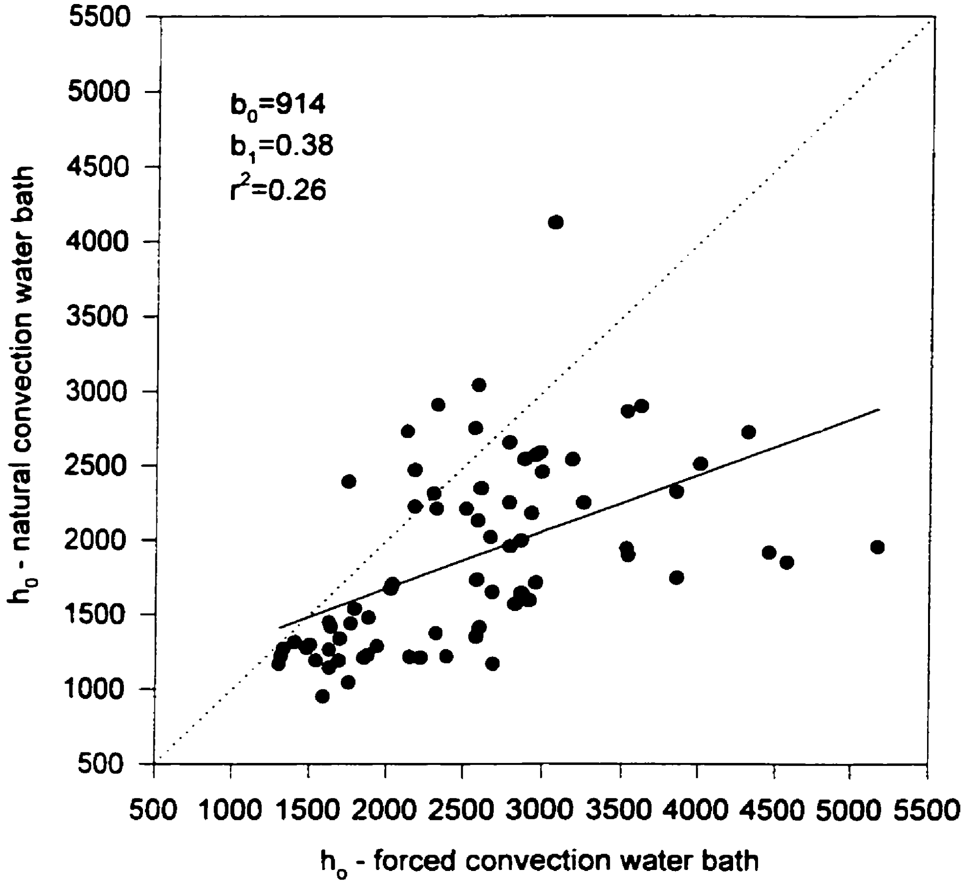

Figure 5.3. Comparison of outer heat transfer coefficients (h_o) obtained in natural and forced convection water bath.

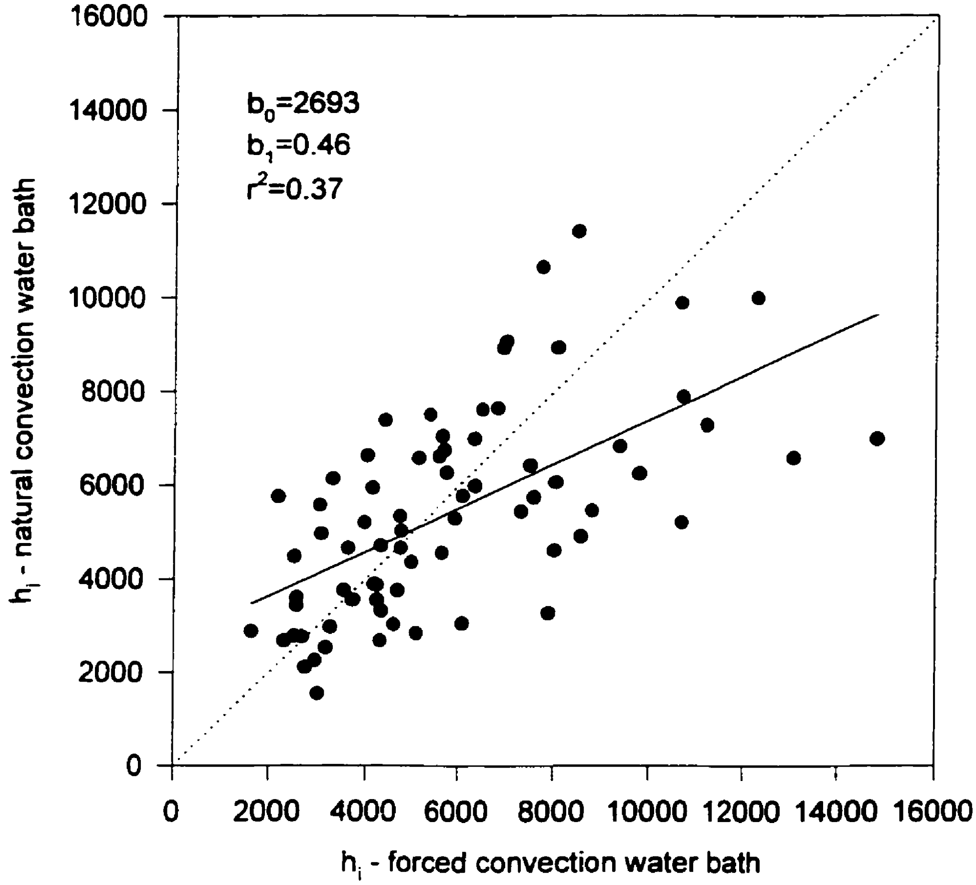

Figure 5.4. Comparison of inner heat transfer coefficients (h_i) obtained in . . . natural and forced convection water bath.

evenly distributed along the 1:1 correspondence line, although the slope of the least squares line is substantially less than 1.0. The t-tests summarised in Table 5.1 indicate that all heat transfer components (inner, overall and outer) were higher due to the water circulation. In the case of the inner heat transfer coefficient, h_i, the difference is significant only at the 0.1 level (ie. borderline).

Table 5.1. Summary of paired t-tests comparing heat transfer coefficients from natural convection and forced convection experiments (n=72).

	Natural Convection		Forced Convection		Joint Statistics		
	Mean	Variance	Mean	Variance	$r_{Pearson}$	t-cal	Prob>t
h_i	5413	4.7×10^6	5792	8.0×10^6	0.61	1.4	0.08
h_t	1284	1.6×10^5	1566	2.7×10^5	0.69	6.3	<<0.001
h_o	1879	3.9×10^5	2536	7.1×10^5	0.51	7.4	<<0.001

Thus, even though the velocity of circulated water near the coil was very low (0.001 m s^{-1}), this was sufficient to improve the outer heat transfer coefficient by 35% and the overall heat transfer noticeably (by 22%). One would expect that inducing greater mixing in the water bath would lead to even higher outside heat transfer and higher overall heat transfer, since in this setup, it was the outer heat transfer coefficient that was limiting. However, there was also an average increase of 7% in the inner heat transfer coefficient due to circulation in the water bath. Thus, one might expect that increasing the outer heat transfer should also lead to further improvement in the inner heat transfer.

The Pearson correlation coefficients between the three heat transfer components are summarised in Table 5.2, for the two water bath regimes. (Note: the Pearson product correlation coefficients are not to be confused with the coefficients of determination from the regressions given in the figures in this chapter).

Table 5.2. Pearson product correlations between inner, overall and outer heat transfer coefficients for natural and forced convection.

	Natural Convection		Forced Convection	
	h_i	h_t	h_i	h_t
h_o	0.80	0.97	0.42	0.82
h_t	0.92		0.81	

These indicate that the overall heat transfer can be expressed directly in terms of either the inner or outer heat transfer coefficient by linear equations (Figures 5.5a,b; 5.6a,b), h_o being somewhat more reliable. The relationships between the h_i and h_o are also shown for the sake of completeness in Figures 5.7a,b.

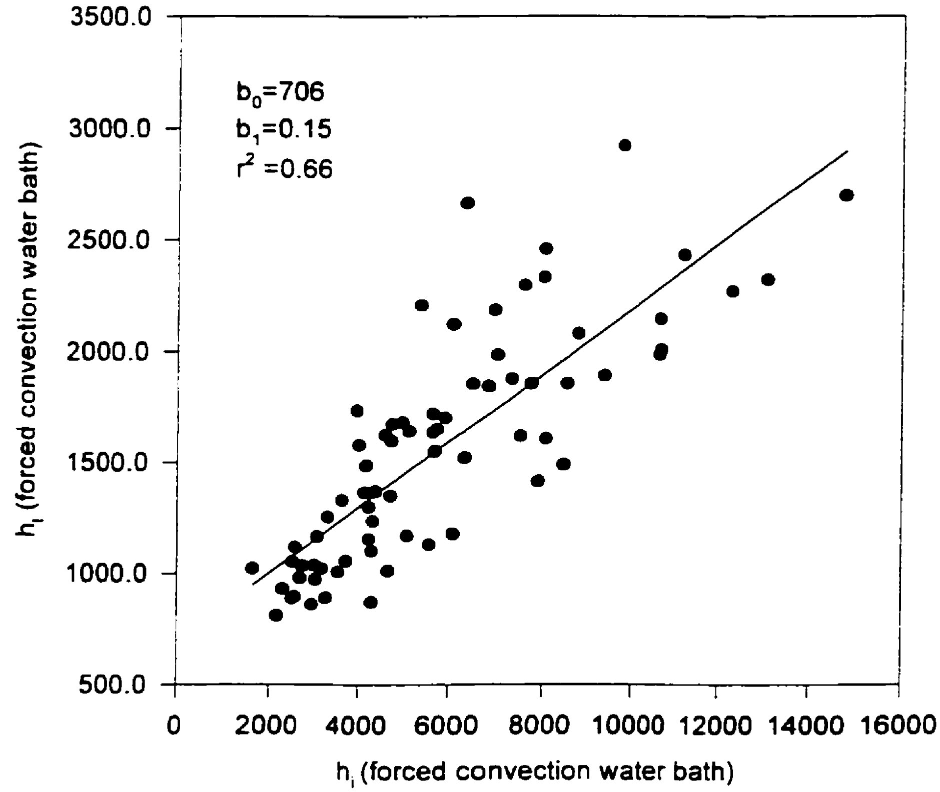

Figure 5.5a. Comparison of inner (h_i) to over all (h_t) heat transfer . . . . coefficients obtained in forced convection water bath.

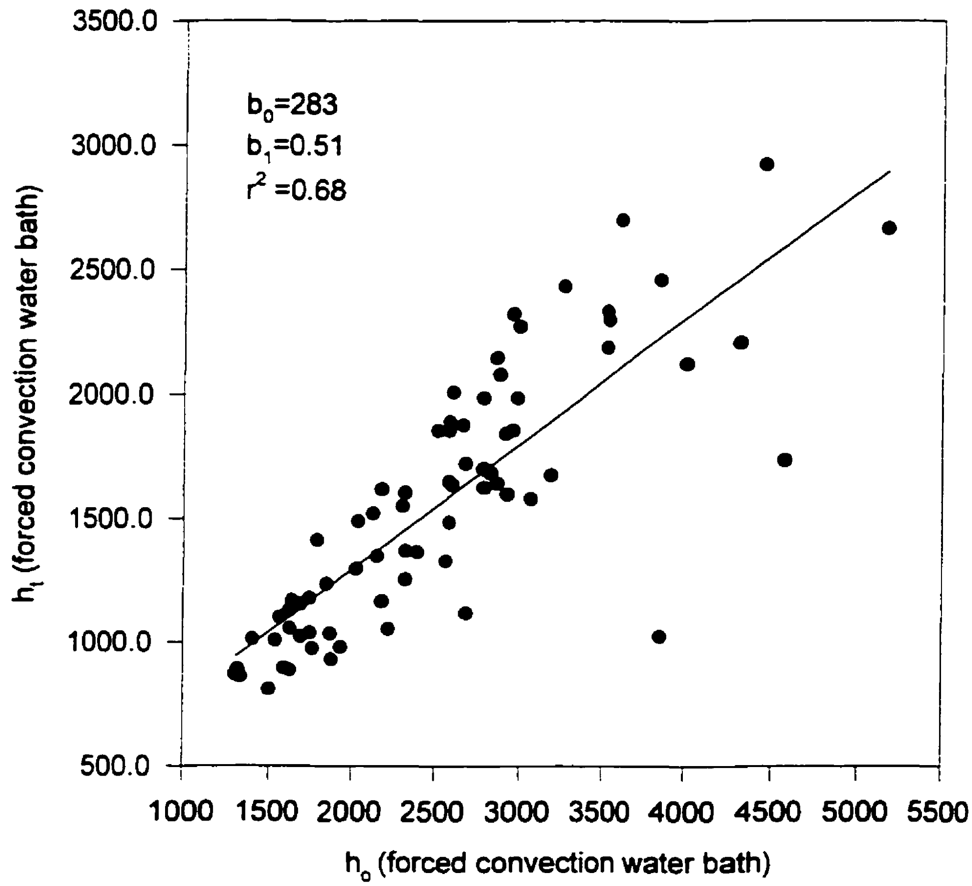

Figure 5.5b. Comparison of outer (h_o) to over all (h_t) heat transfer coefficients obtained in forced convection water bath.

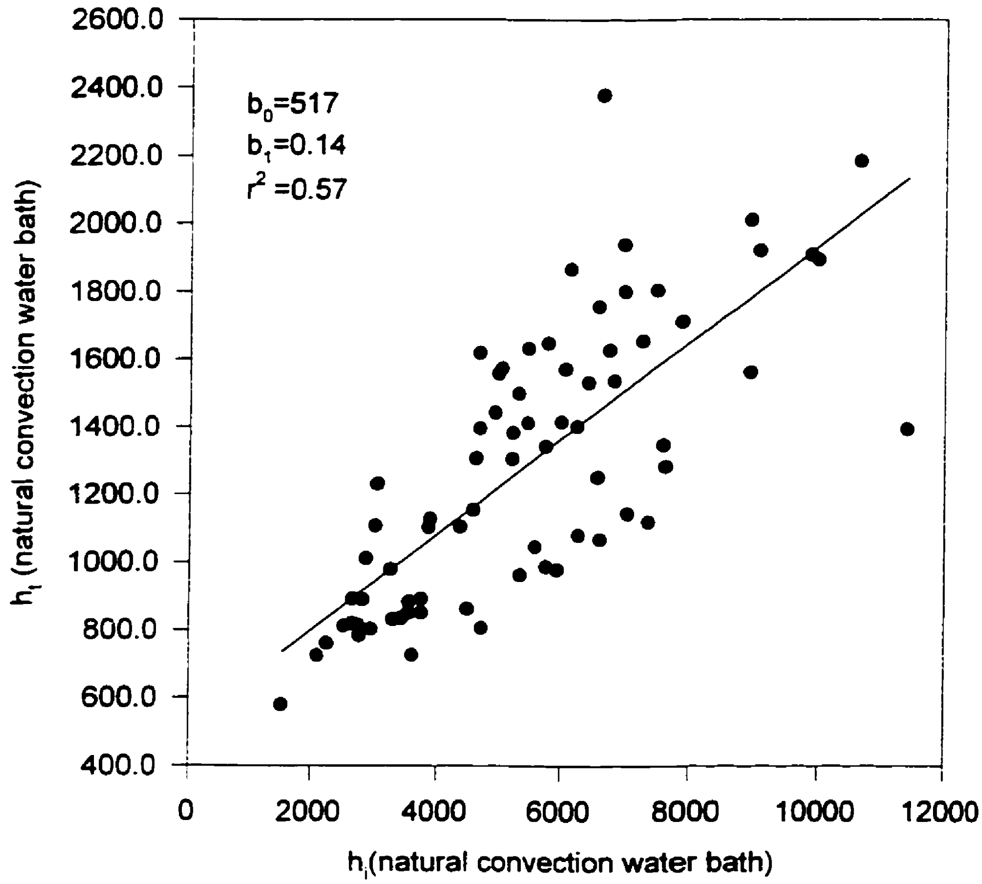

Figure 5.6a. Comparison of inner (h_i) to over all (h_t) heat transfer coefficients obtained in natural convection water bath.

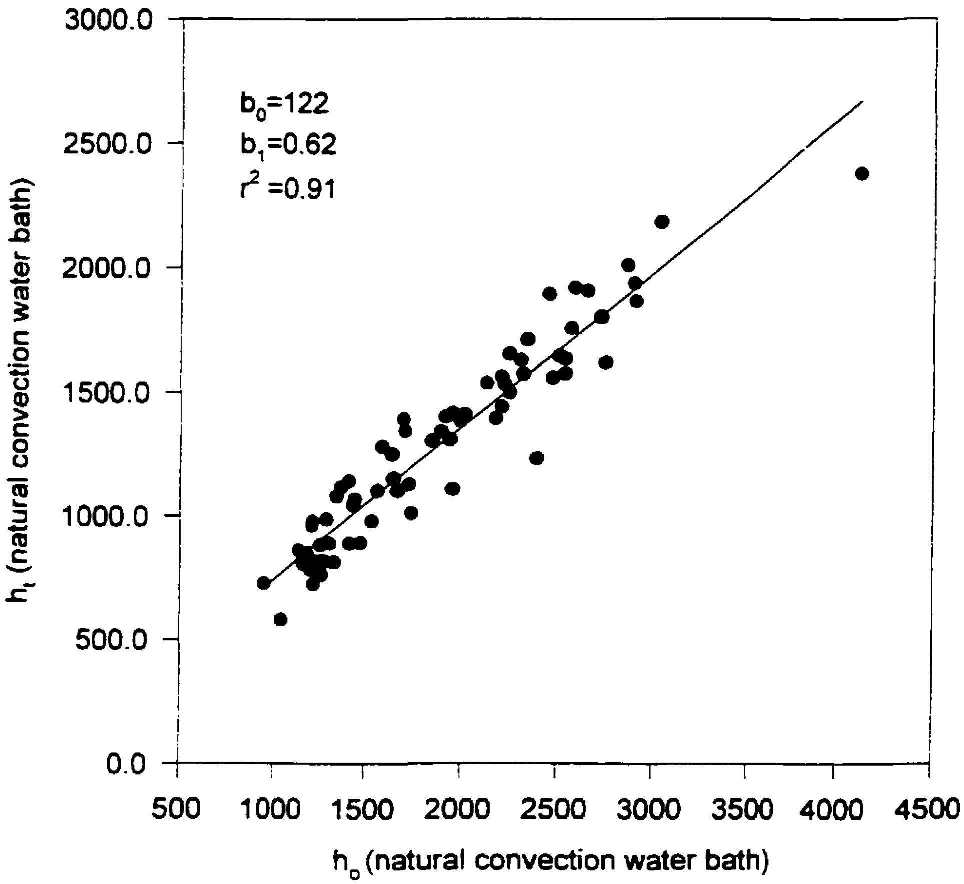

Figure 5.6b. Comparison of outer (h_o) to over all (h_t) heat transfer. coefficients obtained in natural convection water bath.

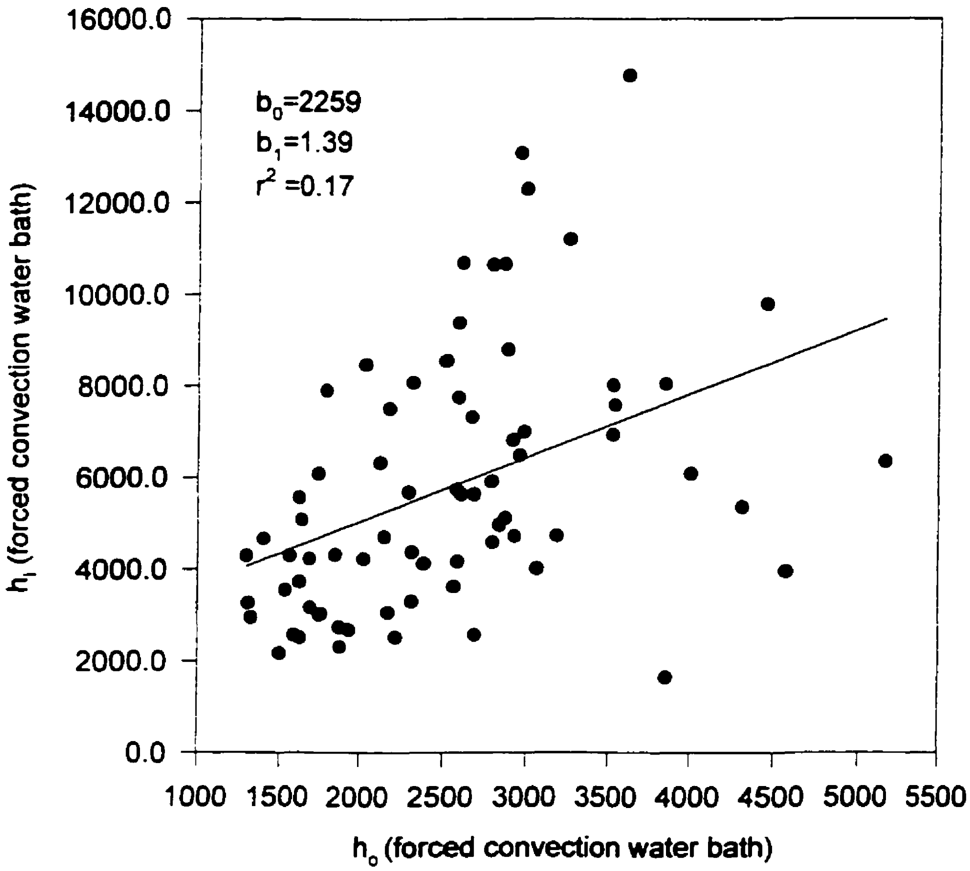

Figure 5.7a. Comparison of outer (h_o) to inner (h_i) heat transfer coefficients obtained in forced convection water bath.

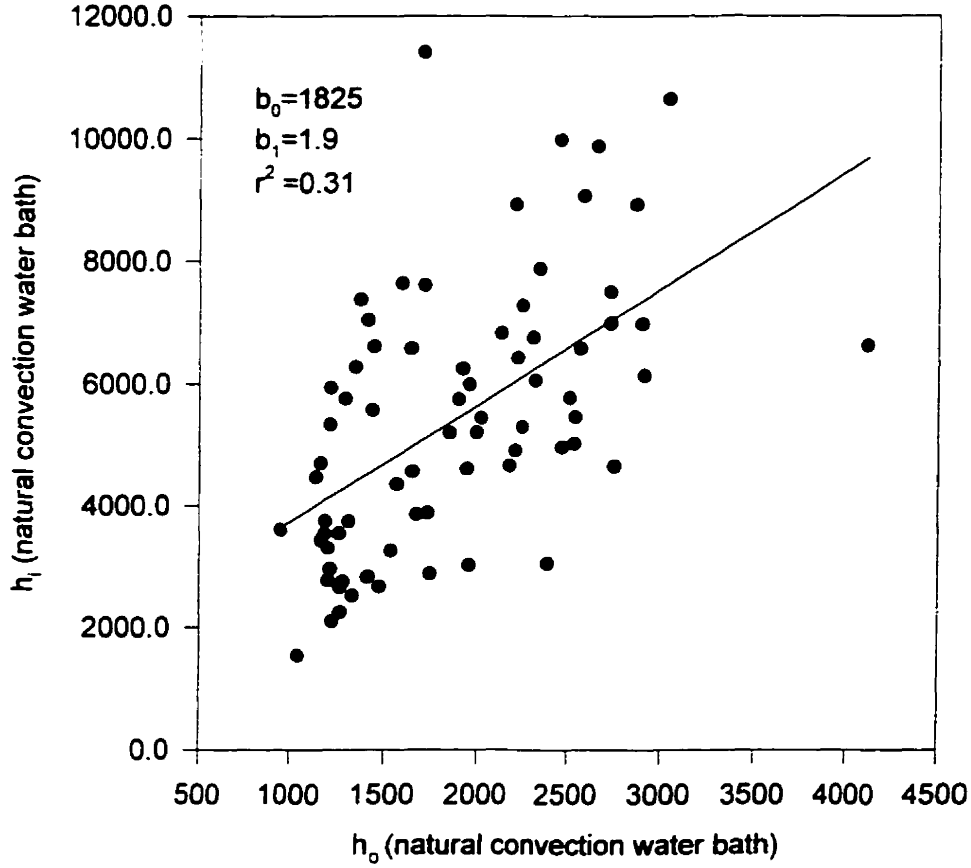

Figure 5.7b. Comparison of outer (h_o) to inner (h_i) heat transfer coefficients obtained in natural convection water bath.

5.1.3. Interaction between outside and inside heat transfer coefficients

As seen in the previous section, improving the heat transfer to the coil increased the inner heat transfer coefficient by 7%. At the same time, the data indicate that increasing the flow rate inside the coil has the effect of increasing the outside heat transfer coefficient, as well as that inside the coil (Figures 5.8a,b,c). Here, the inner and outer heat transfer coefficients, averaged over bath temperature, D_C, D_H, and pitch, are plotted against flow rate inside the coil for each bath regime separately.

Thus, increasing the flow rate inside the coil not only increases the inside heat transfer (as implied by eq. 2.2), but also appears to influence the outer heat transfer characteristics. This is somewhat paradoxical in view of the fact that it was shown that the inner heat transfer coefficient was improved by circulating the water outside the coil. Nevertheless, an explanation may be provided by the data. Figure 5.9 shows the mean outer surface temperature of the coil at the three inner flow rates for the two water bath regimes. The effect of increasing the inner flow rate is to carry heat away from the wall more rapidly, which should be reflected in a lower mean temperature on the outer surface of the coil.

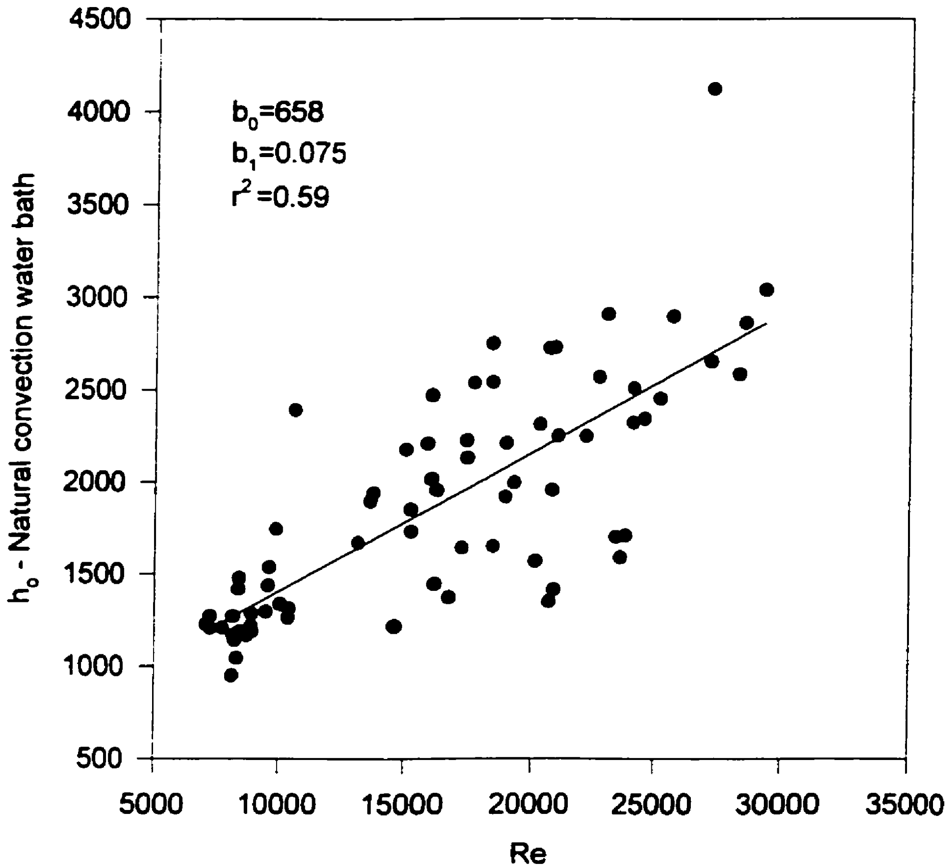

Figure 5.8a. Effect of Reynold's number inside the coil on outer (h_o) heat transfer coefficient (natural convection water bath).

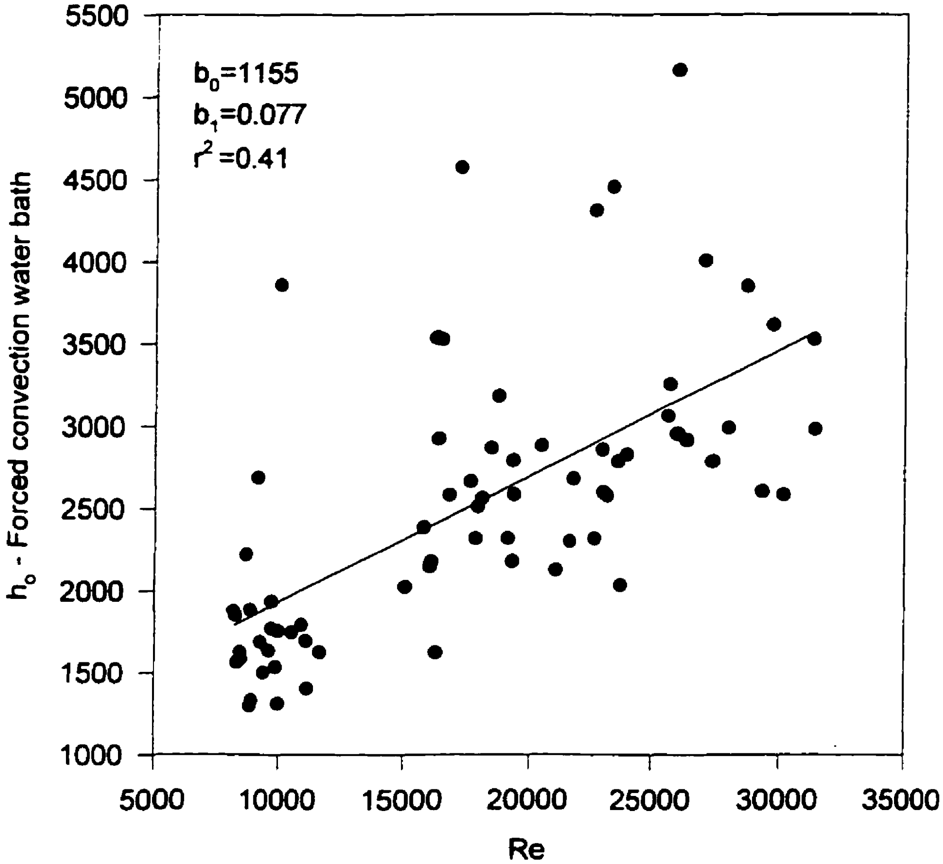

Figure 5.8b. Effect of Reynold's number inside the coil on outer (h_o) heat transfer coefficient (forced convection water bath).

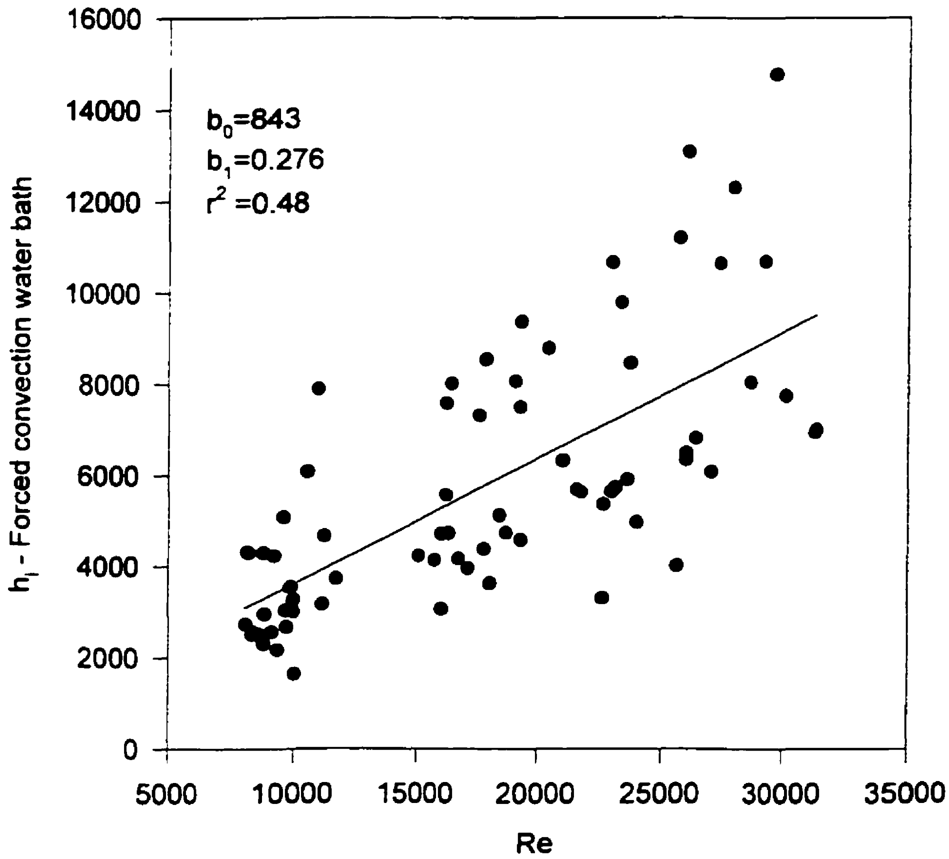

Figure 5.8c. Effect of Reynold's number inside the coil on inner (h_i) heat transfer coefficient forced convection water bath.

This is clearly seen in Figure 5.9. The result is a steeper temperature gradient between the coil surface and the ambient bath water (which is maintained nearly constant). However, the outside heat transfer coefficient is, by definition, independent of the temperature gradient. This makes it difficult to explain why h_0 should increase with a rise in the inner flow rate.

One explanation could be that the greater transfer away from the inner surface results in a steeper temperature gradient in the outer surface boundary layer. This might result in stronger local convection currents on the outside. The greater h_0 could reflect this change in the flow structure near the outer coil surface. Another possibility is that, since the heaters at the bottom must supply energy to the system at a higher rate to maintain constant bath temperature when more energy is drawn away through the coil, there could be an increase in the buoyancy component of the flow in the water bath. This could improve mixing near the coils, due to the interaction between the upward buoyant force and the downward mean flow caused by the recirculating mechanism. Both possibilities could be investigated experimentally.

From the point of view of water bath regime, Figure 5.9 also shows that circulation of bath water significantly increased the outer surface temperature of the coil, thereby increasing the heat transferred to the inner fluid. The temperature difference between regimes at each flow rate rises from about 6°C to about 8°C. The question again arises as to how this might increase the inner heat transfer coefficient (gradient independent). Again, it is possible that the rise is due to stronger buoyancy forces within the coil, or to a consequent increase in the apparent Reynolds number.

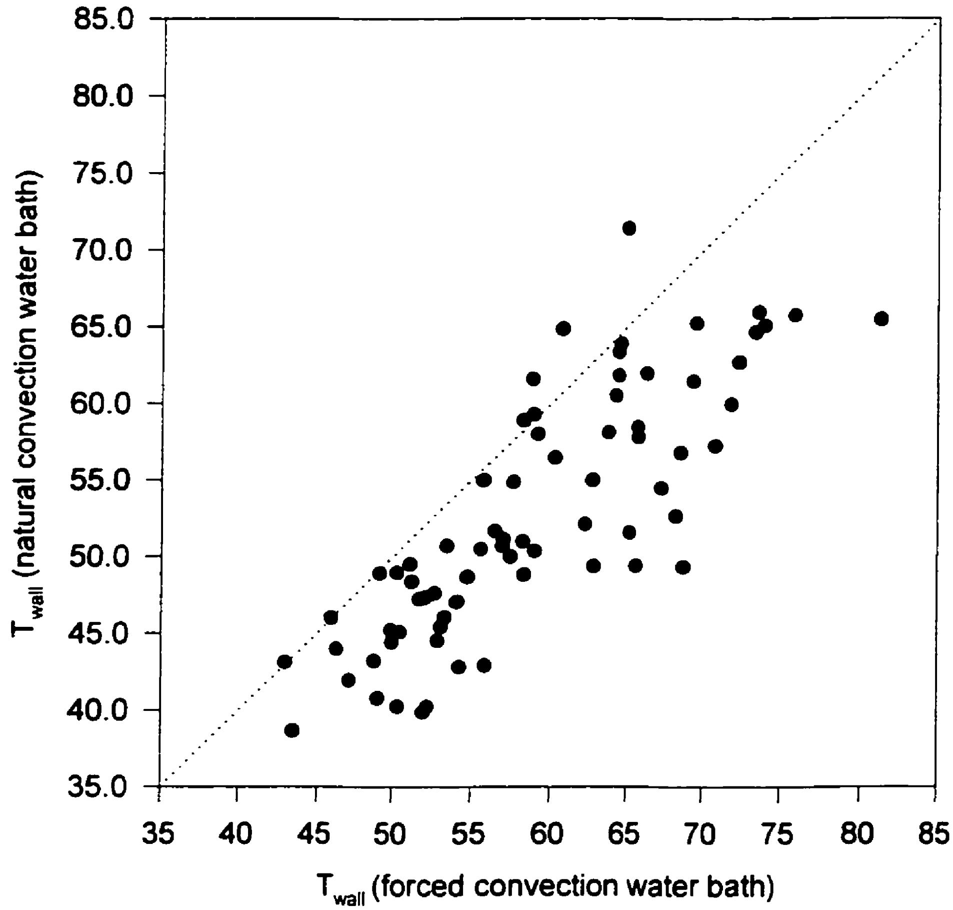

Figure 5.9. Comparison of mean wall temperature (forced to natural) as influenced by forced convection water bath.

As shown in Figure 5.10, the Reynolds numbers inside the coil are higher under the forced convection water bath regime than under natural convection. This is due to the fact that improved heat transfer to the coil raises the average temperature of the coil surface compared to the natural convection situation (Figure 5.9) given the same inner conditions. The consequence of this is to reduce the viscosity of the inner fluid (Figure 5.11), resulting in a higher Reynolds number. Here, it is necessary to assume that the decrease in viscosity is not counteracted by an increase in flow rate, which was not measured during these trials (recall that submersible pumps were used, but were not calibrated at different fluid temperatures).

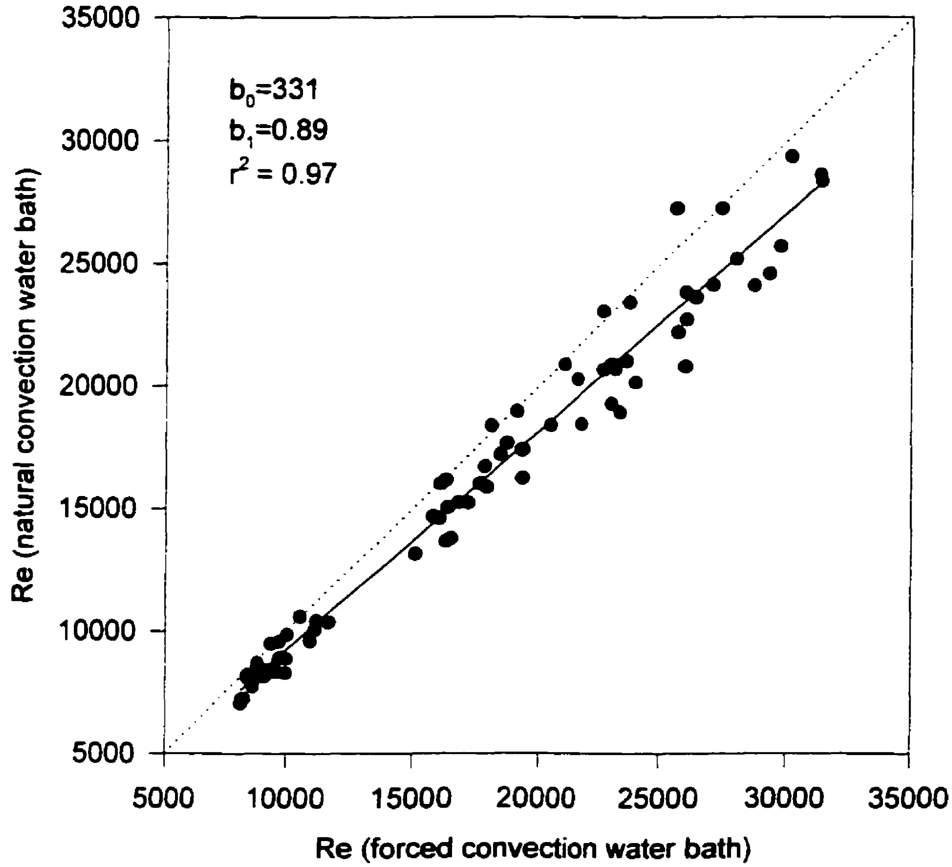

Figure 5.10. Reynolds numbers of water inside the coil obtained under natural convection water bath vs. those from forced convection water bath.

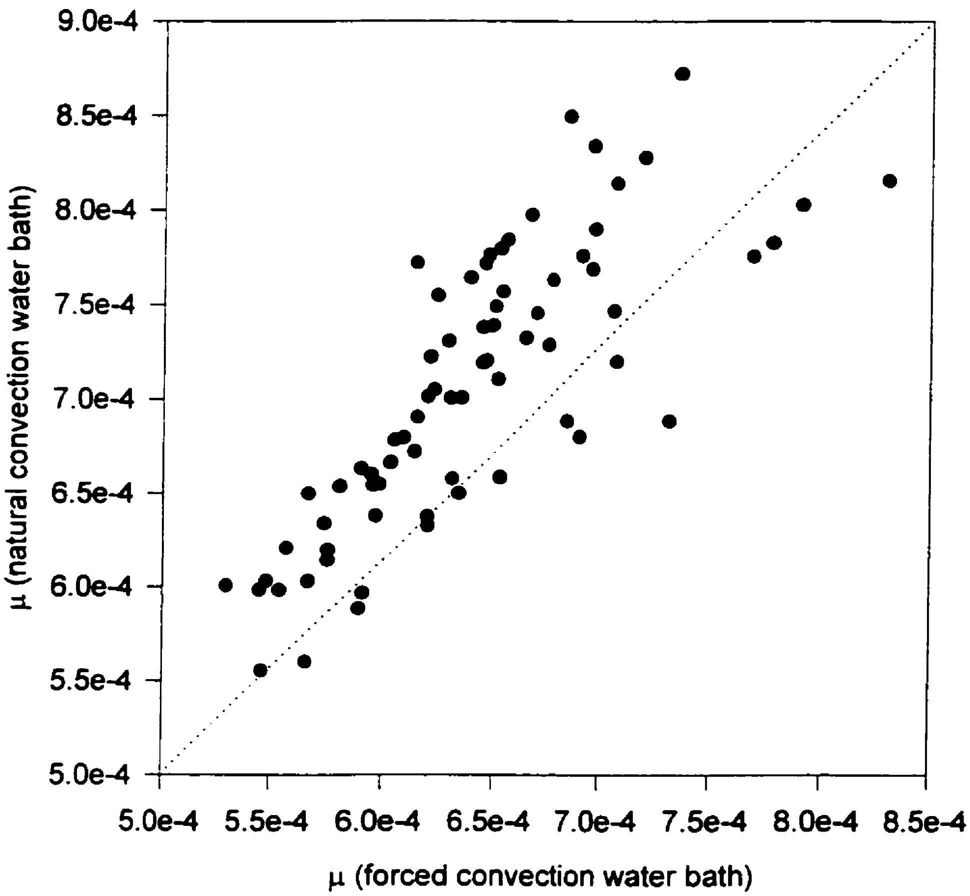

Figure 5.11. Influence of flow rate inside the coil on mean viscosity of water.

5.2. Influence of control parameters on the inner and outer heat transfer coefficients

5.2.1 Analysis in terms of experimental parameters

Analysis of the influence of the control parameters on the inner and outer heat transfer coefficients was performed using the RSREG (Response Surface Regression) procedure from SAS (SAS, 1988). This method was chosen because the coding of control parameter levels leads to an orthogonal parameter space and permits direct evaluation of the relative effects. The data were analysed for each regime separately. The results are presented in Tables 5.3 and 5.4. The mean squares represent the total influence of the parameter in question. This includes its linear and quadratic effects, as well as the interactions with other variables. It should be noted that the original parameter 'pitch' was transformed to the parameter 'torsion' according to the work done by Gong et al. (1994) and Yang and Ebadian (1996). Gong et al. (1994) expressed the effect of pitch in terms of the following definition of the torsion factor λ:

$$\lambda = \text{Pitch}/\pi D_H \tag{5.1}$$

whereas, Yang and Ebadian (1996) redefined λ as:

$$\lambda = \text{Pitch}/(D_H/2) \tag{5.2}$$

The authors recognize torsion to be a twisting force superimposed on the centrifugal force in curved tubes. The torsion factor is greater for tight helices (small D_H) given the same tube diameter. However, increasing the torsion factor does not necessarily improve the heat transfer. Numerical studies by the authors indicate that there is a Prandtl-dependent increase in Nu for small λ, which is followed by a decrease at higher λ. The effect of λ was also shown to depend on the axial flow rate.

This had not been taken into account in the planning of the experiments presented here. It is nevertheless possible to investigate the influence of λ, for which there were 10 levels in this experiment – ie. two pitch levels combined with combinations of two helix diameters and two tube diameters (8 levels), and the 0-pitch (separation distance of 0.001 m) with two different helix diameters. Equation 5.2 was used to transform pitch to λ in the analysis that follows.

Table 5.3. Summary of response surface regression analysis of inner heat transfer coefficients obtained under natural and forced convection conditions in the water bath.

	REGIME					
	Forced Convection			Natural Convection		
Parameter	MS	P>F	Direction of effect	MS	Prob>F	Direction of effect
D_c	$1.2*10^8$	<<0.0001	+ ve	$2.6*10^7$	<<0.0001	+ve
D_H	$4.8*10^7$	0.003	+ve	$2.0*10^7$	0.0002	-ve
Bath Temp	$1.1*10^6$	0.92	n/a	$3.8*10^6$	0.0002	+ve
Flow Rate	$2.4*10^8$	<<0.0001	+ve	$2.1*10^8$	<<0.0001	+ve
Torsion	$9.4*10^7$	0.0007	+ve	$3.6*10^7$	<<0.0001	+ve
Model R^2		0.69			0.89	
CV		31.6%			15.4%	

Table 5.4. Summary of response surface regression analysis of outer heat transfer coefficients obtained under natural and forced convection conditions in the water bath.

	REGIME					
	Forced Convection			Natural Convection		
Parameter	MS	Prob>F	Direction of effect	MS	Prob>F	Direction of effect
D_c	$4.6*10^5$	0 26	n/a	$1.4*10^6$	<<0.0001	+ve
D_H	$1.2*10^6$	0.01	+ve	$2.1*10^5$	0.05	-ve
Bath Temp	$4.4*10^5$	0.28	n/a	$5.5*10^5$	<<0.0001	-ve
Flow Rate	$3.6*10^6$	<<0.0001	+ve	$2.2*10^6$	<<0.0001	+ve
Torsion	$8.4*10^5$	0.03	+ve	$1.8*10^5$	0.07	+ve
Model R^2		0.64			0.83	
CV		23.0%			15.8%	

In both tables, the parameter that most influences the heat transfer coefficients is the flow rate inside the coil (largest mean square contribution, MS), corresponding to the high Reynolds dependence of the Seider-Tate equations. The tube and helix diameters (D_C and D_H), are also significant for h_i in both regimes, whereas D_C does not appear to be influential with respect to h_o in the forced convection regime. The latter observation may be an indication that flow patterns near the outer surface of the coil are independent of helix diameter when the bath water is being circulated, although they are still influenced by the tube diameter. The examination of the relationships between the flow patterns near the outer coil surface, the outer circulation conditions and the inner circulation conditions could be investigated with a more sophisticated instrumentation system.

It is interesting to note that the bath temperature was not significant for heat transfer coefficient under the forced convection regime, but was significant in the natural convection water bath. The average h_i and h_o are plotted for the two bath temperatures in Figure 5.12. The effect appears to be an increase with bath temperature in all cases except h_i in the forced convection regime. Although these results are not completely consistent, there might be a physical basis which could be verified by more detailed experimentation. Essentially, one might imagine that there would be a greater upward velocity due to buoyancy effects resulting from heating from the bottom. The influence could be more important in the natural convection water bath since it would not be counteracted by the downward stream flow caused by the forced convection method used.

The average inner and outer heat transfer coefficients were plotted versus the Re in Figures 5.8 a, b and c. The influence of flow rate inside the coil on both inner and outer heat transfer coefficients in both water bath regimes appear to be the main factor linking the two components of overall heat transfer. Moreover, the effect is almost identical on both h_i and h_o regardless of the conditions in the water bath (forced or natural convection), although one might anticipate a greater separation of the two sets of curves at even higher flow rates. Here again, the question arises as to what might be the influence of stronger flow characteristics in the water bath.

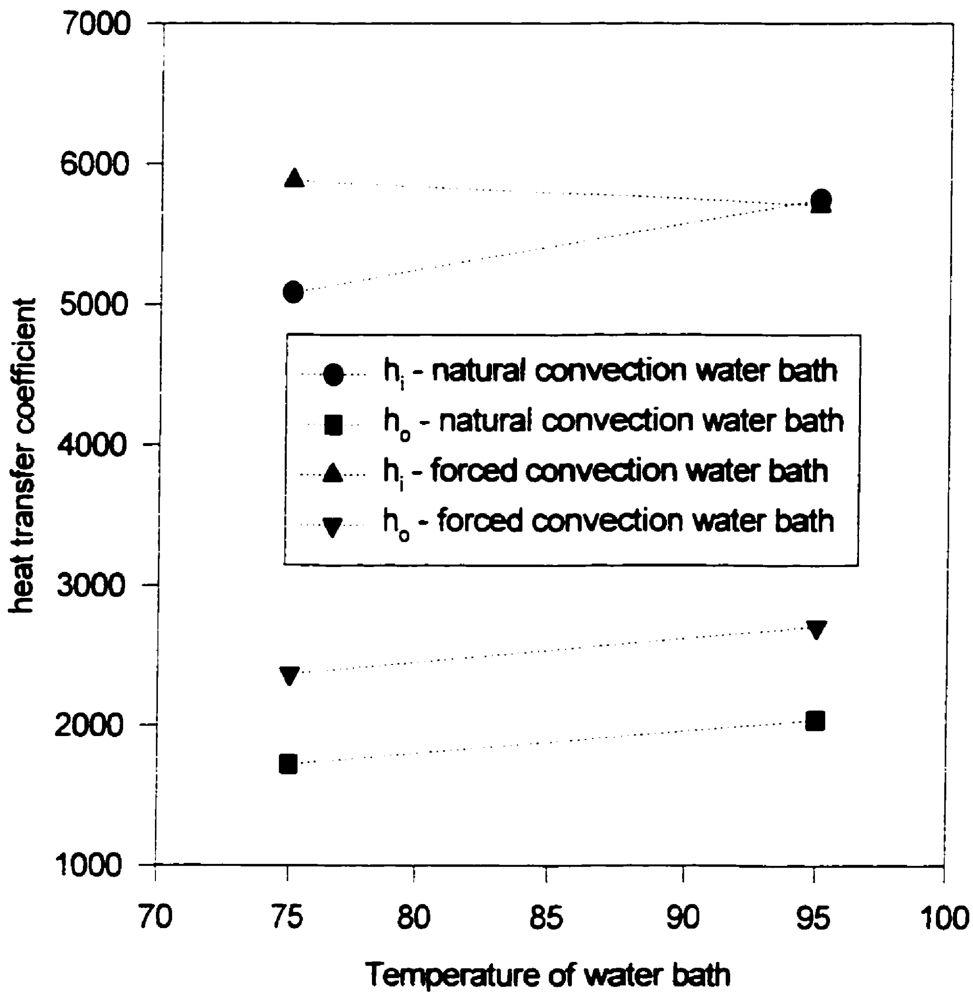

Figure 5.12. Average inner and outer heat transfer coefficients vs. temperature of the natural and forced convection water bath

5.2.2 Influence of torsion factor, λ

The torsion, λ, was found to cause significant variations among the heat transfer coefficients, although the influence was borderline in the case of h_o in the natural convection water bath (Table 5.4). In the case of the forced convection water bath, the influence of λ on h_i was found to be curvilinear (2^{nd} order) and the interaction with D_C and D_H was significant. The influence of λ on h_o was also curvilinear, with significant interaction with D_H. For the natural convection water bath, λ influenced h_i only through interaction with D_H and bath temperature, whereas the linear and quadratic effects were not significant. In the natural convection water bath, λ had no significant influence on h_o, either by itself or through interaction with other variables. Nevertheless, λ accounted for 14% of the variability attributed to the control parameters in this case.

The influence of λ on h_i is curvilinear, as had been noted by Yang and Ebadian (1996). However, the apparent interaction between λ and D_H, is indicative that the functional relationship between λ and D_H is inadequate and could be revised after more extensive experimentation.

The inner heat transfer coefficients are plotted versus the Dean number for various pitch levels in Figure 5.13a-f, for the two water bath regimes separately. Here, it was necessary to split the levels of torsion since it would be otherwise difficult to properly visualize the data. There is clearly a great deal of scatter in many of these figures, which makes it difficult to reach any clear conclusions regarding the influence of λ on h_i from this data set. Nevertheless, there are indications that for some combinations of the other factors, there may be a pitch level that enhances h_i. One of the problems with this data set is that it was difficult to ensure that the pitch was constant at all turns.

The influence of torsion was viewed in a second manner. Given that pitch was defined in equation 5.2 as the separation between turns, in meters, it would appear that the tube diameter is not accounted for. Pitch could be, say 20 mm, for a 13 or 15 mm i.d tube. In fact, Yang and Ebadian (1996) assumed a ratio of helix diameter to tube diameter of 80:1 in their numerical study, which is substantially greater than the ratios for the coils used in the present study.

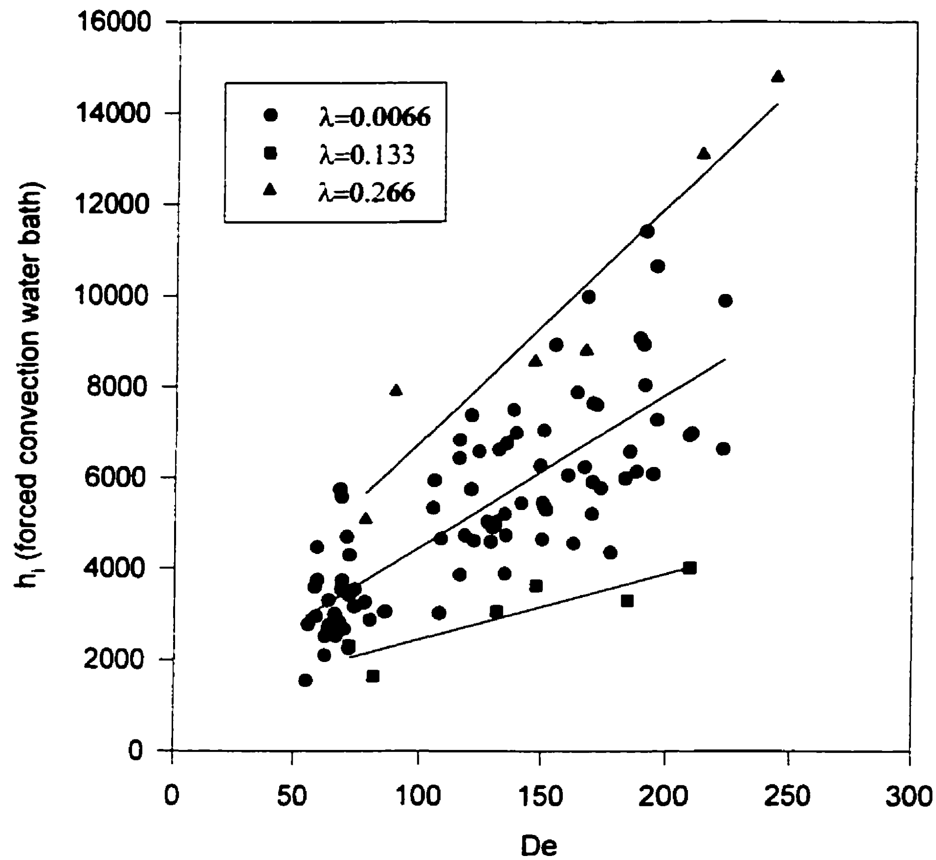

Figure 5.13a. Relationships between Dean no. and inner heat transfer coefficient for forced convection water bath.

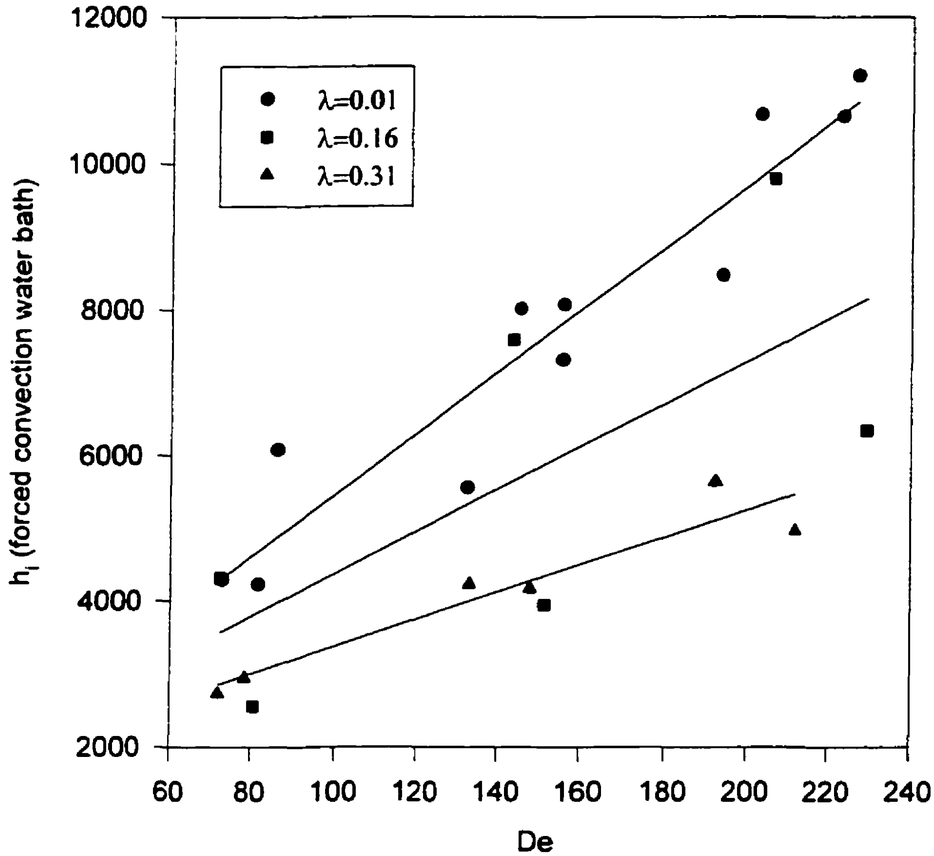

Figure 5.13b. Relationships between Dean no. and inner heat transfer coefficient for forced convection water bath.

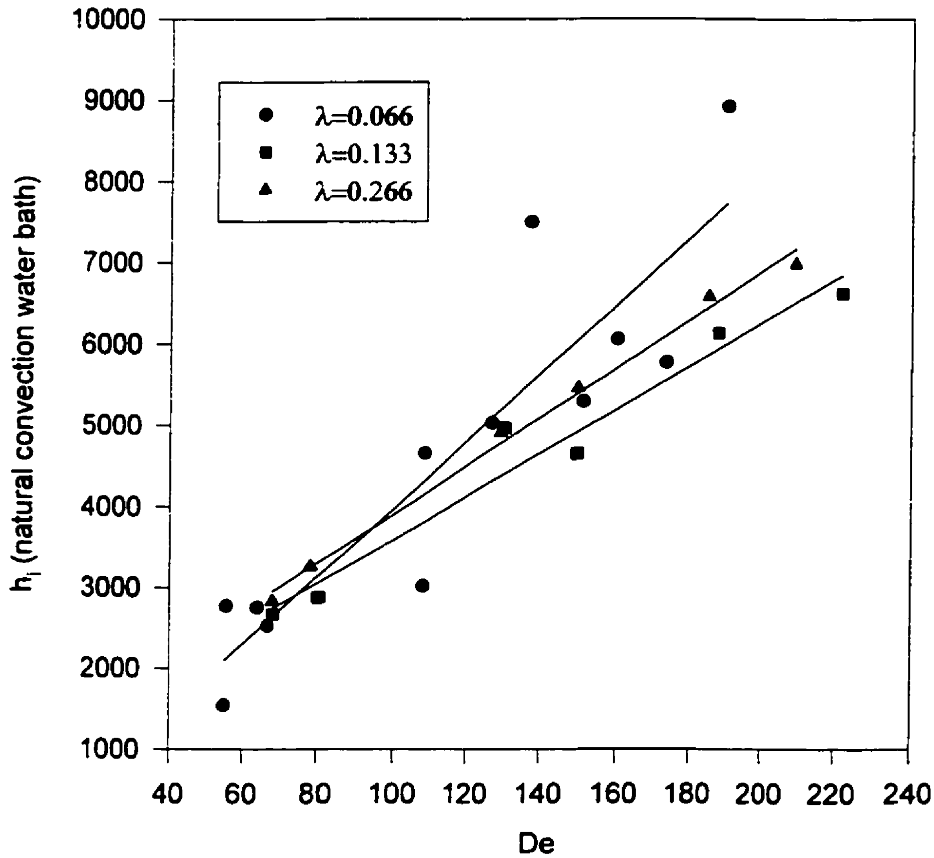

Figure 5.13c. Relationships between Dean no. and inner heat transfer coefficient for natural convection water bath.

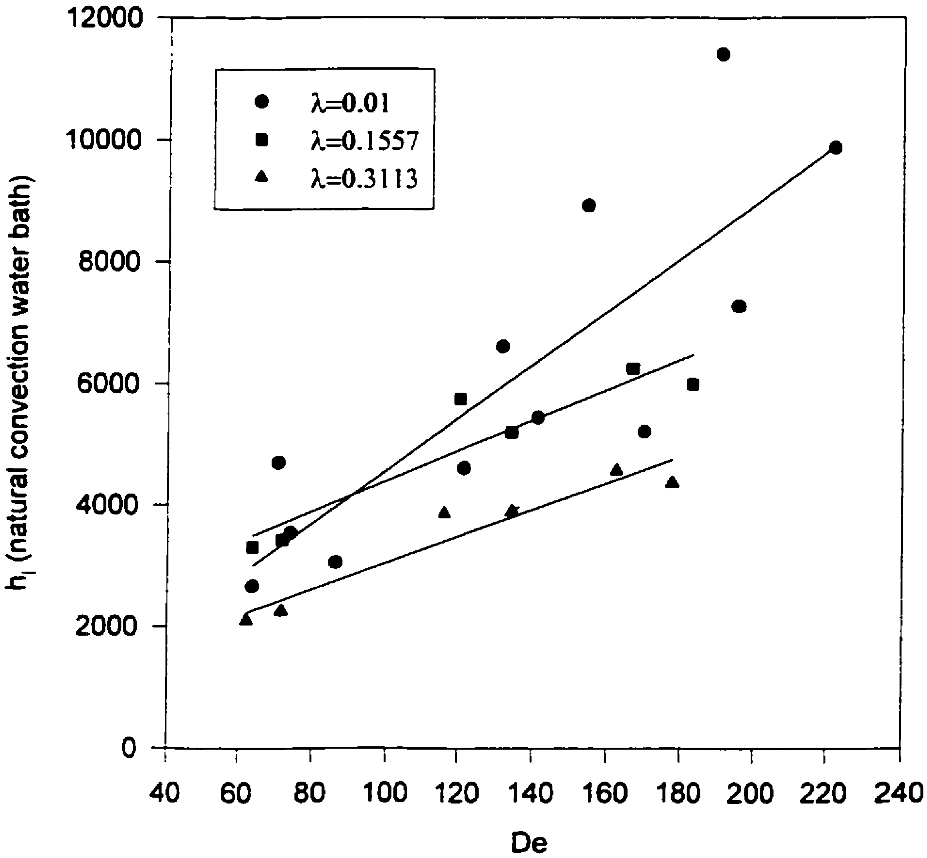

Figure 5.13d. Relationships between Dean no. and inner heat transfer coefficient for natural convection water bath.

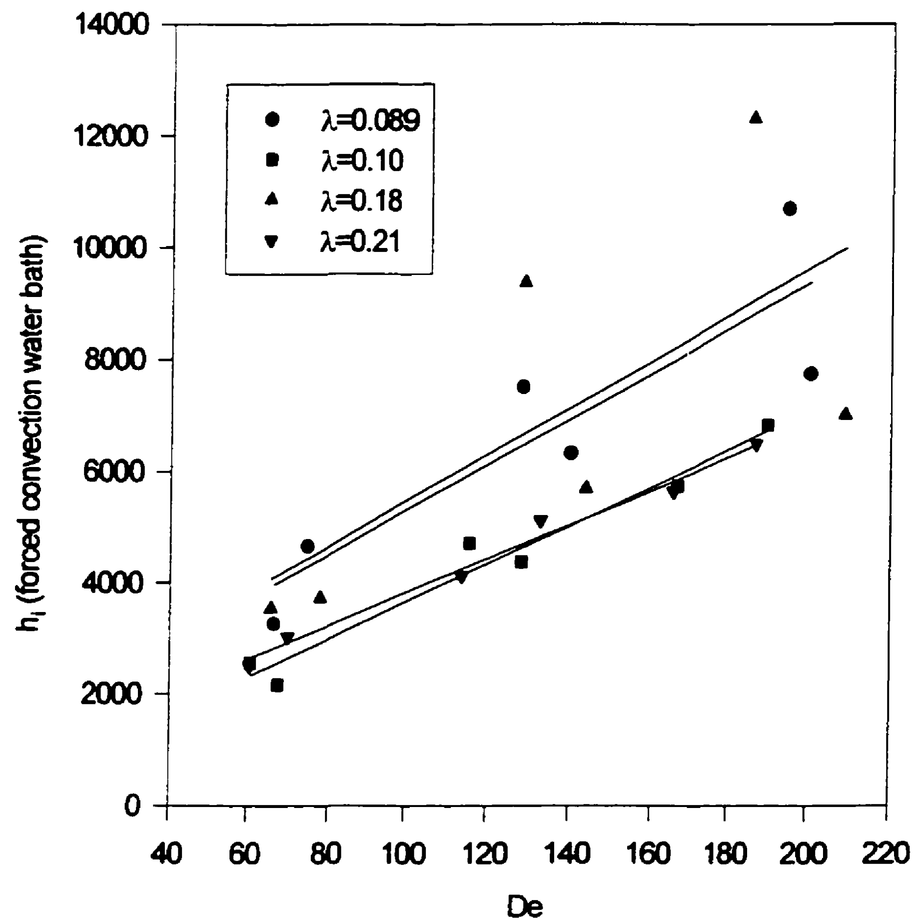

Figure 5.13e. Relationships between Dean no. and inner heat transfer coefficient for forced convection water bath.

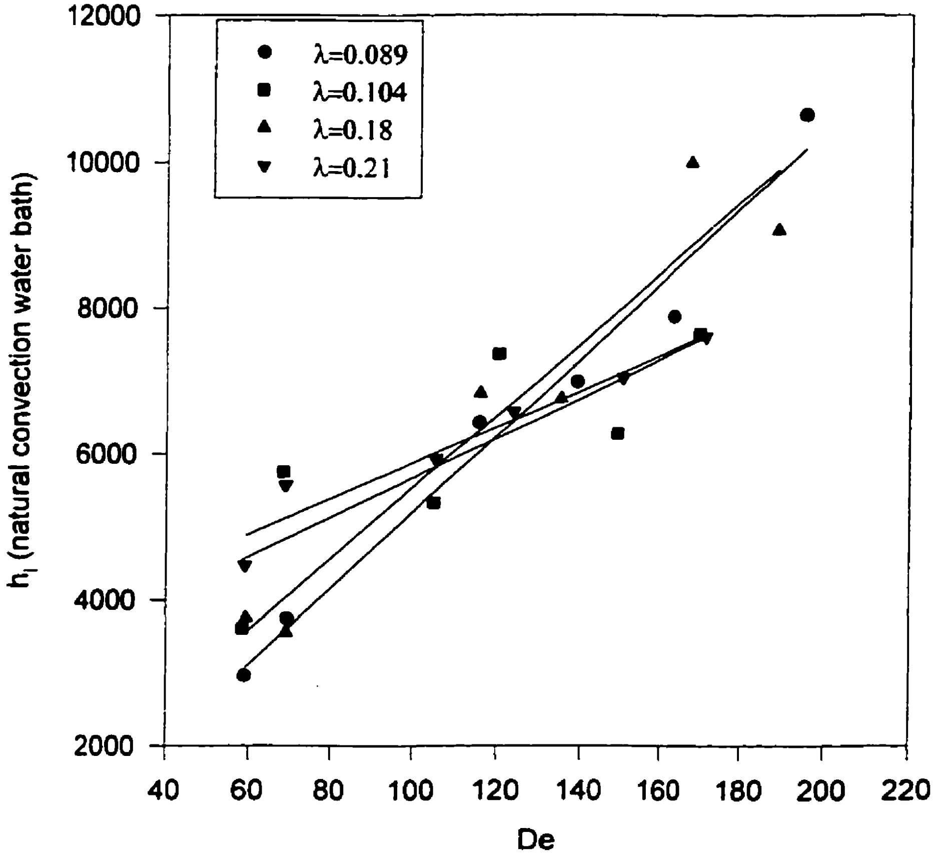

Figure 5.13f. Relationships between Dean no. and inner heat transfer coefficient for natural convection water bath.

In view of this, the effect of pitch or torsion was investigated for each coil separately, albeit over different ranges of the torsion factor. Figures 5.14a-h show the heat transfer coefficients obtained at different pitches with each of the four coils, the values being averages over the flow rates and bath temperatures, and presented in separate graphs for each water bath regime. For ease of comparison, as well as to highlight the fact that different ranges of λ occurred for the different D_H/D_C, ratios, all of these graphs were placed on the same axis scale. There appears to be substantial differences in the responses to λ from one coil to another. In this light, it would be interesting to perform more extensive experiments to elaborate and verify these behaviours at more coherent settings of λ for all the coils.

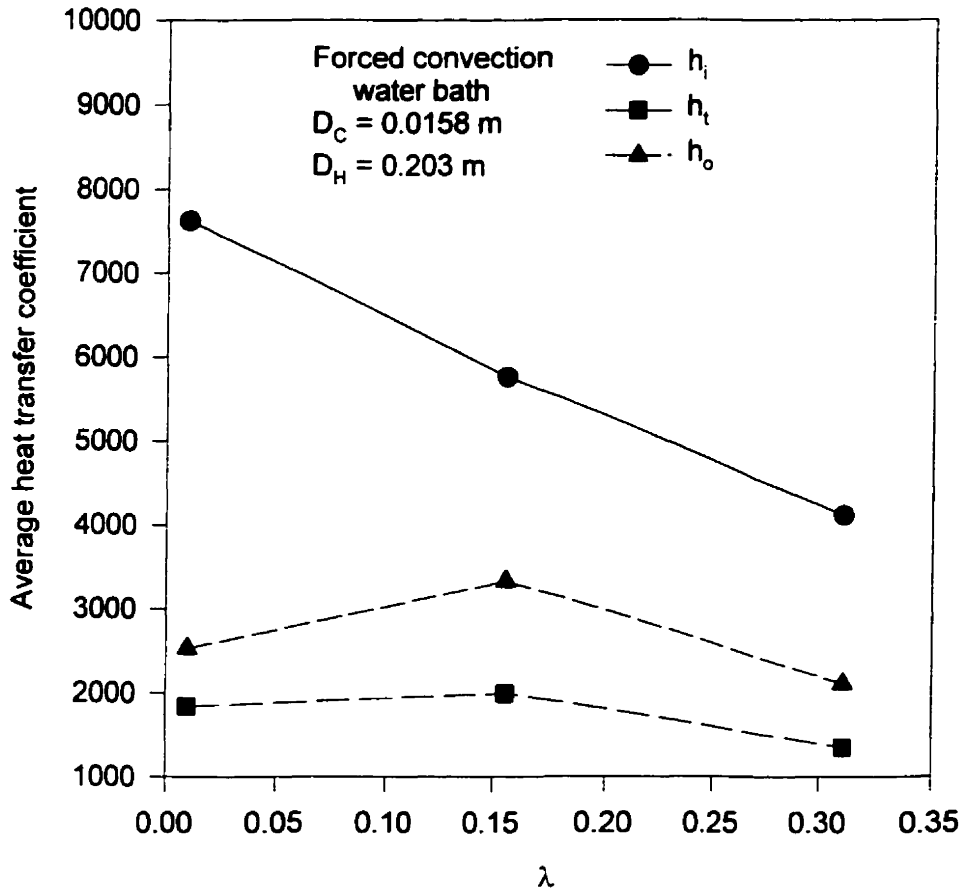

Figure 5.14a. Heat transfer coefficient as influenced by torsion, λ for different coil forced convection water bath.

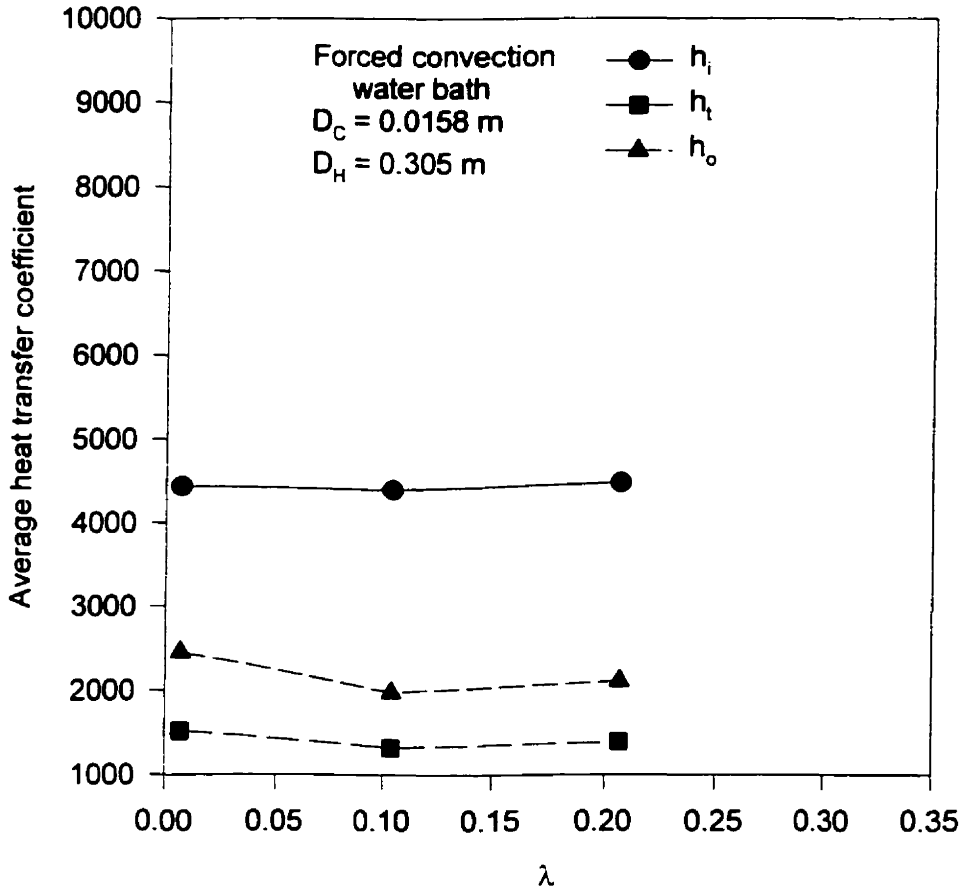

Figure 5.14b. Heat transfer coefficient as influenced by torsion, λ for different coil forced convection water bath.

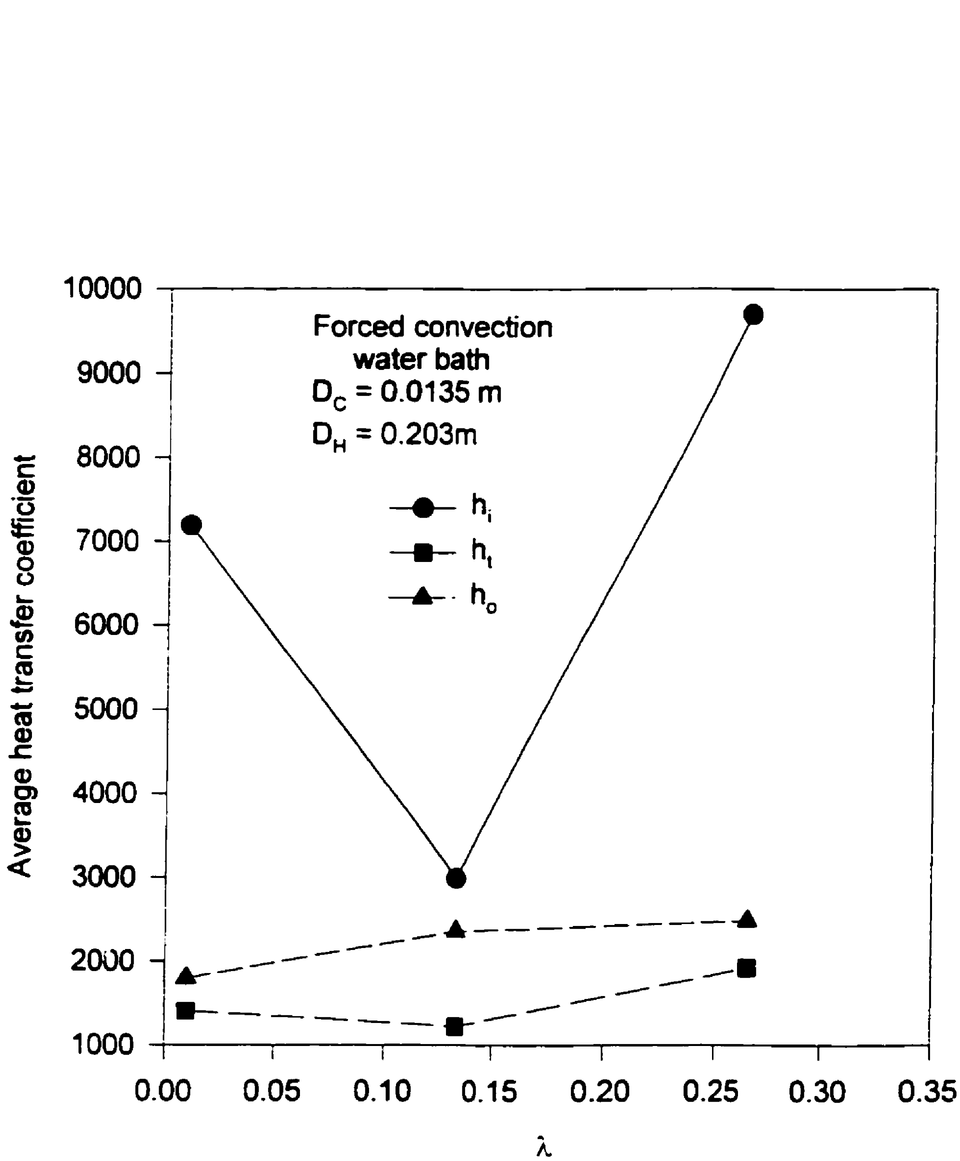

Figure 5.14c. Heat transfer coefficient as influenced by torsion, λ for different coil forced convection water bath.

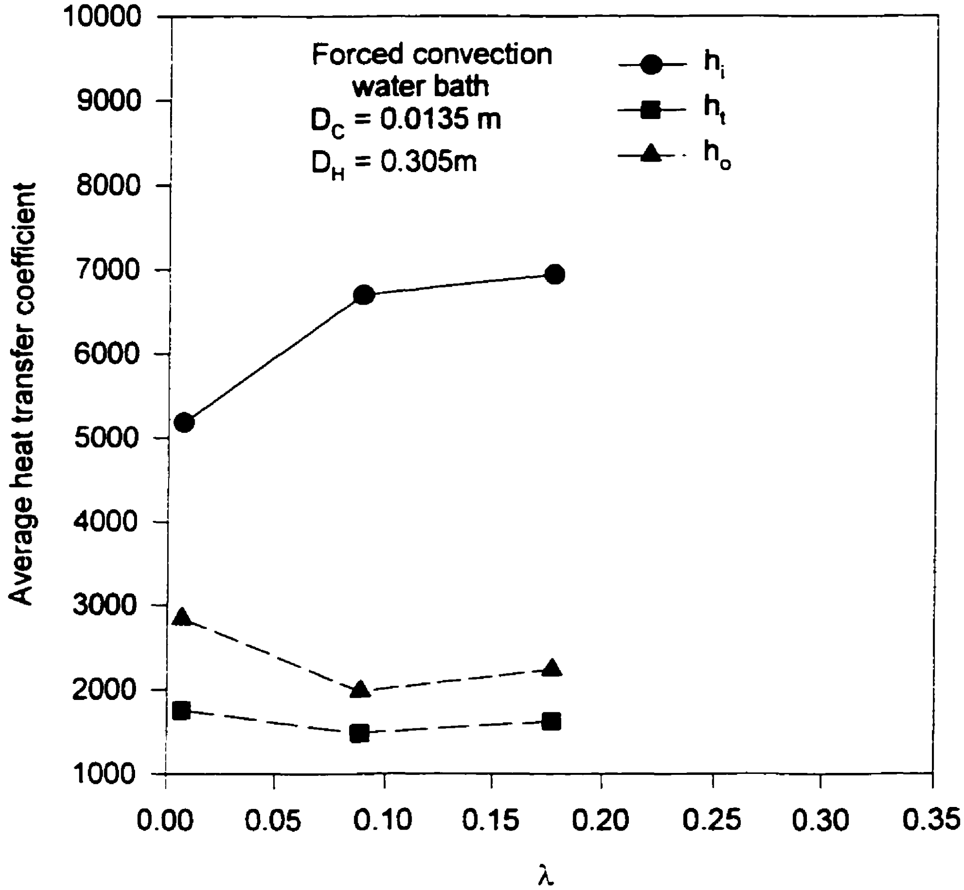

Figure 5.14d. Heat transfer coefficient as influenced by torsion, λ for different coil forced convection water bath.

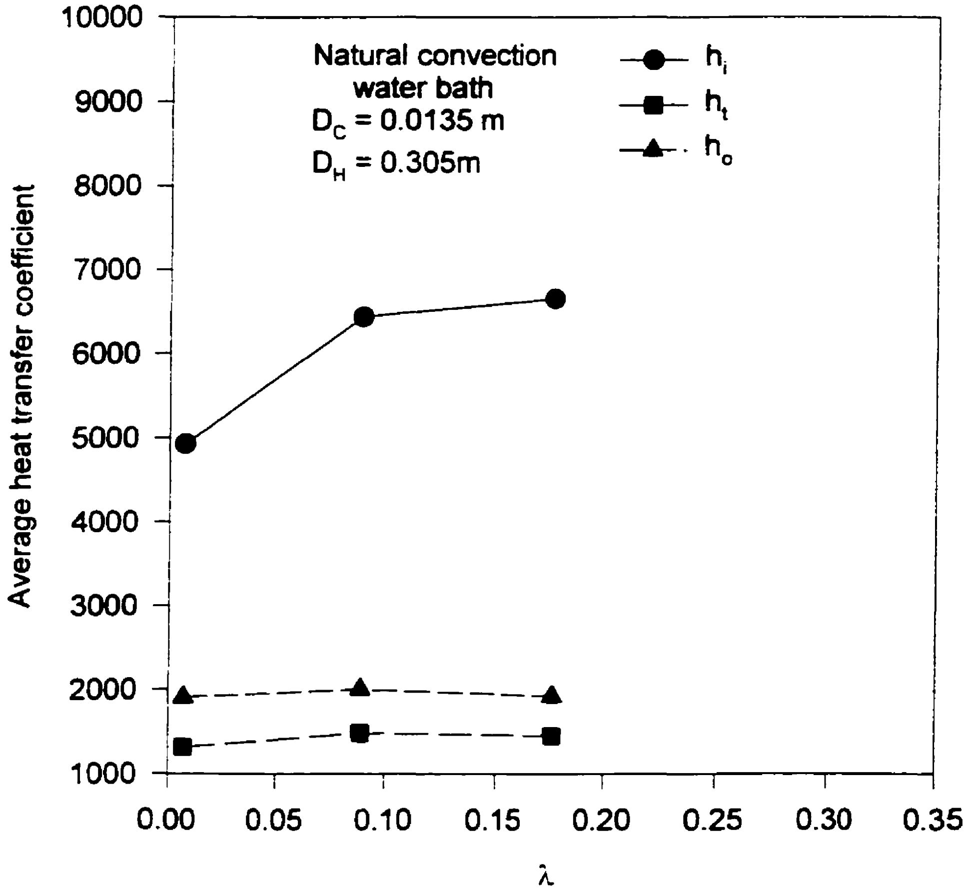

Figure 5.14e. Heat transfer coefficient as influenced by torsion, λ for different coil natural convection water bath.

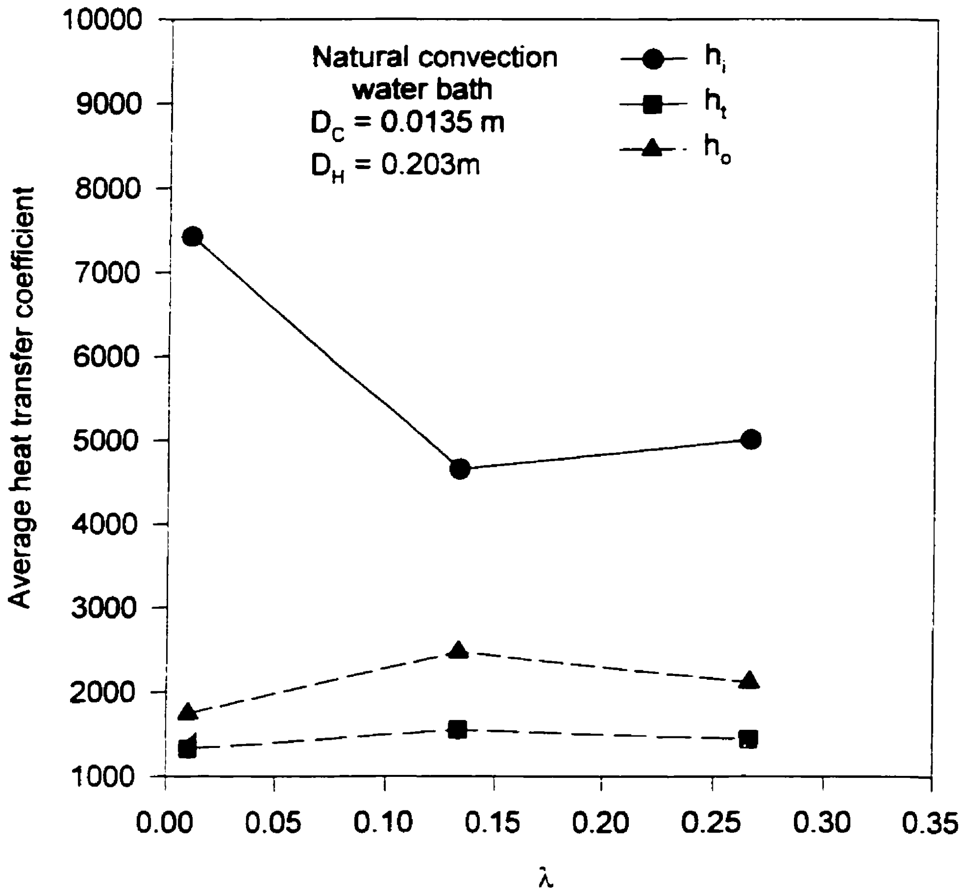

Figure 5.14f. Heat transfer coefficient as influenced by torsion, λ for different coil natural convection water bath.

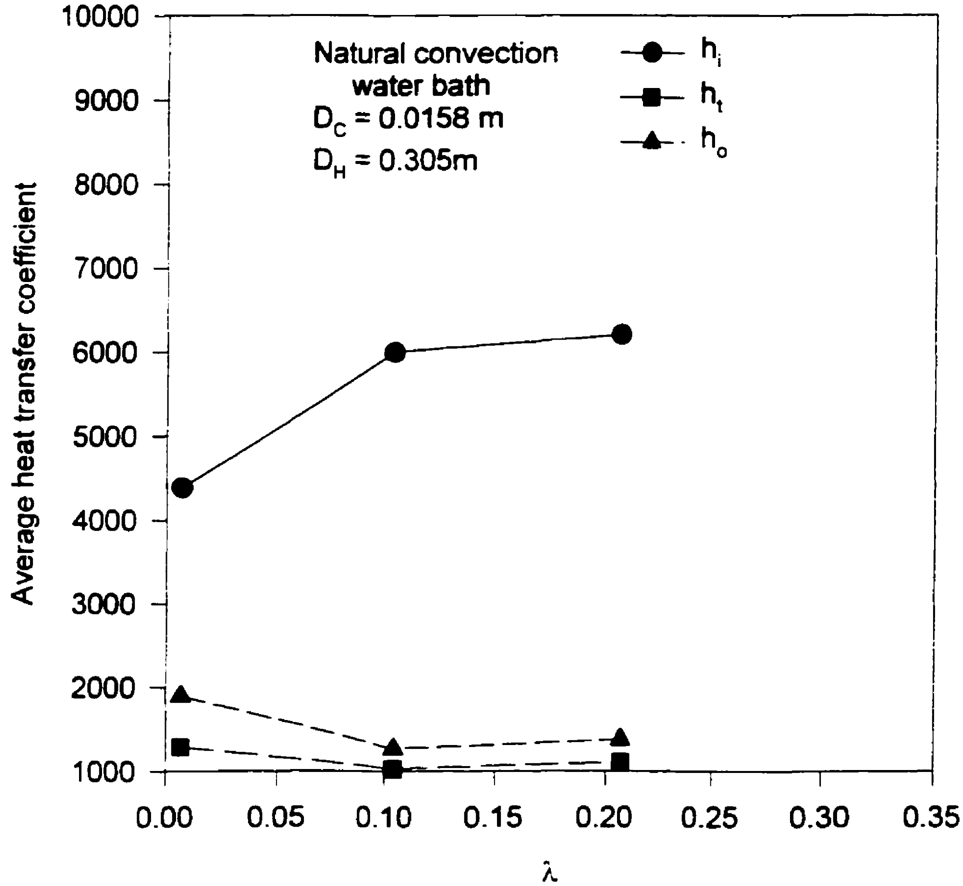

Figure 5.14g. Heat transfer coefficient as influenced by torsion, λ for different coil natural convection water bath.

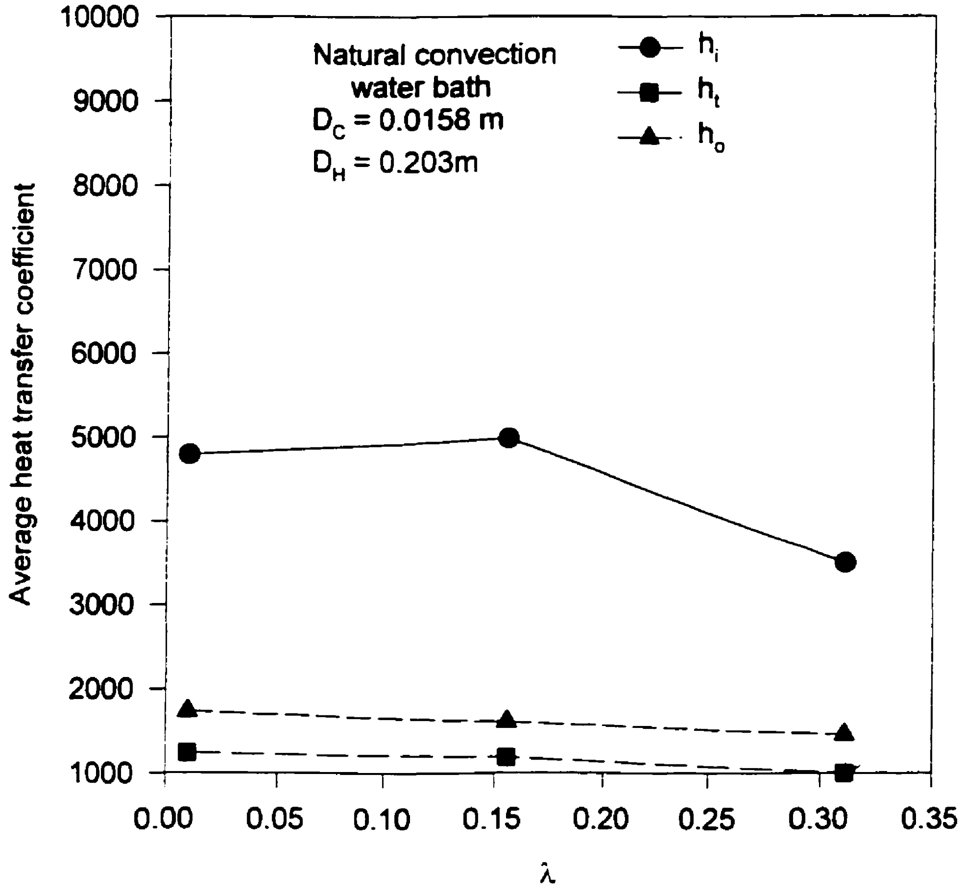

Figure 5.14h. Heat transfer coefficient as influenced by torsion, λ for different coil natural convection water bath.

5.3 Comparison with Seider-Tate predictions augmented by Jeschke's correction factor

The question arises as to how the inner heat transfer coefficients observed here relate to those predicted by the Seider-Tate relations as modified by the Jeschke correction factor (eq. 2.21). Since most of the runs led to Reynolds numbers above 10^4 (Figure 5.10), equation 2.20 can be used. The predicting equation including the correction factor is:

$$Nu_{st} = 0.023\ Re_{st}^{0.8} Pr_{st}^{1/3} (\mu_b/\mu_W)^{0.14} (1+3.5D_C/D_H) \qquad (5.3)$$

The term $(\mu_b/\mu_W)^{0.14}$ is neglected since the required inner wall temperature is not available. However, the maximum underestimate will be less than 5% for the data set, since the ratio of viscosities is not likely to exceed 1.4 in the data set ($1.4^{0.14}=1.05$). This conclusion is based on the fact that the ratio between the mean outer surface temperature (which should be higher than the inner wall temperature) and the mean inner bulk fluid temperature does not exceed that value.

Results are shown in Figures 5.15 and 5.16. The fits are not particularly good in either case ($r^2=0.63$, 0.51, respectively), although the average ratios between the observed and predicted Nu's are almost identically 1.0 in both cases (1.004 and 1.005, respectively). In both of these figures, the data seem to scatter vertically in three approximate ranges of the predicted Nu's, corresponding to the three flow rates used. Since all experimental factors except pitch (torsion) are implicitly included in equation 5.3, analysis of the ratios between the observed and predicted Nusselt numbers as a function of the control parameters should show that torsion explains a good deal of the scatter about the 1:1 correspondence line.

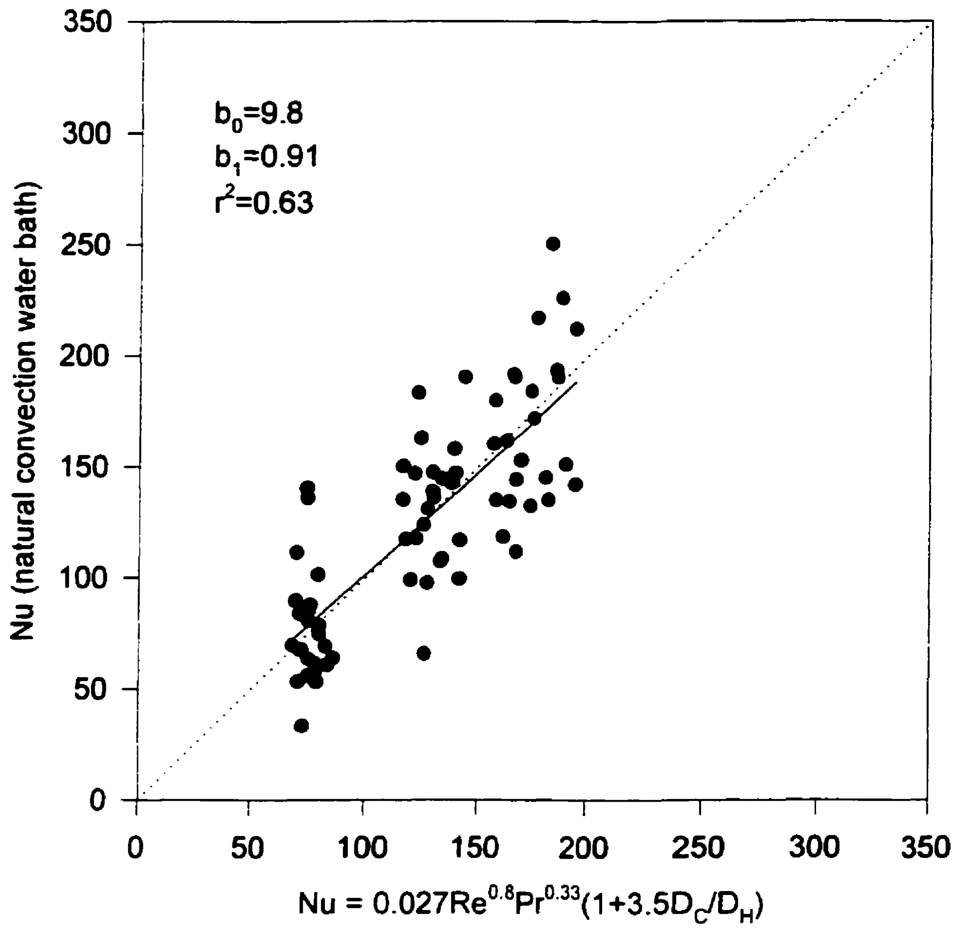

Figure 5.15. Correspondence between observed Nusselt number in forced . . convection water bath and that predicted from the Seider-Tate . . relations corrected by Jeschke's factor.

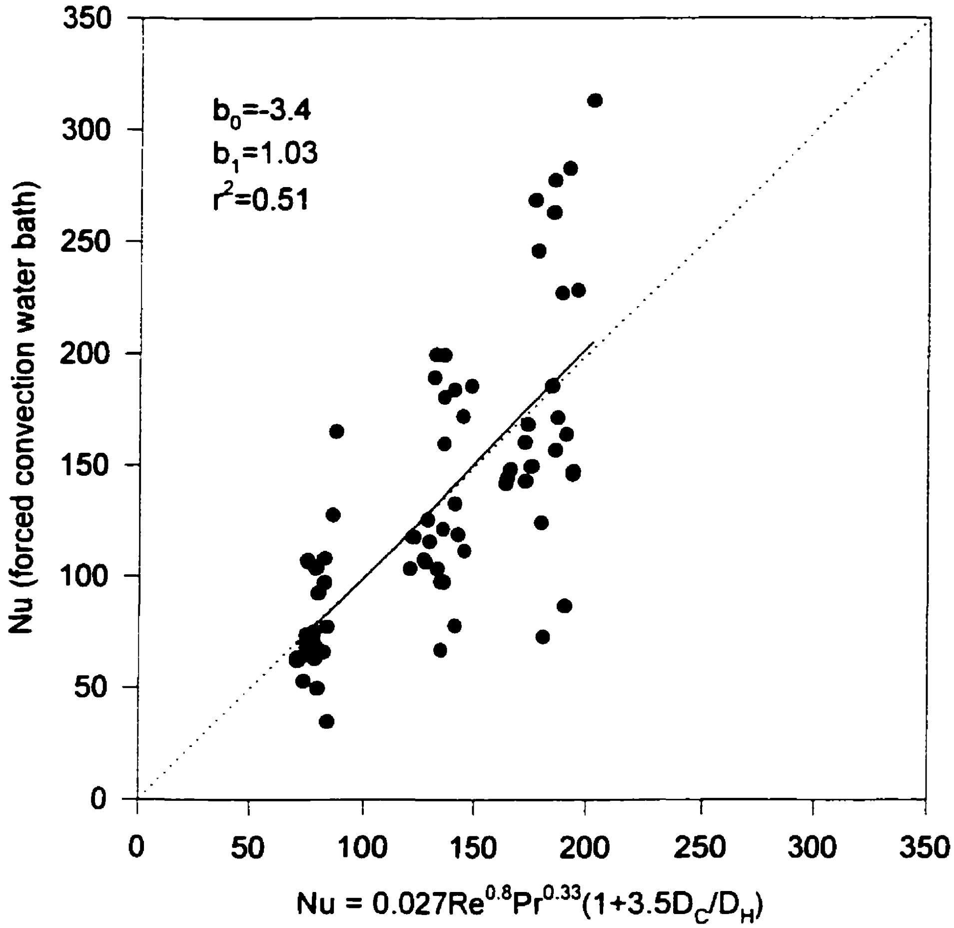

Figure 5.16. Correspondence between observed Nusselt number in natural convection water bath and that predicted from the Seider-Tate relations corrected by Jeschke's factor.

The results of this analysis are shown in Table 5.5, below.

Table 5.5. Summary of response surface regression analysis of the ratio of observed Nusselt number to that predicted by equation 5.3.

	REGIME					
	Forced Convection			Natural Convection		
Parameter	MS	Prob>F	Direction of effect	MS	Prob>F	Direction of effect
D_c	0.29	0.0025	+ve	0.23	<<0.0001	+ve
D_H	0.27	0.0048	+ve	0.17	<<0.0001	-ve
Bath Temp	0.039	0.75	-ve	0.076	0.0096	+ve
Flow Rate	0.019	0.95	-ve	0.101	0.0015	+ve
Torsion	0.37	0.0002	+ve	0.225	<<0.0001	+ve
Model R^2	0.45			0.74		
CV	26.2%			15.4%		

In the case of the forced convection water bath, the torsion, the tube diameter and the helix diameter all have a significant influence on the correspondence between the observed and predicted Nusselt numbers. Bath temperature and flow rate do not influence the correspondence in the forced convection regime, as one would expect given that the predicting equation accounts for flow rate through the Reynolds dependence and for temperature effects through the Prandtl number.

In the case of the natural convection water bath, all factors are significant, although torsion, D_C and D_H are the more influential. Moreover, the slopes of the least-squares fits in Figures 5.15 and 5.16 indicate that, on the average, eq. 5.3 underestimates h_i in the forced convection regime, but overestimates it for the natural convection regime. Again, the question arises as to what extent h_i may be increased by the circulation conditions of a forced convection water bath. Furthermore, the results corresponding to the forced convection water bath show that λ, D_C and D_H are not well accounted for in the predicting equation.

5.4 Comparison of Helical coil data with that of Straight tube.

Table 5.6 below gives the comparison of rise in temperature of the target fluid at different flow rates as affected by bath temperature and radius of curvature of the helix. A comparison is also made with straight tube results for similar bath temperature conditions. A higher rise in temperature of the target fluid was observed for higher bath temperature both in case of helical and straight tubes. Within helical coil heat exchanger, rise in temperature of the target fluid was higher with larger diameter of the helix. At the same time it is interesting to note that the Reynolds number was also higher under similar operating conditions. Higher Reynolds number could be expected because of the physical properties of the fluid persisted with different helix diameter. Difference in temperature of the targeted fluid between the inlet and outlet was dependent on the residence time of the liquid inside the processing tube. At the highest flow rate as the residence time of the fluid was short within the heat exchanger, a lower difference in temperature from inlet to outlet was observed. The least rise in temperature of target fluid was observed with straight tube at low bath temperature of 75° C and maximum flow rate of 12 l/min.

Table 5.6 Rise in temperature of the target fluid at different flow rates (Typical case)

Case Number	Rise in temperature of target fluid at flow rate of 4 l/min	8 l/min	12 l/min
H S 0 8 7	35.5 (7815)	35.3 (15630)	29.2 (20850)
H S 0 8 9	46.7 (9230)	48.4 (18465)	41.3 (26775)
H S 0 12 7	42.6 (9600)	42.5 (19200)	37.6 (24350)
H S 0 12 9	61.6 (10350)	60 .0(21715)	53.2 (26775)
St 7	23.5 (8762)	23.3 (17523)	12.5 (23592)
St 9	32.8 (9842)	35.9 (19685)	18 .0(23706)

Note: Numbers in bracket represent Reynolds number

H = helical coil tube heat exchanger

S = 13.5 mm internal diameter tube

0 = no pitch

8/12 = helix diameter, 203 or 305 mm

7/9 = water temperature in constant temperature bath, 75 or 95°C

St = straight tube heat exchanger

5.5 Nusselt number distribution on first turn of the coil along outer periphery:

At the beginning section of fluid entering the coil, the boundary layer formed is thinner in the first turn, and so the tube curvature has not significantly influenced the heat transfer. Observation made has shown that the heat transfer occurring in the first turn of the coil is almost equal to that of a straight tube setup of similar conditions. Such observations were also made by Merk and Prins (1953), Morgan (1975), and Xin and Eberdian (1996).

Following Table 5.7 gives the range of Nusselt number, Prandtl number and Reynolds number obtained on the outer periphery of the helical coil for a set of smaller tube of diameter 13.5 mm and of helix diameter 203 and 305 mm helix diameter operating at one pitch and different flow rates of 4, 8 and 12 l/min and is compared with that of a straight tube.

Table 5.7 Distribution and comparison of Nusselt number for a helical coil . . heat exchanger on the first turn with that of a straight tube heat . exchanger.

	Nu	Pr	Re
H S 1 8 7 4	15.92	6.88	6333
H S 1 8 9 4	13.99	6.77	6464
H S 1 12 7 4	17.48	6.69	6531
H S 1 12 9 4	16.65	6.11	7036
St 7 4	16.93	6.18	6958
St 9 4	17.82	5.41	7816
H S 1 8 7 8	23.08	7.33	11952
H S 1 8 9 8	23.20	6.88	12666
H S 1 12 7 8	13.92	6.69	13062
H S 1 12 9 8	34.53	5.79	14732
St 7 8	33.35	6.18	13916
St 9 8	39.95	5.38	15632
H S 1 8 7 12	28.03	7.00	18832
H S 1 8 9 12	33.78	6.88	19000
H S 1 12 7 12	33.64	6.97	18827
H S 1 12 9 12	37.70	6.90	19000
St 7 12	24.27	6.99	18735
St 9 12	26.73	6.93	18825

5.6 Comparison of experimental data with other studies

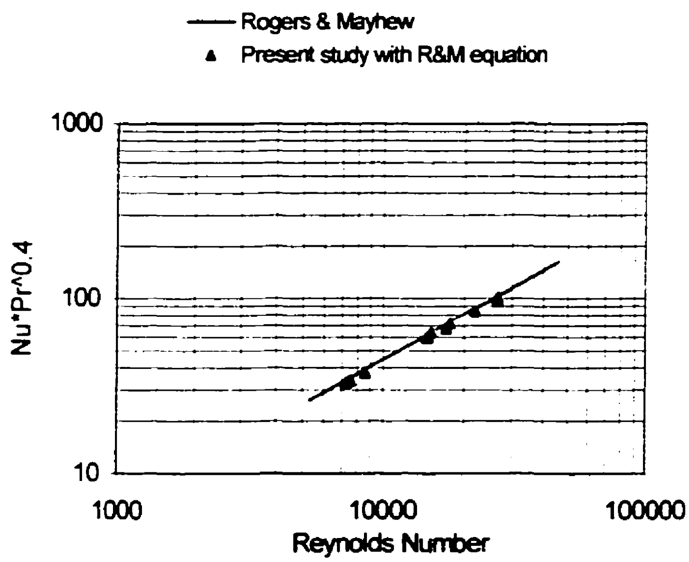

Figure5.17 Comparison of Nusselt number for water (Pr = 5)

The log-log plot of Nusselt number versus Reynolds number was made to estimate the dependency of the heat transfer on the Reynolds number and is compared with that of Rogers and Mayhew's (1964) experimental study. The empirical equation developed by them on heat transfer to water in terms of dimension less Nusselt number is of the form

$$Nu_f = 0.021 * \mathrm{Re}_f^{\ 0.85} * \mathrm{Pr}_f^{\ 0.4} * (d / D)^{0.1} \tag{5.4}$$

where suffix 'f' stands for the film temperature. In this data the properties of the fluid are evaluated at the film temperature and the average heat-transfer coefficient is based on the arithmetic average of the inlet and outlet temperature difference. Data obtained from the present study which had Prandtl number close to five was chosen for plotting and compared with other authers study which had water with Prandtl no. 5 in their analysis. By replacing the logarithmic mean temperature difference term with arithmetic mean temperature difference to calculate the heat transfer coefficient, Nusselt number was fitted to the above equation (Figure 5.17). The figure demonstrates that the results from present study agree well with Rogers and Mayhew (1964). With this validation one could suspect that the temperature distribution of the processing fluid inside the helical coil would follow the same pattern as shown by Yang and Ebadin (1996) who used k-ε model in his numerical study for modeling the convective heat transfer in a helical coil tube with substantial pitch for flow with turbulent behaviour (Figure 2.10). However discrepancy lies with the fact that while calculating the heat transfer coefficient Rogers and Mayhew (1964) have taken the arithmetic mean temperature difference between the liquid entering the heat exchanger and that while leaving the system. As the rise in temperature of the processing fluid is nonlinear from inlet to outlet of the heat exchanger, logarithmic mean temperature difference would be more appropriate to calculate and the Nusselt number value would decrease .

5.7 Comparison of Nusselt number distribution on outer and inner periphery at first turn of coil:

The outer and inner peripheral Nusselt number distribution on the first cross section are plotted in the Figure 5.18 shown below. Those in the dotted line represent that of smaller diameter tube and the one with larger diamet

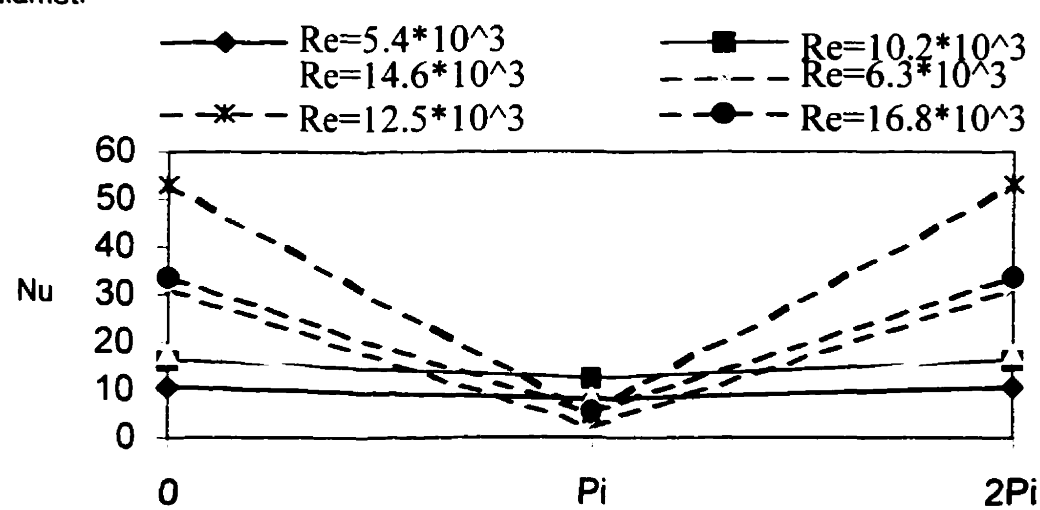

Figure 5.18 Peripheral distribution of local Nusselt number

Boundary layers formed are thicker on the inner periphery of the coil ($\psi = \pi$)than those on the outer periphery ($\psi = 2\pi$). As fluid enters the curved section of the tube because of the nature of flow due to restriction in the tube size and the thickness of boundary layer developed in case of smaller diameter tubes the Nusselt number will have a steep fall on the inner periphery of the tube compared to that with a larger diameter tube. Theoretical explanation for this is given by Yang and Ebadian (1996). Though there is variation in Nusselt number distribution along the inner periphery compared to outer periphery, the fall in distribution of Nusselt number is comparatively low with larger diameter tube. With this one could conclude that the boundary layer thickness formed is more uniform along the inner and outer periphery as the diameter of the tube increases, hence allowing a more uniform temperature distribution.

5.8 Local Nusselt number distribution along the length of coil:

Most of the research in the area of heat transfer from the tube to the fluid circulating inside have considered the variation of the Nusselt number in the axial direction, peripheral variation of Nu at a given axial position, thermal entry length, influence of a/R, influence of De,. However, the influence of pitch, which is an interaction factor for heat transfer has not been considered by any of the early researchers. This section gives a comparison of heat transfer to the fluid inside the pipe along the outer and inner periphery, as fluid travels from inlet to the outlet of the pipe.

A comparison of Nusselt number distribution along the length of coil from beginning to end on inner and outer periphery is made and is shown in the Figure 5.19 a, b below.

For a given cross section of the tube, the thermal boundary layer develops from the outer periphery region of the coil, and becomes thick on the inner periphery of the coil. Because of the curvature of the tube, the flow temperature and boundary layers are thicker on the inner periphery of the coil

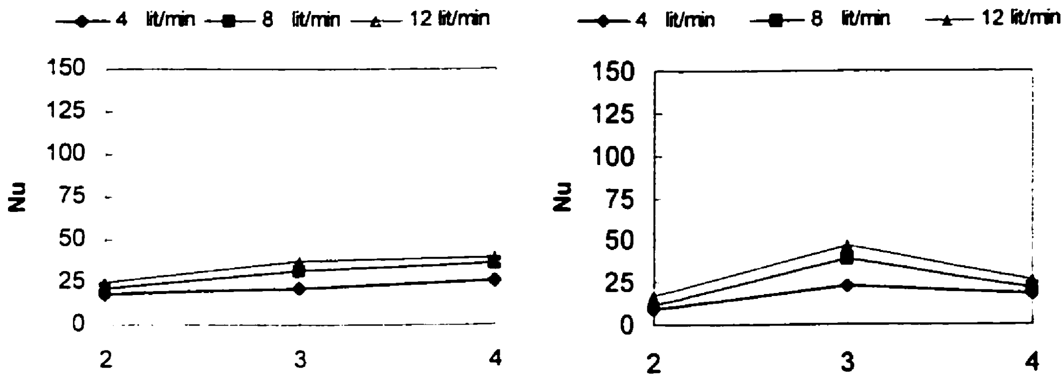

15.7 mm dia tube, 2 pitch, 203 mm helix dia

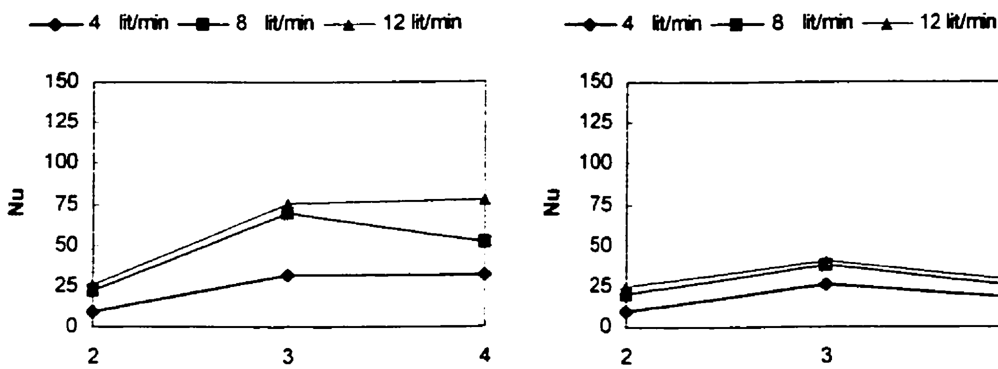

13.5 mm dia tube, 2 pitch, 203 mm helix dia

Figure 5.19 a. Variation of Nusselt no. along the length of the coil at different thermocouple locations (Natural Convection)

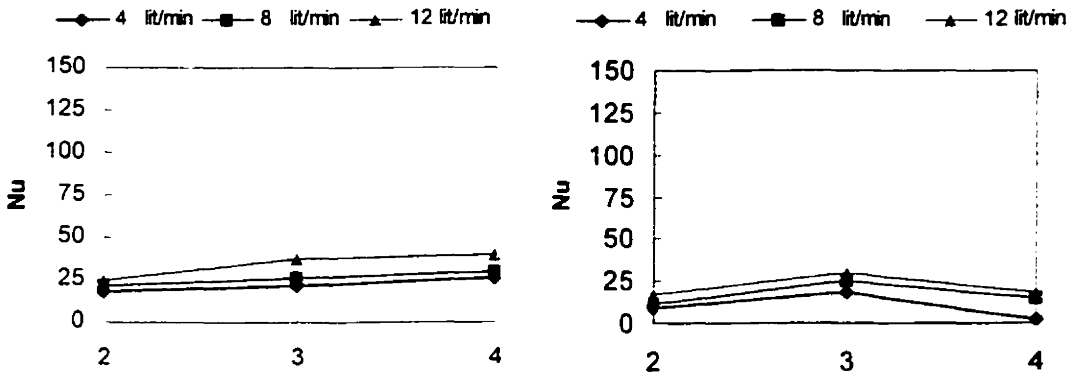

15.7 mm dia tube, 2 pitch, 203 mm helix dia

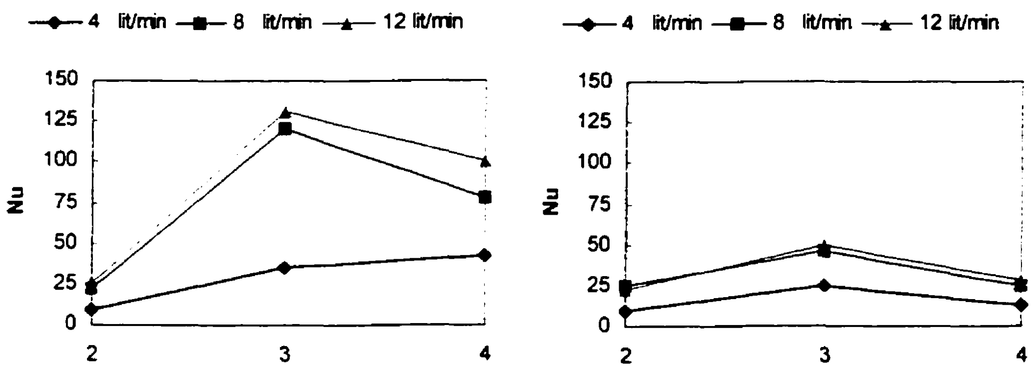

13.5 mm dia tube, 2 pitch, 203 mm helix dia

Figure 5.19 b. Variation of Nusselt no. along the length of the coil at different thermocouple. locations (Forced Convection)

($\psi = \pi$) than those on the outer periphery ($\psi = 2\pi$). Thicker the boundary layer lower the heat transfer. Thus, the Nusselt number on the outer periphery of the coil is always higher than on the inner periphery of the coil where little end effect exists. From Figure 5.19a, b one could see that there is an oscillatory behaviour of Nu number as the fluid travels along the length of the coil. This oscillation could be explained as the propagation of a step-change in temperature at the thermal boundary layer some distance from the entrance, which is due to the rapid transport of heat from the wall near the entrance energy which is driven around the tube periphery then back through the centre to meet the thermal boundary layer at the same peripheral position further down stream. The meeting of the warmer fluid with the wall causes a drop in thermal gradient and consequently, decreases in flux. Similar effect has been observed by Dravid et.al., (1971) Tarbell and Samuels (1973) and Patankar et al. (1974). Janssen and Hoogendoorn (1978) recognised the variablitty of results of previous workers and measured the heat transfer in several oils under a wide range of condition and with liquids of different viscosities. Their data also exhibited oscillations similar to those predicted by early workers. Since the data acquisition system did not have enough channels to permit measurement of coil surface temperatures at all turn of the coil, it was necessary to interpolate linearly using the available data at turns one and ten.

There are several general comments one might make with respect to these graphs. First, assuming that the flow rate is constant throughout the coil, the heat transfer coefficient should tend to increase from inlet to outlet end, based on the effect of the bulk fluid temperature, which increases throughout the length of the coil. This can be seen in Figure 5.20, where the Reynolds and Prandtl numbers relative to their values at a bulk fluid temperature of 10°C are plotted versus temperature. The Reynolds number increases at a faster rate than the Prandtl number decreases in this context.

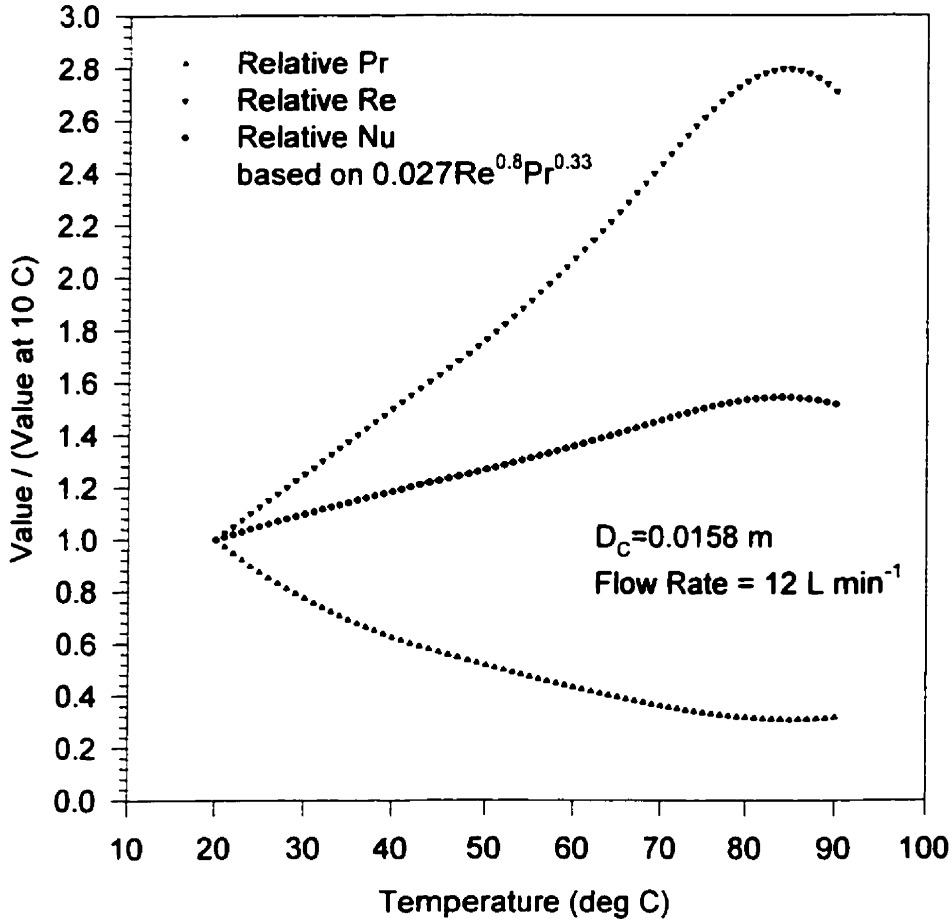

Figure 5.20. Variation of Reynalds and Prandtl numbers relative to the bulk temperature of the bath.

The relative estimate of the Nusselt number expressed in terms of Re and Nu ($0.027Re^{0.8}Pr^{0.33}$) is also seen to increase. The only factor that has been assumed to remain constant in the calculations is the flow rate used in calculation of the Reynolds number. It is based on the mass flow rate (kg s^{-1}), divided by the cross-sectional area of the coil. This element was calculated as mass flow rate based on estimates of the outputs of the three submersible pumps that were used, which were not calibrated for each coil. This may have introduced significant error in all of the downstream calculations.

Secondly , in order for this function to remain constant over the length of the coil, one would expect that the flow rate would decrease to a certain extent.

5.9 Conclusion:

The results obtained in the course of the experiments described in this chapter indicate that:

1) the flow characteristics of the carrier fluid may have an influence on the inner heat transfer; and conversely,

2) that the inner flow conditions influence the heat transfer characteristics outside the coil,

3) inducing greater mixing in the water bath lead to higher outside and higher overall heat transfer since in this setup, it was the outer heat transfer coefficient that was limiting.

4) there was significant effect of bath temperature in natural convection regime on heat transfer coefficient which was not there in forced convection conditions

5) existing engineering relationships do not adequately predict the heat transfer characteristics of helical coils, primarily because the interactions between pitch (torsion factor), tube diameter and helix diameter are not adequately represented.

VI EXPERIMENTAL DATA VERIFICATION

6.0 Introduction

Helical coiled pipes are effective as heat transfer equipment due to their compactness and increased heat transfer coefficients in comparison with straight tube heat exchangers. Helical coils are used for heat exchange in the air conditioning, nuclear power, refrigeration, and chemical engineering fields (Xin and Ebadian, 1996).

While the inside heat transfer coefficient can be compared to flow through a straight tube, the outside heat transfer can not be related directly to the flow around the outside of a tube of similar dimensions. At any given location on the outside of the coil, the heat transfer is influenced by the previous or subsequent turn. Thus, in natural convection conditions, the flow of the fluid on the outside is not due only to the local tube temperature difference, but also due to the momentum or pressure difference induced by the previous or subsequent turns. The horizontal helical coil may have a flow field similar to that of a vertical cylinder in which there are several relationships of the Nusselt number developed for laminar and turbulent natural convection. However, the flow conditions would be more similar to a vertical cylindrical shell. The natural convection in the inside of the helix would be considered to be confined space natural convection rather than free space natural convection (Xin and Ebadian, 1996). For the vertical helical coil, comparisons could be made with a horizontal cylinder, but the results would expect to deviate greatly as the pitch is increased, as the idealized cylinder would become more and more porous.

Much work has been preformed on the heat transfer coefficients in the inside of the pipe. However, little work has been reported on the outside heat transfer coefficients of helical coils. Ali (1994) obtained average outside heat transfer coefficients for turbulent natural convection heat transfer from horizontal (Note: what Ali (1994) considers vertical coils is considered as horizontal in this work) helical coils in water. Hot water was pumped through the helical coil and cooled by the water in a constant temperature water bath for two different diameters of the tube. Five different pitch-to-helical diameter ratios were used and two different number of coil turns. The total heat transfer was based on the difference of the inlet and outlet temperatures, the mass flow rate, and the specific heat of water. The overall heat transfer coefficient was calculated from

$$Q = UA\Delta T_{lm} \tag{6.1}$$

where T_{lm} is the log mean temperature difference between the bulk fluid in the tube and the water bath. All physical properties of the hot water in the tube were assumed to remain constant over the length of the coil and were evaluated at the average bulk temperature. Once the overall heat transfer coefficient was obtained, the outside heat transfer could be deduced from the following relationship

$$h_o = \frac{1}{\frac{1}{h_i} + \frac{A_i \ln\left(r_o / r_i\right)}{2\pi kL} + \frac{A_i 1}{A_o h_o}} \tag{6.2}$$

The inside Nusselt number was calculated based on the following correlation of Rogers and Mayhew (1964)

$$Nu = 0.023(\mathrm{Re})^{0.85}(\mathrm{Pr})^{0.4}\left(\frac{a}{R}\right)^{0.1} \tag{6.3}$$

where physical properties for the dimensionless numbers were based on the arithmetic mean of the bulk temperature of the fluid. Once obtained, all the parameters were known with the exception of the outside heat transfer coefficient. Once found, the outside Nusselt number was evaluated using the characteristic length as the length of the tube. A least squares method was used to relate the Nusselt number to the Rayleigh number (also based on a characteristic length equal to the total length of the tube). The following relationships were developed for outside diameters of 0.012 and 0.008 m, respectively.

$$Nu_L = 0.685(Ra_L)^{0.295} \tag{6.4}$$

$3\times 10^{12} \le Ra_L \le 8\times 10^{14}$

$$Nu_L = 0.00044(Ra_L)^{0.516} \tag{6.5}$$

$6\times 10^{11} \le Ra_L \le 1\times 10^{14}$

Ali (1994) stated that from the observations that h_o decreases slightly with boundary layer length for an outside diameter of 0.012 m while it increases rapidly with the boundary layer length for a diameter of 0.008 m. Ali (1994) also suggested that increasing the tube diameter for the same Rayleigh number and tube length will enhance the outer heat transfer coefficients. Xin and Ebadian (1996) state that the large behavior differences between different tube diameters in Ali's (1994) experiments is inexplicable. Neither of the expressions for the Nusselt number given above takes the pitch into consideration. However, Ali (1994) also used the data to develop the Nusselt relationship with the Rayleigh number based on the height of the coil, which considered both the pitch and the tube diameter. For an inner tube diameter of 0.012 m and for R/a ratios of 20.792, 13.923, and 9.914, the best power law fit obtained was

$$Nu_H = 0.257(Ra_H)^{0.323} \tag{6.6}$$

$6\times 10^{8} \le Ra_H \le 3\times 10^{11}$

As the exponent is just under 1/3, it indicates that h_o is decreasing very slightly or that it may be along the coil height (Ali, 1994). For a tube diameter of 0.008 m and R/a ratios of 19.957 and 9.941 two distinct regions were obtained, one for laminar flow and the other for turbulent flow. The following correlations were obtained for the transition region for both R/a ratios:

$$Nu_H = 0.016(Ra_H)^{0.433} \tag{6.7}$$

$2X10^{'} \leq Ra_{H} \leq 5X10^{''}$

$$Nu_H = 0.0023(Ra_H)^{0.494} \tag{6.8}$$

$3.5 \times 10^{8} \leq Ra_H \leq 7 \times 10^{10}$

From these correlations it can be deduced that h_o increases rapidly with H in the transition zone, unlike that in the laminar zone (Ali, 1994). Interestingly, Ali (1994) considered that there was a laminar, transitional, and turbulent regions in his experiments for an inner diameter of 0.008 m and correlated only for the transitional region. For the correlation of Nu_L the same data was used but it was not divided into the three zones but all considered in one correlation. If Ali (1994) is correct in deducing that three flow regimes exist for the diameter of 0.008 m using H as the characteristic length, then there should be three regimes when using the characteristic length as L, which is not consider in the correlation.

Ali (1994) also correlated the Nusselt number to the number of turns and the Rayleigh number, with L as the characteristic length for two R/a ratios for each tube diameter. Five and ten coil turns were used. The outside heat transfer coefficient was found to slightly decrease for an increasing number of turns with the same Rayleigh number for the inner diameter of 0.012m. For the 0.008 diameter tube, h_o was found to strongly increase with increasing number of coil turns.

Xin and Ebadian (1996) used three different helicoidal pipes to determine the outside heat transfer coefficients for vertical and horizontal natural convection in air-cooling of the coil. The tube wall was heated by passing a high dc current through the tube wall. Thus, as the radial temperature gradient was much larger than the axial gradient, it was considered that the boundary condition was a uniform heat flux on the surface. By measuring the power input to the tube the average heat flux was determined.

The calculations for the outside heat transfer coefficient of Xin and Ebadian (1996) were based on the difference between the heat flow through the wall and the heat transfer due to radiation. The temperature difference was based on the difference between the reference temperature and the wall temperature. Average Nusselt numbers were based on the average wall temperature, in which the variation in temperature was small compared to the overall temperature difference. The relationship of the Nusselt number as a function of the Rayleigh number was based on the outer diameter of the tube. The thermal properties of the air were based on the film temperature. Unlike the experiment of Ali (1994), the outer heat transfer coefficient was based on temperature measurements on the outside of the tube and not on a back calculation from the determination of the inside heat transfer coefficient. Xin and Ebadian (1996) found that the heat transfer for the first turn was similar to that of a single horizontal pipe as the boundary layer is thinner in the first turn and the curvature would have little effect. The local Nusselt numbers around the periphery were also similar to those of a single horizontal cylinder. Local Nusselt numbers were calculated for each turn on the coil. It was found that the local Nusselt numbers were lowest on the top of the tube and the highest on the bottom for all the turns except the final turn. The location of the lowest Nusselt number on the top is due to the thermal boundary layer that develops from the bottom and becomes thickest at the top. For the fifth and final turn, the lowest local Nusselt was seen to move towards the inner part of the tube. This could be due to the curvature of the tube so that the plume on the inside develops such that it converges along the helix axis. Xin and Ebadian (1996) also showed that for a coil of 10 turns, the Nusselt number decreased, increased, and then decreased again along the height of the coil. This increase could be caused by the transition from laminar to turbulent flow (Xin and Ebadian, 1996). The plume on the lower turns has two effects on the heat transfer from the upper turns. The first effect is to make the boundary layer thickness increase on the subsequent turns. Additionally, there is an increased initial velocity about the subsequent turns, which increases advective heat transfer. The effects on the second turn were dominated mainly by the increase in the boundary layer thickness, and hence decreasing the conductive heat transfer, whereas for the third and fourth turns the increased advection is becoming more important (Xin and Ebadian, 1996). Xin and Ebadian (1996) also showed the change in the Nusselt number along the height of the coil at each location on the periphery. It was shown that the top and bottom Nusselt numbers decreased slowly. The Nusselt numbers for the inner and outer positions were identical on the first turn but as the flow developed the Nusselt number on the inner became less than the outer and this difference increased along the height of the coil. The explanation for this is that due to the curvature the boundary layers would increase more quickly in the inside of the helix. The average Nusselt number was calculated for each of the test sections. It was found that the coil with 10 turns had higher average Nusselt numbers that the coil with similar dimensions but of only 5 turns and roughly a third of the pitch. The average Nusselt number for the two test sections with 5 turns was correlated with the Rayleigh number and the following empirical equation was obtained (Xin and Ebadian, 1996)

$$Nu_{o.d.} = 0.290\left(Ra_{o.d.}\right)^{0.293} \tag{6.9}$$

$4 \times 10^3 \leq Ra_{o.d.} \leq 1 \times 10^5$

It should be noted that this correlation cannot be directly compared to those of Ali (1994) as the characteristic length of Ali (1994) was used as the length of the coil and the height of the coil, and not based on the outer diameter.

Xin and Ebadian (1996) also studied the natural convection from the outside of helical coils for the case of a horizontal coil. They instrumented the coil to measure the peripheral Nusselt numbers at nine locations around one turn of the helix. The turn was in the middle of the coil. They showed that the variation in the Nusselt number along the peripheral was much smaller compared to the variation around the turn and hence the results were given in the variation of the Nusselt number around one turn by averaging the peripheral Nusselt numbers for each cross-section. The local Nusselt numbers were higher on the top and the bottom of the coil than on the sides. The average Nusselt number correlation obtained was the following (Xin and Ebadian, 1996)

$$Nu_{o.d.} = 0.318\left(Ra_{o.d.}\right)^{0.293} \tag{6.10}$$

$5 \times 10^3 \leq Ra_{o.d.} \leq 1 \times 10^5$

The two correlations of Xin and Ebadian (1996) showed that the average heat transfer coefficient of the vertical coil was about 10% higher than for the horizontal coil in the laminar flow regime.

Ali (1998) criticized the work of Xin and Ebadian (1996) stating that their correlation for the vertical orientated coil was not useful for practical applications as the correlation did not take into account the end effects which would be important to consider in real applications. Ali (1998) set up an experiment to measure the average Nusselt number for the whole coil, including end effects, for a coil exposed to air with constant heat flux. Ali (1998) calculated the average Nusselt number for each turn using temperature measurements at three locations (spaced 120° apart around the turn). The correlation between the Nusselt number and the Rayleigh number was based on the outer tube diameter as the characteristic length. The coils were made from electric stove oven replacement elements and coiled to the different helix sizes. Different heat fluxes between the ranges of 500 to 5000 $W{\cdot}m^{-2}$ were used. It was assumed that the heat flux was constant along the length of the tube and was equal to the total heat input divided by the total surface area. Ali (1998) used four different coils, each with the same inner diameter and outer diameter but with two different helix diameters and with 4 different number of turns, 4, 5, 6, and 8.

For the coil with three turns, the average Nusselt for each turn decreased for the first three turns and then increased for the fourth. The same general trend was found for each of the different heat fluxes used, ranging from 500 to 5000 $W \cdot m^{-2}$. Ali (1998) deduced from this that until up to turn 3 the boundary layer was increasing and causing the heat transfer coefficient to drop and then the 4^{th} turn was subjected to end effects. Ali (1998) stated that up to the third turn the flow was laminar and after this point the flow was transitional to turbulent. However, if the helix is setup for a constant heat flux, and there are no specific differences between the wall boundaries at each end, then the Nusselt number distribution should be symmetric about the middle turn. For example, if there was fluid flowing in the pipe that changed temperature along the tube and a constant heat flux was applied then it would be expected to go from laminar flow to turbulent flow along the helix axis. But with the given setup, it would be expected that both ends would be laminar and if turbulence existed that it would be in the middle portion of the helix. Ali (1998) used the same logic when showing laminar and transitional regions for the results of the other three coils as well. Intuitively, it would be expected that the onset of turbulence in a natural convection system would also be a function of the heat flux, with greater heat fluxes causing turbulence more readily. However, Ali (1998) indicates that the onset of turbulence is at the same turn for each of the different heat fluxes encountered. Ali (1998) correlated the Nusselt number as a function of the Rayleigh number for each of the different heat fluxes used. It was found that the Nusselt number decreased with increasing Rayleigh numbers. However, it must be considered that the determination of the relationship used only one size of tube diameter, which questions the value of these correlations for design purposes. It is true that the Rayleigh number varied, but what is the true effect of the tube diameter? That remains to be answered. However, the correlation for 5000 $W \cdot m^{-2}$ will be presented to compare with the correlation developed by Xin and Ebadian (1996).

$$Nu_{o.d.} = 4.988 \times 10^{45}\left(Ra_{o.d.}\right)^{-14.061} \quad (6.11)$$

$1531 \le Ra_{o.d.} \le 1567$

The range of Rayleigh numbers is very small since the tube diameter was not changed and only fluid properties determined the Rayleigh number. However, the pitch, the helix diameter, and number of turns were varied during the experiment. These changes were not taken into account and could have significantly affected the heat transfer coefficient. It appears that the true relationship between the Nusselt number and the outside heat transfer characteristics cannot be fully explained by a simple power law relation with the Rayleigh number, despite the linear relationships developed. The combination of low range of Rayleigh numbers, and the fact the Nusselt number was developed on only one diameter size greatly reduces the usefulness of these relationships of engineering design.

In all, the number of studies on the outside natural convection heat transfer is not sufficient to properly design heat exchange equipment and there exists a need for more studies involving different helical configurations and flow rates.

6.1 Objective

The objective of this experiment is to:

1) Measure the temperature distribution on the outside of the coil.
2) Determine the Nusselt number correlation for natural convection from a horizontal helical coil.

Both objectives are to be preformed on a fluid-to-fluid helical heat exchanger where the processing fluid is pumped through the tube and the carrier fluid is unmixed.

6.2 Materials and Methods

The general setup and equipment used is described in chapter III. The physical dimensions of the four coils that were used are given in Table 6.1. The first three coils were used to gather data for the development of the models of heat transfer and the fourth coil was used to validate the models. However, data from all four coils was used to determine the influence of the different parameters on the temperature distribution. The fluid was pumped through a set of horizontal coils using a positive displacement pump connected to a variable speed motor. The speed of the motor was adjusted to obtain the desired flow rates. The flow rates used were 0.10, 0.15, and 0.20 $kg \cdot s^{-1}$. These corresponded to Reynolds numbers in the range of 11 000 to 27 000, obviously in the turbulent flow regime as the critical Reynolds numbers were 7756 and 8401 for the tube diameter to helix diameter ratios of 0.052 and 0.067, respectively, based on the correlation of Ito (1959). The purpose of using different flow rates was to change the temperature distribution along the tube, as this was a fluid-to-fluid heat exchanger. The flow of the water in the coil was from the top of the coil to the bottom. Tap water was used for both the processing fluid and the heat carrier. The water in the bath was heated using four 5 kW heating elements that were controlled with an on-off PID controller. The water in the bath was not stirred or pumped, however the heating elements may have caused some fluid movement due to buoyancy effects.

Temperature measurements were made using type K (nickel-chromium vs. nickel-aluminum) thermocouples with 30-gauge extension wire. The temperatures were recorded with DATAshuttle Express (StrawberryTree, Sunnyvale, CA) data acquisition system. This system had 16 analog inputs with a 13-bit resolution. Temperature measurements were recorded at a rate of 1 Hertz. Two thermocouples were used to measure the water inlet temperature, 4 for the water bath temperature, and 10 for the outside surface temperature of the coil, one on each turn. The outlet temperature was measured using a type-k thermocouple attached to a handheld temperature display. The location of the thermocouples is shown in Figure 6.1. The bath temperature was measured in four locations, two in the center of the coil and two outside the coil.

The total amount of heat transferred were calculated based on the mass flow rate, inlet and outlet temperatures, and the specific heat of the processing fluid. The outside heat transfer coefficient was calculated by the relationship

$$h_o = \frac{q}{A_o \Delta T} \tag{6.12}$$

The modeling of the heat transfer coefficient in such a situation is open to interpretation. The area that is used should be the effective area of heat transfer. For a straight pipe this is obviously the length multiplied by the circumference. However, with a helix of no pitch, it resembles a hollow cylinder with ribs, and thus the effective heat transfer area would be the helix circumference multiplied by the height of the helix. As the pitch is increased, it would be expected that the effective heat transfer area would be the length of the tube multiplied by the circumference of the tube. Both configurations were used to develop the heat transfer coefficients calculation in this study. The corresponding dimensional length in the Nusselt number (and the Grashof number) would reflect the choice of area used in the heat transfer coefficient determination. The characteristic lengths that were used included: the tube diameter, the helix diameter, the total height of the helix, and the effective height of the coil. The Nusselt number was modeled as a function of the Grashof and the Prandtl number in the following form

$$\mathrm{Nu} = a(\mathrm{Gr}\,\mathrm{Pr})^b \tag{6.13}$$

which is a general form used in most Nusselt number correlations for natural convection systems. The symbols *a* and *b* are empirical constants based on experimental data.

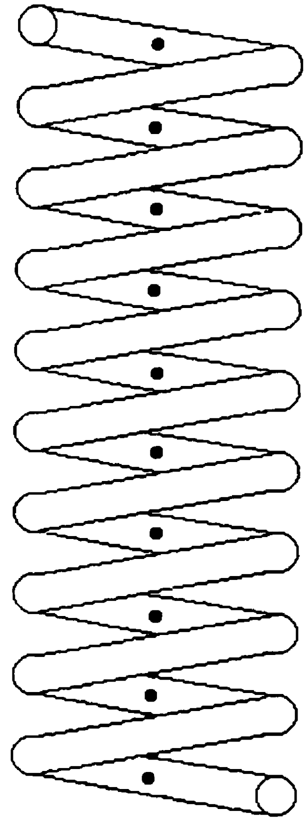

Figure 6.1 Location of thermocouples on inner and outer surface of the coil

The fluid properties used in the Grashof and Prandtl numbers were based on the mean film temperature as discussed by Holman (1992). The specific heat of the processing fluid was based on the average bulk temperature of the fluid. All fluid property values were based on interpolation functions that were generated from data from Holman (1992).

6.3 Results and Discussion

The orientation of the coil and the direction of the flow in the coil affect the natural convection from the coil. As well, if the coil is being heated or cooled by the carrier fluid will make a difference on the direction of the natural convection currents. In this case, the bath temperature was hotter than the outside temperature of the coils, and hence, fluid would be cooled at the edges of the coil and tend to flow downwards, which would result in an up-flow away from the coil. However, as the cold processing fluid entered the coil at the top and was heated as it flowed down through the coil, the temperature of the coil tended to increase from the top of the coil to the bottom. Thus, as the carrier fluid was cooled at one turn and began to drift downwards, it would encounter the next tube that tended to heat it up again. Thus, it is not easy to predict the direction of the flow, as there are influences that would tend to make it flow in opposite directions. However, if the direction of the processing fluid had been reversed, it would have been obvious that the direction of the flow would have been downward, as the fluid flowing downwards would be further cooled, and in effect would increase its tendency to descend.

Figures 6.2 through 6.5 show the temperature on the outside surface of the coil for each turn. Each graph shows the data points for 6 trials, for the combinations of three flow rates and two water bath temperatures. Figures 6.2 and 6.3 are for the same coil except that in Figure 6.3 it was stretched to obtain a pitch of 2. Both graphs show a linear increase of temperature along the length of the coil. Table 6.2 shows the temperature gradients for each of the trials show in Figures 6.2 through 6.5. The gradients are based on (a) the temperature change per turn, (b) temperature change per distance from one turn to the next, and (c) the temperature change per unit length of coil. For coils 3 and 4, some of the data points were thrown out due to obvious errors in the data acquisition. The calculations for the temperature gradients were evaluated with the data that was deemed reliable for these two coils.

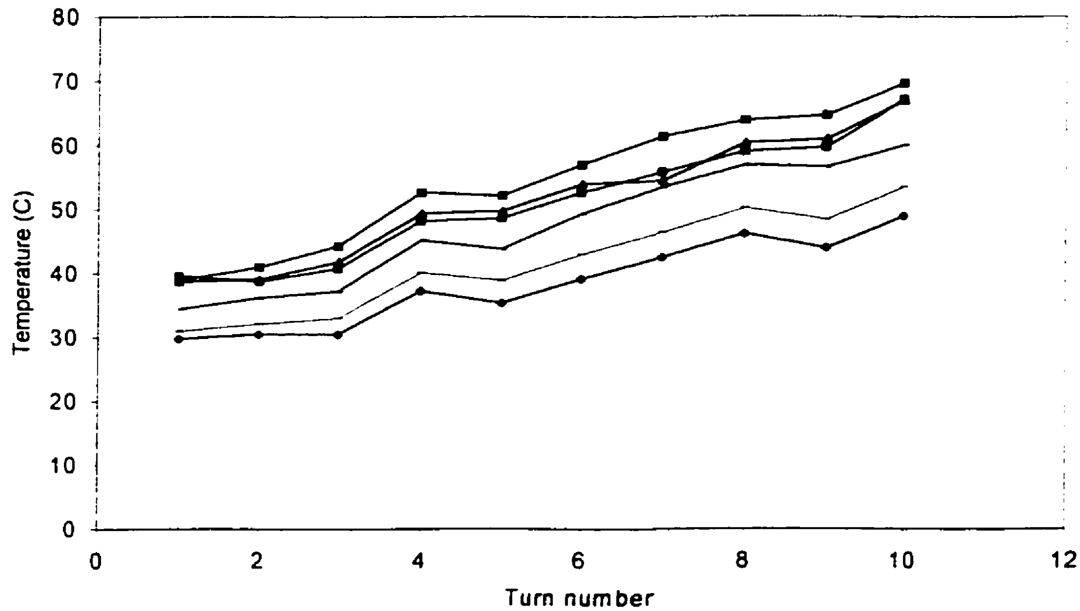

Figure 6.2 Temperature measurements on the outside of coil 1 for each turn

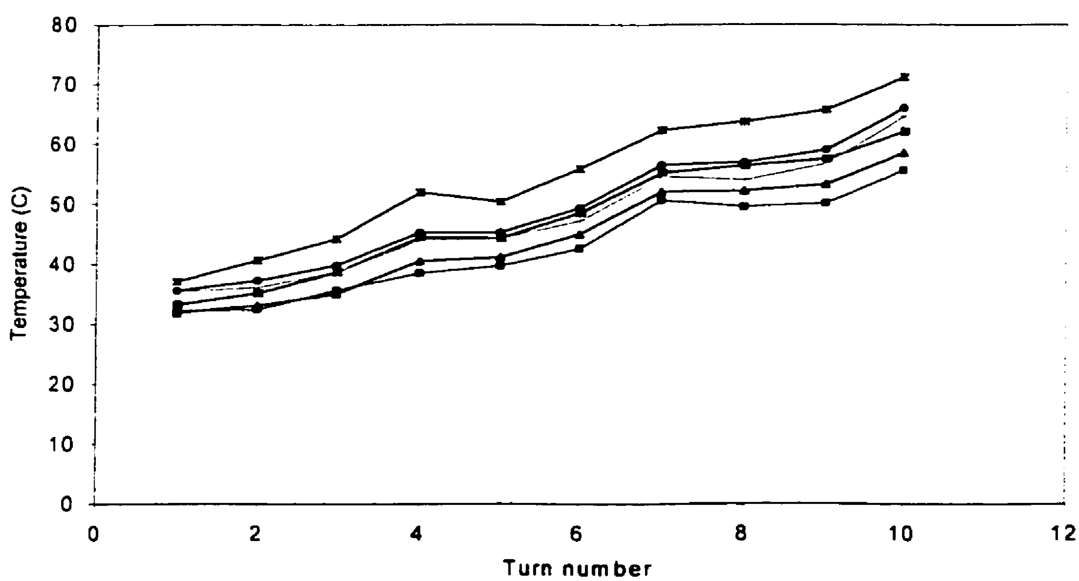

Figure 6.3 Temperature measurements on the outside of coil 2 for each turn

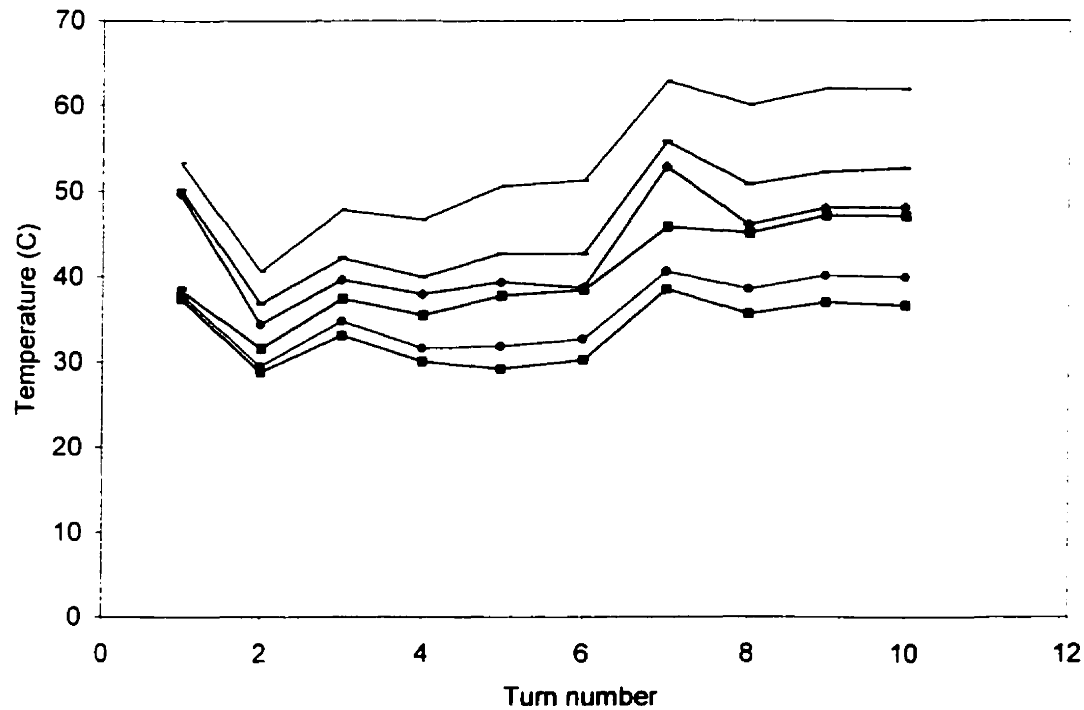

Figure 6.4 Temperature measurements on the outside of coil 3 for each turn

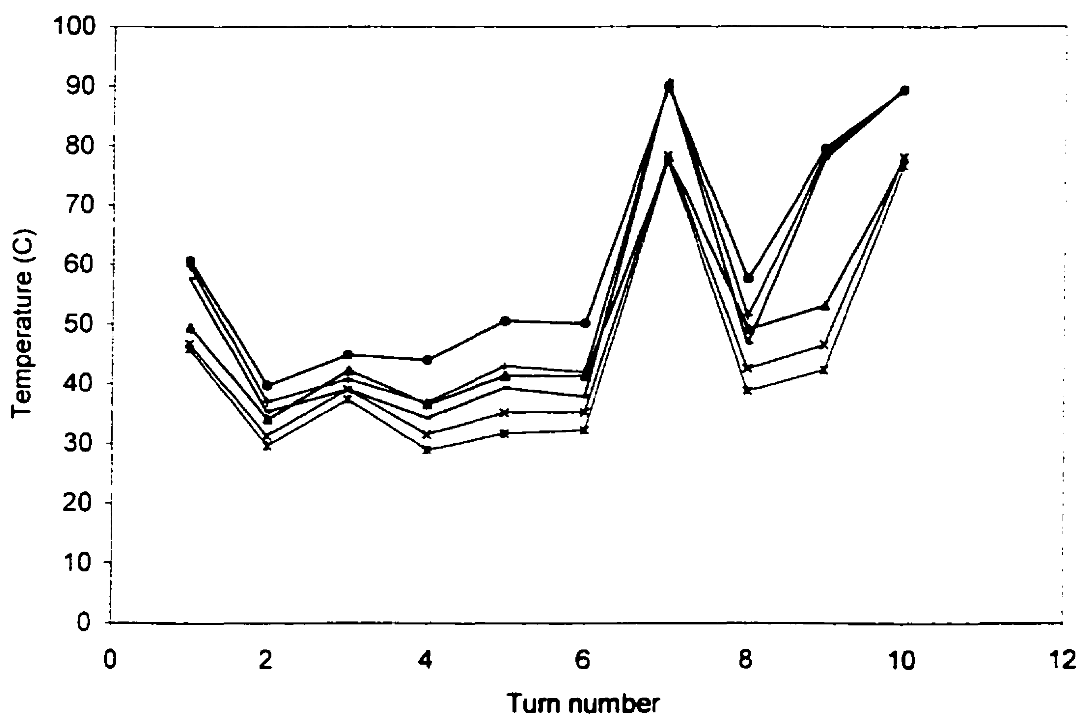

Figure 6.5 Temperature measurements on the outside of coil 4 for each turn

Figure 6.6 shows a plot of Nusselt number versus the Rayleigh number. The characteristic length taken in both the Nusselt number and the Rayleigh number is the diameter of the tube. The validation of this model is shown in Figure 6.7 where the predicted Nusselt number based on the model is plotted against the observed Nusselt number. It can be seen that the model underestimates the Nusselt number. The percent differences for the prediction and the observed for water baths of 75 and 95 were 27.33 and 33.73 percent, respectively. The higher observed, and predicted, Nusselt numbers were for the bath temperature of 95°C. In general, it would be expected that the higher bath temperature would result in a higher Nusselt number for the same inlet conditions, which were fairly constant for this experiment. The larger temperature difference would result in greater buoyancy forces to drive the flow. This higher mass transfer on the outside of the coils would increase advection, effectively increasing the heat transfer ability. However, Figure 6.7 also shows that changing the flow rate had a slight effect on the model, but not drastic. The lower flow rates in the inside of the tube resulted in the higher Nusselt numbers. Interestingly, this only held true for the smaller coil. For the larger coil, the opposite was observed, with an increase in the flow rate causing an increase in the Nusselt number, except for one case where the 9.1 kg/s flow rate resulted in the lowest Nusselt number and the 6 kg/s flow rate had the highest Nusselt number. Figure 6.8 shows the Nusselt number plotted against the flow rate in the tube. It shows that changing the bath temperature has more of an effect on the Nusselt number than changing the flow rate. Both changes are in effect doing the same thing, but at different levels of magnitude. A change in the water bath temperature increases the convective currents around the coil, due to an increased temperature difference. The same thing can happen with the flow rate. By changing the flow rate, the temperature distribution along the tube will be changed, and hence, the temperature difference outside the coil, which is responsible for the buoyant forces, will also be changed. The correlation developed for this Nusselt number relationship is:

$$Nu = 0.0052 Ra^{0.521} \qquad (6.14)$$

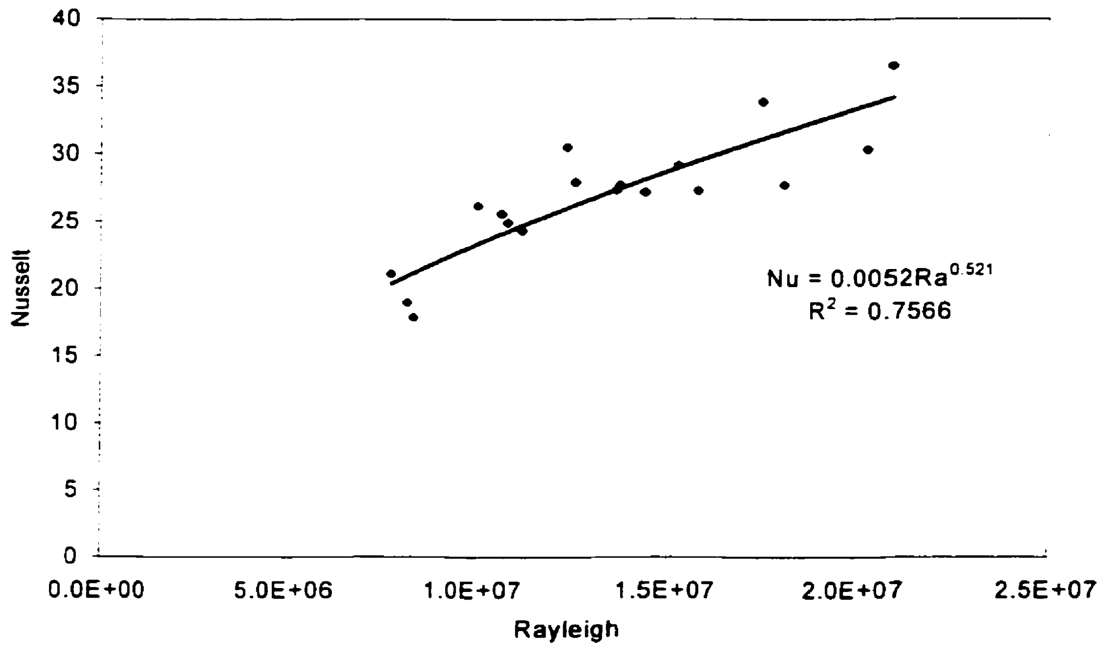

Figure 6.6 Nusselt versus Rayleigh based on a power law distribution

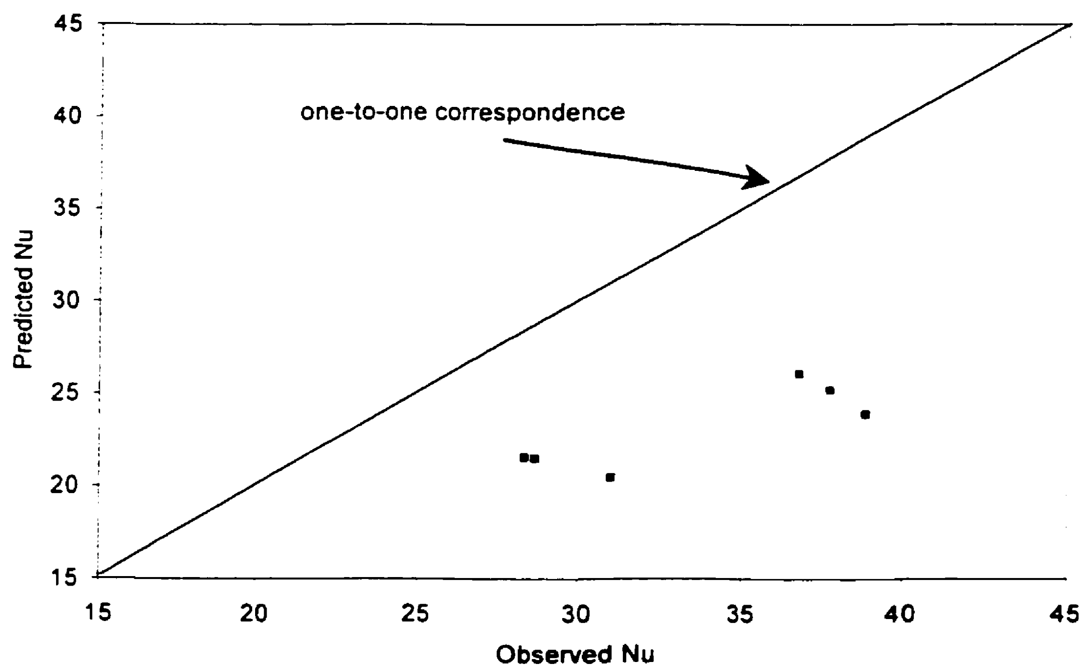

Figure 6.7 Predicted versus Observed Nusselt number for validation of power law distribution for coil modeled with tube diameter

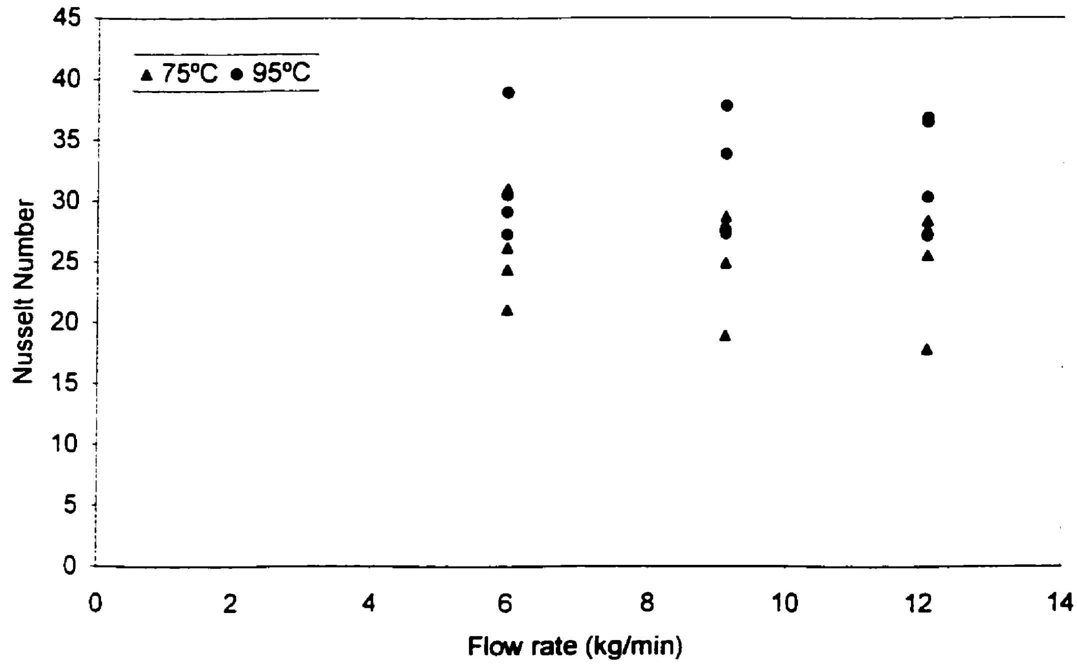

Figure 6.8 Nusselt number versus flow rate for different bath temperatures

Increasing the bath temperature increased the Nusselt number by 22.97, 6.26, 31.85, and 22.40 % for coils 1, 2, 3, and 4, respectively. It should be noted that coils 1 and 2 are the same coil but at different pitches, as are coils 3 and 4. Percentage wise, the Nusselt number increase due to the increase in temperature is greater with 2-pitch for the 12-inch coil, while it is greater for the no pitch 8-inch coil.

The heat transfer from the coil was modeled with the assumption that the flow around the coil would be similar to that of a vertical cylinder with a diameter equal to the diameter of the helix. The Nusselt number and the Rayleigh number were both based on the total height of the coil. Figure 6.9 shows the relationship between these two parameters. There is a distinct difference between the two pitches. However, it must be considered that in the Grashof number, the characteristic length, which in this case is the height, is cubed. Thus, when the

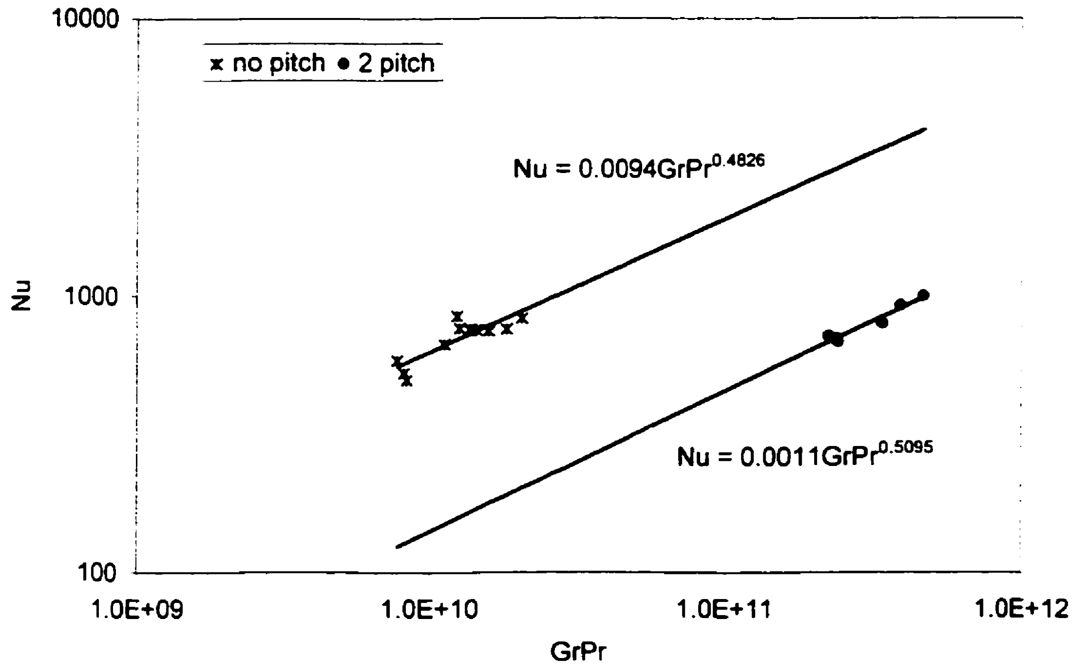

Figure 6.9 Nusselt versus Grashof-Prandtl for coil model as a vertical cylinder

total height is used, and the pitch is greater than 1, the actual height which is contributing to heat transfer and the total height of the coil is different. The choice to use the total height for the characteristic length in the Grashof number is based on the length available for the buoyancy and the viscous forces to act. The correlations developed were the following for the no pitch and the 2-pitch coils, respectively:

$$Nu = 0.0094Ra^{0.4826} \tag{6.15}$$

$$Nu = 0.0011Ra^{0.5095} \tag{6.16}$$

The main difference between these two correlations is the constant that is multiplying the Rayleigh number. The power is nearly the same for both.

Figure 6.10 shows the plot of the predicted Nusselt versus the observed Nusselt numbers for the model based on the height of the coil. The values are under-predicted by 25.83 and 32.25 % for water bathes of 75 and 95°C, respectively. This graph also shows the slight effect of the flow rate on the Nusselt number. However, it could be seen that the bath temperature has a much larger effect.

The helical diameter was used as the characteristic length to model the heat transfer from the coil. The area available for heat transfer was assumed to be the height of the coil multiplied by the helix diameter. This was used in the calculation of the heat transfer coefficient, and hence the Nusselt number. The characteristic length in both the Nusselt number and in the Rayleigh number was the helix diameter. The correlation developed with this characteristic length was:

$$Nu = 0.0417 Ra^{0.4153} \tag{6.17}$$

Figure 6.11 shows the plot of Nusselt number versus the Rayleigh number for this characteristic length.

The model validation is shown in Figure 6.12. The values of the Nusselt number are under-predicted by 28.11 and 36.30 % for the water baths of 75 and 95°C, respectively. The major flaw with this model is that using the helix diameter, as the characteristic length does not truly represent the physical significance of the Rayleigh number. It would work fine if the coil was mounted horizontally, as then the comparison could be made with a horizontal cylinder.

When modeling the coil as a vertical cylinder, the pitch posed a problem, as correlations had to be made for both the no-pitch and 2-pitch cases. To avoid this problem, another model was developed based on the effective height of the coil. This effective height was the actual height of the coil if non-stretched, regardless of the pitch. The correlation developed was the following:

$$Nu = 0.005Ra^{0.5112} \tag{6.18}$$

The Rayleigh number is raised to a power quite similar to the other models. It seems that changing the characteristic length does not have a great effect on the power but does on the constant. However, it must be kept in mind

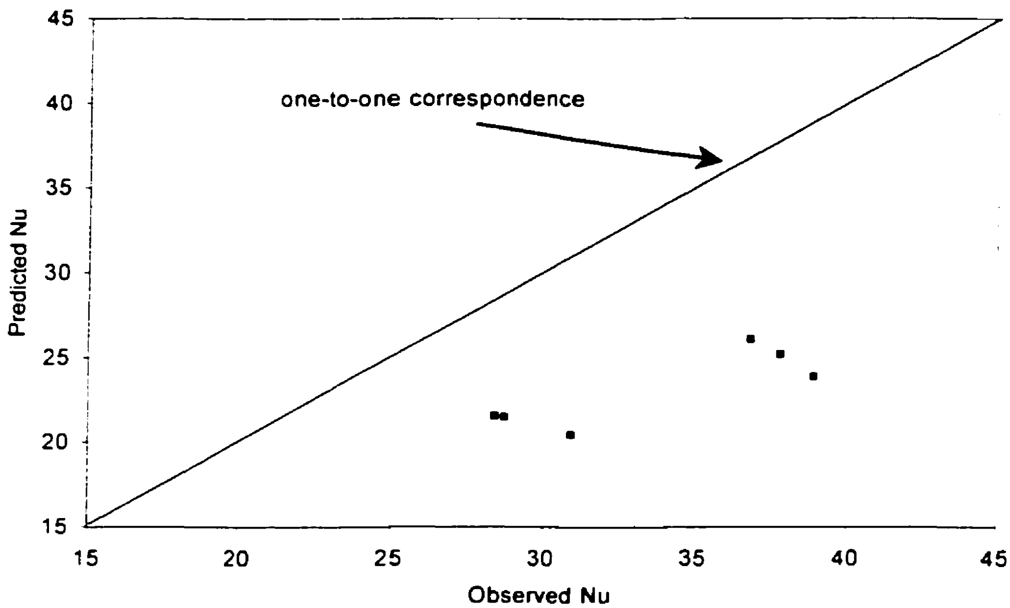

Figure 6.10 Predicted versus Observed Nusselt number for validation of power law distribution with coil model as a vertical cylinder

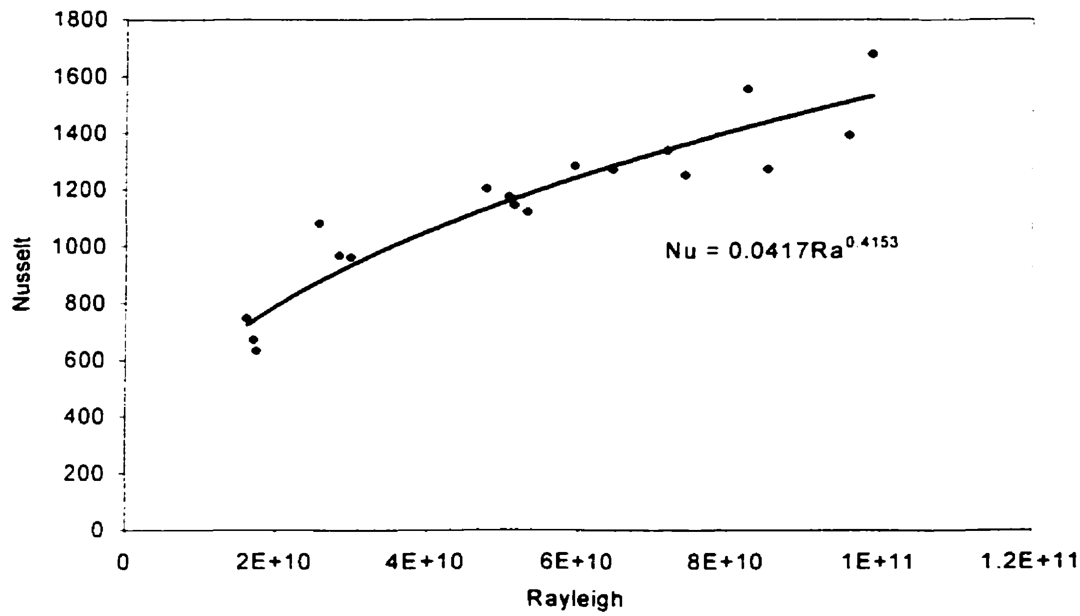

Figure 6.11 Nusselt versus Rayleigh for coil model using helix diameter

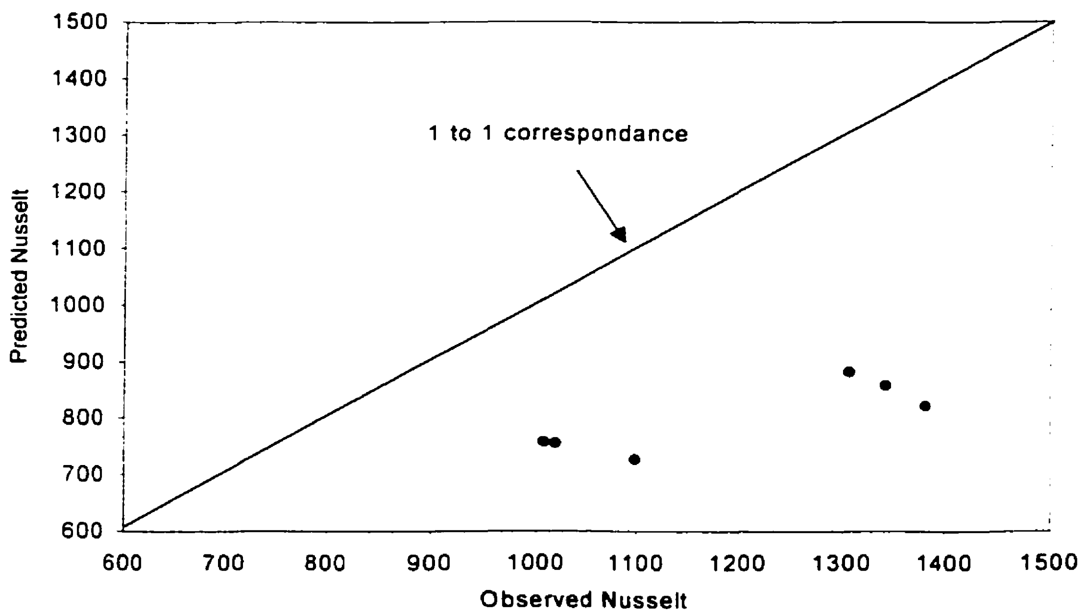

Figure 6.12. Predicted versus Observed Nusselt number for validation of power law distribution with coil modeled with the helix diameter.

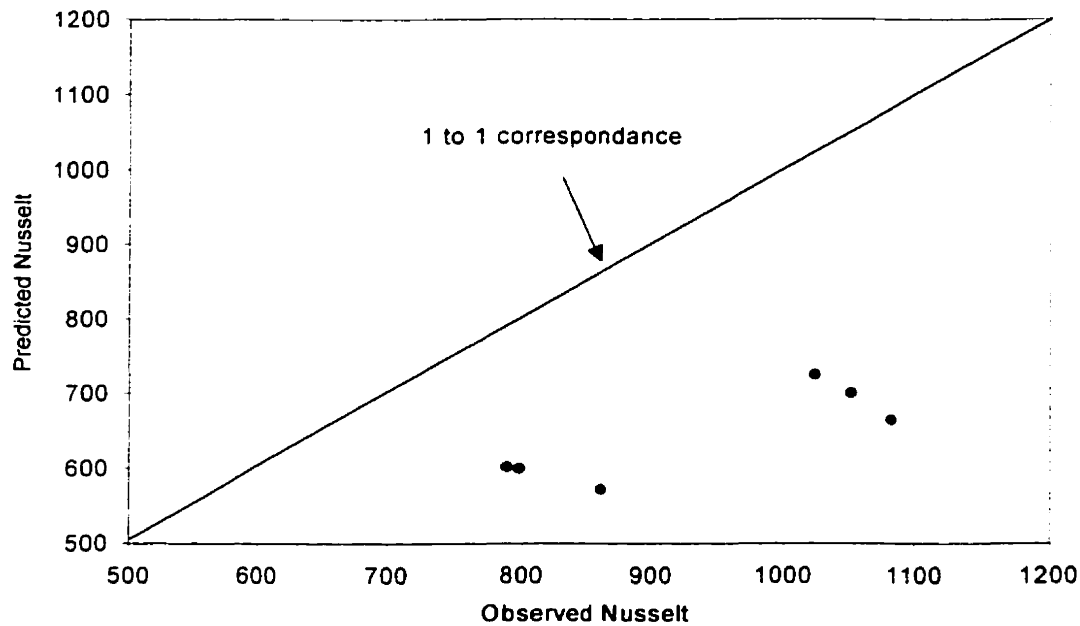

Figure 6.13 Predicted versus Observed Nusselt number for validation of power law distribution with coil modeled with the effective height

that there is not a great variance in the characteristic lengths and this may mask the effect of the characteristic length on the power. Figure 6.13 shows the results of the validation of this model. Similar to the other models, the Nusselt number was under-predicted by 27.36 and 33.61 % for water baths of 75 and 95°C.

6.4 Conclusion

The models developed in this experiment all followed the same trend, despite the fact that the characteristic length was changed in the models. The Nusselt number was under-predicted in all cases by 25 to 37 % for water baths of 75 and 95°C, respectively. The flow rate inside the tube was shown to have a slight effect on the Nusselt number, but not great. The reason for this effect is due to the change in the temperature gradient along the length of the tube. This effect is therefore accounted for in the temperature difference used to calculate the Rayleigh number. It is not conclusive which method is best for the determination of the Nusselt number for different dimensions of the coil. However, in this experiment, the best results for the validation came from the model that was based on the total height of the coil. This model had only been developed for the 2-pitch case as there were two distinct groups in the Nusselt-Rayleigh plot, one for each pitch. It may be possible to develop a similar relationship that also takes into account the pitch. Such a model would have the pitch (non-dimensional) as a multiplying factor in the Nusselt-Rayleigh function. This could be incorporated as the power in the equation seems to be somewhat constant, that is, it is independent of the pitch. However, more than two pitches would have to be used to determine the functionality of the multiplying factor.

Table 6.1 Coil dimensions used in the experiment

Coil	Tube diameter (mm)	Helix diameter (mm)	Pitch (mm)
1	15.8	305	31.6
2	15.8	305	0
3	13.5	203	0
4	13.5	203	27.0

Table 6.2 Temperature gradients

Coil	Flow rate (kg/s)	Bath Temp (C)	Temp/turn (C)	Temp/height (C/m)	Temp/length (C/m)	Temp/flow rate (C/kg/s)
1	6	75	3.05	55.86	3.18	0.53
1	9.1	75	2.58	47.33	2.70	0.30
1	12.1	75	2.22	40.62	2.31	0.19
1	12.1	95	3.11	57.01	3.25	0.27
1	9.1	95	3.16	57.80	3.29	0.36
1	6	95	3.47	63.56	3.62	0.60
2	12.1	75	2.68	147.37	2.80	0.23
2	9.1	75	3.06	167.95	3.19	0.35
2	6	75	3.28	180.34	3.43	0.57
2	6	95	3.73	205.20	3.90	0.65
2	9.1	95	3.33	182.92	3.47	0.38
2	12.1	95	3.14	172.71	3.28	0.27
3	12.1	75	0.98	61.83	1.54	0.13
3	9.1	75	1.27	80.02	2.00	0.22
3	6	75	1.92	120.49	3.00	0.50
3	12.1	95	1.67	105.18	2.62	0.22
3	9.1	95	2.00	125.65	3.13	0.34
3	6	95	2.66	167.36	4.17	0.69
4	12.1	75	1.44	30.11	2.25	0.19
4	9.1	75	1.80	37.70	2.82	0.31
4	6	75	2.36	49.56	3.71	0.62
4	12.1	95	1.607	33.69	2.52	0.21
4	9.1	95	2.18	45.61	3.41	0.37
4	6	95	2.82	59.18	4.43	0.74

VII HEATING OF VISCOUS MINERAL OILS IN AN IMMERSED HELICAL-COIL

7.0 INTRODUCTION

Helical coil heat exchangers are used in many industrial processes because they can provide better mixing and higher heat transfer coefficients than straight-tube heat exchangers. This can result in significant savings in time, energy and/or space requirements for thermal processing. The heat transfer in a coil can be estimated as a function of the straight tube case and the ratio of tube diameter, D_C, to helix diameter, D_H:

$$h_H = (1 + 3.5\, D_C/D_H)\, h_{st} \qquad (7.1)$$

where h_{st} is the heat transfer coefficient in a straight tube, all other parameters being equal (i.e. fluid characteristics and flow rate). Various authors (Haraburda, 1995; Patil et al.1982) have described design procedures for helical exchangers based on this correction, having estimated h_{st} using the appropriate Seider-Tate relationship for the flow regime. For a 13.5 mm diameter tube and a 203 mm helix diameter, the correction amounts to a 22% higher heat transfer coefficient inside the coil. However, it should be noted that in terms of the improvement of the overall heat exchange coefficient h_t, the effect depends on how close the inner and outer h's are, and on which is the larger, as embodied in the fundamental resistance relationship for tubes:

$$h_n = \frac{1}{\dfrac{1}{h_i} + \dfrac{A_i \ln\left(r_o/r_i\right)}{2\pi k L} + \dfrac{A_i 1}{A_o h_o}} \qquad (7.2)$$

An illustration of the relationship between the overall heat transfer coefficient and the inner heat transfer coefficient is given in Figure 7.1 for fixed wall conductivity and thickness and fixed outside heat transfer coefficient. Improvements in h_i result in rapid increase in h_t when h_i is limiting.

However, once h_i becomes larger than h_o, improvements in h_t decrease asymptotically towards the value of h_o.

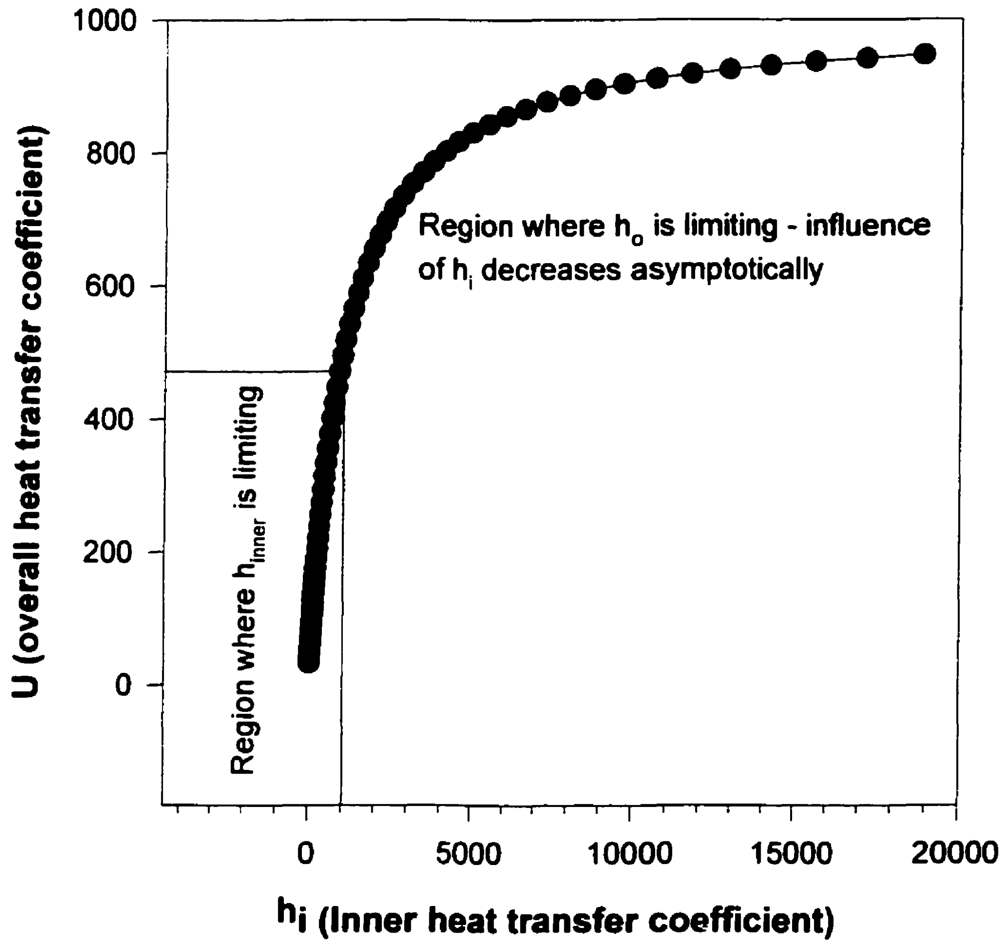

Figure 7.1 Relation between h_t and h_i for h_o =1000 and x/k_c = 350000.

There is a substantial literature on the flow patterns and temperature distributions in helical coils. Some work has focused on convection away from a coil (eg. Ali, 1994; Xin and Ebadian, 1996), but most of the recent literature is concerned with the inner heat transfer coefficient. In the latter case, experiments have been done in setups where there is no external fluid transfer. Heat to the coil surfaces has been provided by electrical resistance wires and the assemblies are insulated such that air movement on the outside of the coil is negligible. Although research of this kind has provided valuable information for applications involving radiative transfer to the coil (eg. microwaves, induction) not requiring carrier fluids, it is not clear as to what extent the relationships developed on those bases would apply to a fluid-to-fluid heat exchanger.

The objectives of this study were therefore to study the heat transfer coefficients associated with fluid-to-fluid heat exchange through copper helices and evaluate the relevance of equations proposed for design of helical fluid-to-fluid exchangers.

7.1 RESULTS AND DISCUSSION

7.1.1 Viscosity of the Oils

It was found that the viscosities were substantially different (Figure 7.2 a, b), P005 having a viscosity at 20°C that is over an order of magnitude less than the others.

a) the viscosity of oil at 23°C prior to use;

b) the viscosity at 23°C after having been heated to the temperature shown in parentheses, cooled to 10°C, stored for one day, then equilibrated to 23°C;

c) after 9 runs through helix at various operating conditions (Table 7.2), stored at 10°C, then reheated to shown temperatures and equilibrated to 23°C.

The viscosity of the oils was also determined at 23°C after they had been used in the experiments. The data is presented in Table 7.1:

Table 7.1 Dynamic viscosity (Ns/m^2) of petroleum base oils at 23°C

	(a)	(b)			(c)		
	23°C	20°C	60°C	80°C	20°C	60°C	80°C
P005	0.0017	0.0014	0.0012	0.0013	0.0011	0.0011	0.0011
P022	0.0180	0.0170	0.0170	0.0160	0.0160	0.0160	0.0160
P032	0.0560	0.0480	0.0500	0.0500	0.0400	0.0400	0.0400

Within the limitations of experimental error, it appears that there is some loss in viscosity due to usage. After heating once and recooling, the reduction in viscosity didn't change much. A significant difference in viscosity was observed after heating the oil for several times. Further work would be needed to verify the extent and reasons for viscosity loss.

7.1.2 Heat Exchange

The overall, inner and outer heat transfer coefficients were calculated for each experimental run, as given in Table 7.2. The overall coefficient was obtained using the difference between bath temperature and mean temperature of the fluids inside the coil. The inner heat transfer coefficient was based on the difference of the mean outer surface temperature of the coil and that of the fluid inside, whereas the outer coefficient was based on the difference between bath temperature and outer surface temperature of the coil. The Reynolds and Prandtl numbers were also computed in order to permit evaluation of the data in the non-dimensional framework common to heat and mass transfer. However, it should be noted immediately that the Re numbers, Pr numbers and oil types were confounded in that the ranges of Re associated with the 3 fluids were distinct over the 27 runs. For P005, the Re was 8173±2696 (ie. ±2 standard errors), and could be considered to represent turbulent flow in curved tubes (Ali, 1994). The range of Re was 1008±196 for P022 and 375±122 for P032. The Pr numbers were 14±2, 109±24 and 296±62 for P005, P022 and P032, respectively. Thus, each fluid was heated in a distinctly different flow regime than the others and there was no overlap between the fluid property ranges, all of which made any statistical analysis physically meaningless. The data are nevertheless described in other terms in the following paragraphs.

The predicted values of the inner Nusselt numbers are based on the Seider-Tate relation for turbulent flow, $Nu=0.23\ Re^{0.8}Pr^{0.33}(\mu_b/\mu_s)^{0.14}$ multiplied

Table 7.2. Summary of experimental results

Tube Dia (mm)	Pitch (mm)	Helix Dia (mm)	Temp (°C)	Flow Rate (L/min)	Oil Type	Re (oil)	Pr (oil)	h_t (W/m²K)	h_i (W/m²K)	h_o (W/m²K)	Nu_i (cal)	Nu_i (pred)
13.5	1	203	60	6	P005	7430	13	492	896	1460	88	106
13.5	1	305	75	8	P005	8775	14.7	367	824	878	80	126
13.5	1	305	95	10	P005	18675	8.6	471	955	1230	94	219
15.7	15.7	305	62	10	P005	6516	18.3	321	489	1555	55	122
15.7	15.7	305	78	6	P005	6725	10.6	265	394	1216	45	110
15.7	15.7	203	95	8	P005	5840	16.3	272	377	1825	43	170
15.7	31.4	305	60	8	P005	5599	17	341	660	905	75	102
15.7	31.4	203	75	10	P005	6977	17	382	813	836	92	135
15.7	31.4	305	95	6	P005	7017	10.2	211	438	486	50	117
15.7	1	203	60	8	P022	634	146	284	524	761	57	22
15.7	1	305	75	10	P022	1070	108	351	862	949	94	19
15.7	1	305	95	6	P022	1022	67.6	226	507	672	55	17
13.5	13.5	305	60	6	P022	1220	76.6	365	712	943	67	15
13.5	13.5	305	75	8	P022	1405	88.8	357	805	762	75	18
13.5	13.5	203	95	10	P022	947	165	137	192	896	18	36
15.7	31.4	305	60	10	P022	855	135	333	667	822	73	19
15.7	31.4	203	75	6	P022	560	124	237	421	686	46	21
15.7	31.4	305	95	8	P022	1355	68	280	552	701	60	20
15.7	1	203	60	10	P032	244	464	321	629	779	66	28
15.7	1	305	75	6	P032	196	346	233	579	556	61	19
15.7	1	305	95	8	P032	423	213	282	705	650	74	22
15.7	15.7	305	65	8	P032	240	377	324	511	1205	54	22
15.7	15.7	305	78	10	P032	436	258	391	568	2037	60	25
15.7	15.7	203	95	6	P032	321	210	191	265	1199	28	46
13.5	27	305	60	6	P032	347	263	446	836	1384	75	18
13.5	27	203	75	8	P032	354	344	539	815	2684	74	27
13.5	27	305	95	10	P032	811	187	437	1161	835	105	23

by the correction factor given in the introduction, when oil P005 was used. Although this relationship is intended for higher Reynolds number (Re> 10,000), it gave a reasonable fit (Figure 7.2), although it appears that under certain situations, the helix geometry gives much higher heat transfer rates than predicted. The average difference between the observed and predicted values of Nu_i was only 4.4. In the case of P032 and P022, Re was very low (Re<1500). Thus, the Seider-Tate equation for laminar flow was used,

$Nu = (RePr)^{0.33}(d/L)^{0.33}(\mu_b/\mu_s)^{0.14}$, also multiplied by the correction factor.

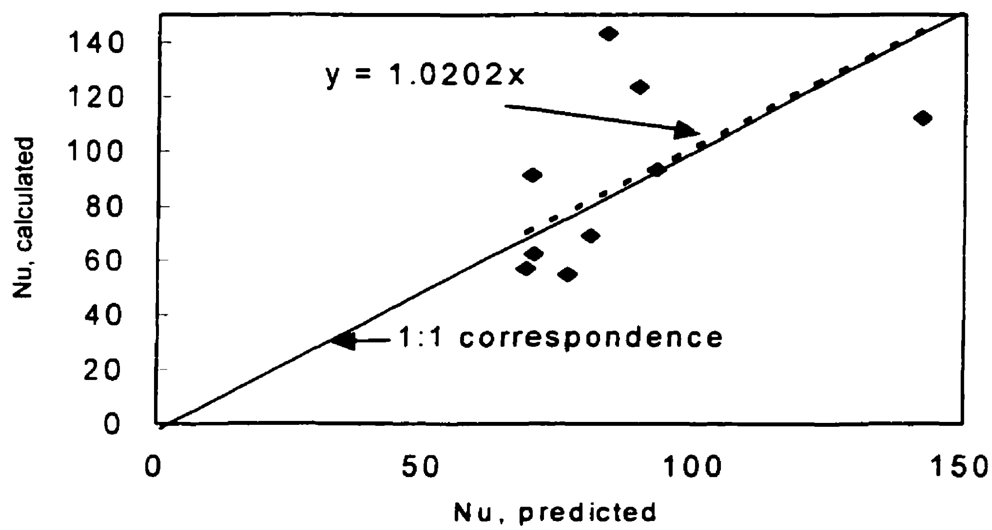

Figure 7.2 Correspondence between observed Nu and that predicted by the Seider-Tate relationship for turbulent flow, multiplied by the correction factor $(1+3.5\ d_t/D_H)$.

As can be seen in Table 7.2, the observed Nu inside the coil for low Re, is substantially higher than the predicted values, and often as much as an order of magnitude greater. This is not entirely surprising given that Dean vortices are present even at very low flow (Webster and Humphrey, 1993).

Since the vortices operate in a three-dimensional framework, they could very well result in an increase in heat transfer normally associated with the eddy structures seen at higher Reynolds flow in the conventional two-dimensional flow.

Figure 7.3 shows the relationship between h_o based on the temperature data described earlier and h_o calculated from the resistance relationship

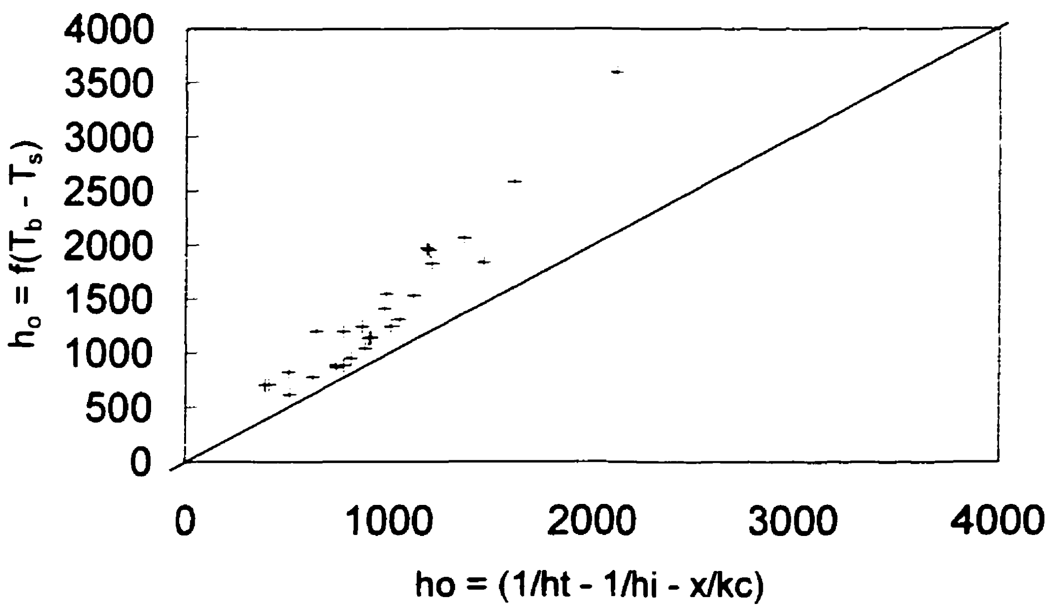

Figure 7.3 Plot of outside heat transfer coefficient obtained from temperature data and that obtained by back-calculation from h_t and its other components.

between components. It is interesting to note that the 'observed' h_o is greater than the back-calculated one and that the difference increases at higher values. Since the heat absorbed by the fluids inside the coil varied from one run to the next, the heater outputs likely varied in total output and in cycling, such that buoyancy forces were not the same from one run to the next. A more detailed analysis would require an array of thermocouples within the water bath. On the other hand, the outer surface temperature on the coil might have been measured at more locations since it is not evident that the surface temperature varies linearly along the length of the coil given the particularities of the setup. An analysis of the outer heat transfer coefficient, based on natural convection conditions involving the relationship between the Nusselt number and the Rayleigh (Ra) number (Kreith and Black, 1980) was preformed using the empirical equation, $Nu = c(Ra)^a$, where the coefficient c is 0.53 and a is 0.25 for Rayleigh numbers ranging between 10^4 and 10^9 (Holman, 1992). The results indicate that, neglecting the low circulation rate of water within the bath, h_o should range from 700 to 1200 W/m^2-°K and can be approximately described by (see also Figure 7.4):

$$h_o = 573 + 4.6\,T_b \qquad R^2=0.35 \qquad (7.4)$$

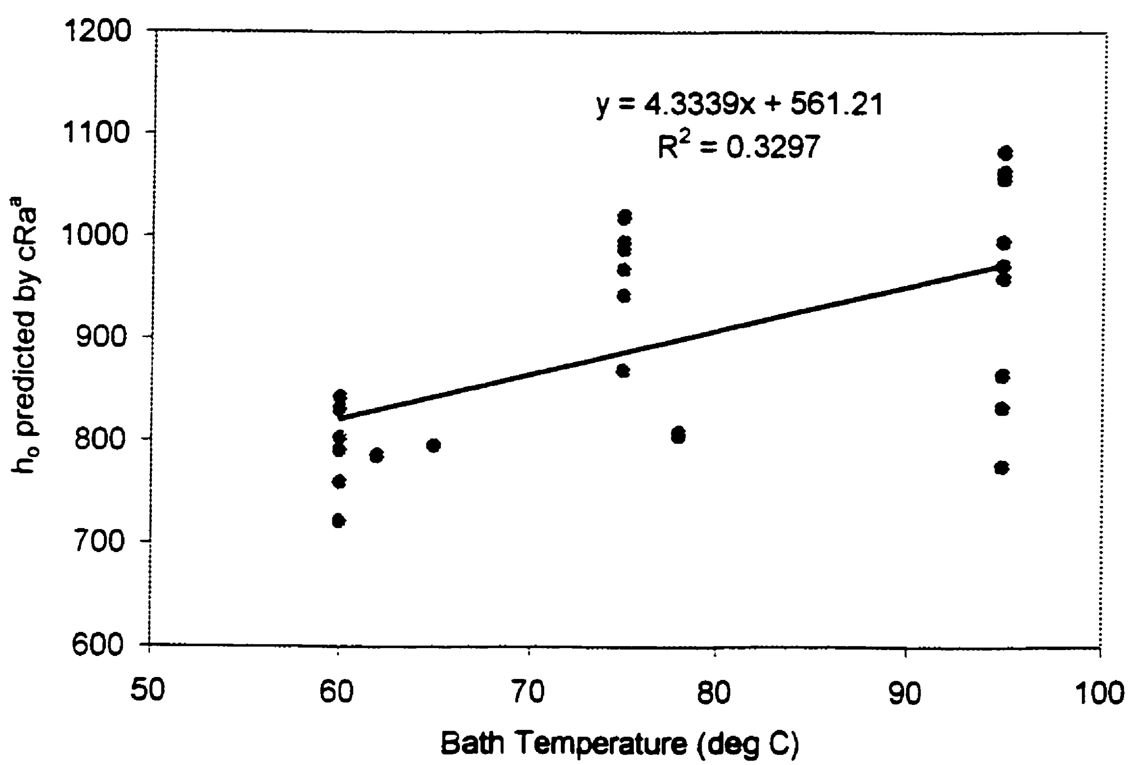

Figure 7.4. Outside heat transfer coefficient based on natural convection . . considerations, plotted versus bath temperature.

The observed h_o's fall in this range for 15 of the 27 runs. For the others, h_o is higher, possibly due to the influence of circulation rate and possibly to some unexplained interaction with the conditions inside the coil. These aspects warrant more detailed investigations. It is rather unfortunate that the bath temperature was assumed to be that set on the PID controller and was not monitored precisely at different locations. We believe this to be a considerable source of error in the calculations since it is unlikely that bath temperature could be the same everywhere within a given distance of the coil.

The outside Nusselt number was predicted by $Nu=0.257Ra^{0.323}$ as proposed by Ali (1994), though the Ra numbers are outside the range for this correlation. This correlation was based on a helical coil immersed in water. The outside Nusselt number was also predicted using $Nu=0.59Ra^{0.25}$, which is a correlation for a vertical cylinder (Kreith and Black, 1980). Both these predictions, along with the observed Nu, are plotted in Figure 7.5. The helical coil predictions were higher than those for the vertical cylinder, indicating that helical coil design has some beneficiary characteristics on the outside heat transfer coefficient as well as the inside coefficient. The observed Nu did not follow either of the trends.

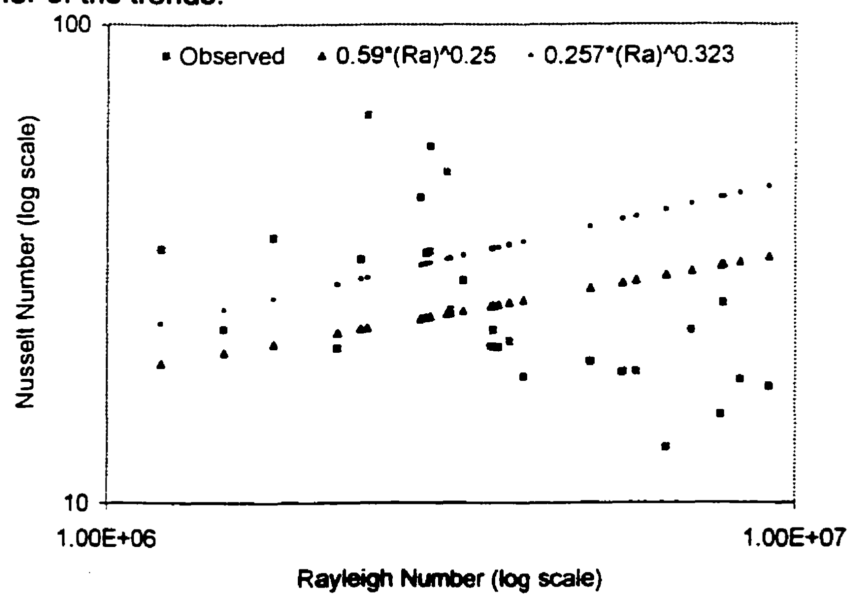

Figure 7.5. Observed and predicted outer Nusselt no. Vs Ra no, Log Scale

The Reynolds number and the Prandtl number were greatly affected by temperature changes. When heated fron 20 to 50° C, the viscosity of the P005 and the P032 oil decreased by 3 and 4 times, respectively. This results in an increase of the Reynolds number proportional to the change in viscosity, as the diameter, and the product if the density and the velocity remain constant. The Prandtl numbers were also highly affected by the changes in the fluid temperature. Though existing correlations for Nusselt numbers based on the Reynolds and the Prandtl numbers do attempt to take into consideration changing fluid properties by the use of average bulk temperatures, they may not be adequate to fully account for changes when highly temperature sensitive fluids are used. A change in Reynolds number by a factor of 3 or 4 can have a large impact on the flow characteristics, especially when the operating parameters are close to the transition zone.

7.2 CONCLUSIONS

Loss in viscosity was observed due to repeated usage. By running more experiments, and a closer look at the analysis of data may provide the reason for loss in viscosity.

This study indicates that the presently used relationships to describe heat transfer in helical coils do not fully account for behavior when fluid-to-fluid heat transfer is involved. However, there were several sources of error in this study and further experiments are planned to verify the relationships between our results and the experimental conditions.

There were several unforeseen circumstances regarding the fluids used that prevented analysis under better comparative conditions, flow conditions in particular (i.e. distinctly different ranges of Reynolds number for the three fluids). Nevertheless, this experience has provided a suitable basis for planning further experiments in this area.

VIII. CONCLUSIONS, CONTRIBUTIONS TO KNOWLEDGE AND RECOMMENDATIONS FOR FUTURE STUDY

8.0 Summary and Conclusions

The purpose of this study was to develop a relationship between hot water bath and coil parameters that influence heat transfer to the fluid processed passing thorough a curved tube and express in terms of dimensionless numbers. The study describing the flow field in the tube and the heat transfer across the surface of the coil lead to the following conclusions.

1. Forced convection water bath gave a higher heat transfer compared to natural convection water bath. Inducing greater mixing in the water bath would lead to even higher outside heat transfer and higher overall heat transfer, since in this setup, it was the outer heat transfer coefficient that was limiting. However, there was also an average increase of 7% in the inner heat transfer coefficient due to circulation in the water bath. Thus, one might expect that increasing the outer heat transfer should also lead to further improvement in the inner heat transfer.

2. Improving the heat transfer to the coil by increasing the temperature of the water in the bath increased the inner heat transfer coefficient by 7%. At the same time increasing the flow rate inside the coil has the effect of increasing the outside heat transfer coefficient, as well as that inside the coil.

3. The bath temperature was not significant for either heat transfer coefficient under the forced convection regime, but was significant in the natural convection water bath. The influence of flow rate inside the coil on both inner and outer heat transfer coefficients in both water

bath regimes is quite striking, and would appear to be the main factor linking the two components of overall heat transfer.

4. For the natural convection water bath, the torsion factor λ influenced h_i only though interaction with D_H and bath temperature, whereas the linear and quadratic effects were not significant. In the natural convection water bath, λ had no significant influence on h_o, either by itself or through interaction with other variables.

5. Bath and flow rate do not influence the correspondence in the forced convection regime, as one would expect given that the predicting equation accounts for flow rate through the Reynolds dependence and for temperature effects through the Prandtl number.

6. As for as oil experiments are concerned, loss in viscosity to some extent was observed due to the usage. It appears that this is because of repeated use of oil to run the experiments. A closure examination of this by running more number of experiments would verify the reason for loss in viscosity.

7. The range of Reynolds number and Prandtl number for three fluids were distinct and thus each had different flow regime. There was no overlap of the properties of the oils and hence statistical analysis of the data was meaningless.

8. The predicted values of the inner Nusselt number based on Sider-Tate relation for turbulent flow multiplied by the correction factor gave a reasonable fit. The average difference between the observed and predicted Nu_i was as low as 4.4 at higher Re.

9. For low Re, the Nu_i was of an order of magnitude greater. Since the vortices operate in a three-dimensional framework, they could very well result in an increase in heat transfer normally associated with the eddy structures seen at higher Reynolds flow in the conventional two-dimensional flow.

10. This study indicates that the presently used relationships to describe heat transfer in helical coils do not fully account for behaviour when fluid-to-fluid heat transfer is involved.

8.1 Contribution to knowledge.

This thesis has made original contribution to knowledge by providing basic and applied information on influence of coil characteristics on Heat transfer to Newtonian fluids expressed in terms of inner, outer and overall heat transfer coefficients. The main contribution are as follows:

1. The amount of heat transferred was dependent on the flow characteristics of the carrier fluid and that of the processing fluid inside the coil.

2. Relationship between inner, outer and overall heat transfer coefficient was developed. The overall and outer heat transfer coefficients are significantly lower in case of natural convection. The outer and overall heat transfer coefficient was higher with water in the bath being circulated.

3. The flow characteristics of the carrier fluid may have an influence on the inner heat transfer coefficient to a little extent compared to outer and overall heat transfer coefficient.

4. The inner flow conditions influence the heat transfer characteristics outside the coil.

5. It was possible to express the over all heat transfer directly in terms of either inner or outer heat transfer coefficient by linear equation.

6. The torsion factor had significant influence on heat transfer coefficients. Its influence on h_i was curvilinear and of 2nd order in case of forced convection water bath.

7. The study showed that the presently used relationships to describe heat transfer in helical coils do not fully account for behaviour when fluid-to-fluid heat transfer is involved.

8.2 Recommendations for further studies

The main points that are yet to be addressed are whether this process could be used as a substitute for asceptic processing of liquid foods. A cost and/or energy benefit study would enable us to the limitation of this process.

Since there is an improvement in heat transfer by circulating water in the bath, it would be more interesting to conduct studies at different conditions where outer heat transfer coefficient is not limiting the heat transfer inside the coil.

A measurement of circulating flow rate near the coil would explain the process better. This could also be done by developing technique to look at the eddy structure near the coil surface.

This study was conducted keeping the coil in vertical position inside the coil. Alternatively studies could be conducted by placing the coil in horizontal or at different angles inside the water bath and see the effect of gravity on the processing fluid.

Different technique of heat source on to the coil like having water jets inside the bath to impinge upon the coil or use of microwave as heat source sould be tried to make the process more flexible.

The processing fluid used in this study was Newtonian fluids at different viscosities. Studies could be conducted with Non-Newtonian fluids and fluids with particulate for processing.

Food grade quality materials may be used for fabricating the unit and for pumping system so that the results could be taken direct to the food processing industry.

REFERENCES

Ali, M.E. 1994. Experimental investigation of natural convection from vertical helical coiled tubes. Int. J. Heat Mass Transfer 37(4):665-671.

Ali, M.E. 1998. Laminar natural convection from constant het flux helical coiled tubes. International Journal of Heat and Mass Transfer. 41(14):2175-2182.

Ashim K. Datta. 1992. Thermal sterilization of liquid foods. Encyclopedia of Food Science & Technology. John Wileys & Sons Publication. 4:2566-2578.

ASHRAE guide and data book. 1997. New York : American Society of Heating, Refrigerating and Air-Conditioning Engineers

Berger, S.A. and Talbot, L. 1983. Flow in Curved Pipes. Amn. Rev. Fluid Mech. 15:461-512.

Daily, J.W. and D.R.F. Harleman. 1966. Fluid Dynamics. Addison_Wesley (Canada), Don Mills, Ontario. 454 pp.

Dean, W.R. 1927. Note on the motion of fluid in a curved pipe. Phil. Mag. 14:208.

Dean, W. R. 1928. The streamline motion of fluid in a curved pipe. Philos. Mag. 20:208-23

Dravid, A. N., K.A. Smith, E.W. Merrill, and P.L.T. Brain. 1971. Effect of secondary fluid motion on laminar flow heat transfer in Helically coiled tubes. A.I.Ch. E. Journal, 17(5):1114-1122.

Eustice, J. 1910. Flow of water in curved pipes. Proc. R. Soc. London Series A. 84:107-118.

Eustice, J, 1911. Experiments on streamline motion in curved pipes. Proc. R. Soc. London Series A. 85:119-131.

Futagmi, K. and Y, Aoyama. 1988. Laminar heat transfer in a helically coiled tube. Int. J. Heat Mass Transfer. 31(2):387-396.

Germano, M. 1982. On the effect of torsion in a helical pipe flow. J. Fluid . Mech. 125:1-8.

Germano, M. 1989. The Deans equations extended to a helical pipe flow J. Fluid Mech. 203:289-305.

Gong, Y., G. Yang., and M.A. Ebadian. 1994. Perturbation analysis of convective heat transfer in helicoidal pipes with substantial pitch. J. of Thermophysics & Heat Transfer. 8(3):587-594.

Haraburda, S., 1995. Three-phase flow. Consider helical-coil heat exchangers. Chemical Engineering, July 1995: 149-151.

Holman, J.P., 1992. Heat Transfer. McGraw-Hill Book Company, London. 713pp.

Ito, H. 1959. Friction factors for turbulent flow in curved pipes, J. Basic Engng, Trans. A.S.M.E. D, 81, 123-124.

Ito, H. 1970. Laminar flow in curved pipes. Rep.no 224. Inst. High Speed Mech. Japan. 22:161.

Janssen, L.A.M. and C.J. Hoogendoorn. 1978. Laminar convective heat transfer in helical coiled tubes. Int. J.Heat Mass Transfer, 21:1197-1206.

Jeschke, D. 1925. Heat transfer and pressure loss in coiled pipes Ergaenzungsheft Z. Ver. Disch. Ing. 68:24-28.

Kao, H.C. 1987. Torsion effects on fully developed flow in a helical pipe. J. Fluid Mech. 184 335-356

Kreith, F., 1955. The influence of Curvature on Heat Trasnfer to . incompressible fluids. The Am. Soc. Mech. Engrs. Transaction, . 77:1247

Kreith, F. 1973. Principles of Heat Transfer. 3rd Edition. Intext Press, Inc. New York, NY. 656 pp.

Kreith, F. and W.Z. Black, 1980. Basic Heat Transfer. Harper and Row Publishers, New York. 556 pp.

Mikheev, M.A. 1947. Elements of Heat Transfer. Gosdarstvennoje, Energetitchoskoje, Izatehtz. P 291.

Mishra, P., S.N. Gupta. 1979. Momentum transfer in curved pipes. I. Newtonian fluids. Industrial and Engineering Process Development 18(1):130-136.

Mori, Y., and W. Nakayam. 1965. Study on forced convective heat transfer in curved pipes (1st report, Laminar region). Int. J. Heat Mass Transfer. 8:67.

Mori, Y. and W. Nakayama. 1967. Study on Forced Convective Heat Transfer in Curved Pipes (2nd Report, Turulent Region). Int. J. Heat Mass Transfer, 10:37-59.

Morton, B.R. 1959. Laminar convection in uniformly heated horizontal pipes at low Rayleigh numbers. Q.J. Mech. Appl. Math. 12:410-420.

Murata, S., Y. Miyake., T. Inaba and H. Ogawa. 1981. Laminar flow in a helically coiled pipe. Bull. JSME 24:355-362.

Nikuradse.J. 1932. "Gesetzmassigkesten der turbulenten Stromung in glatten Rohren" Forschungsheft 356.

Ozisik, M.N. 1985. Heat Transfer: A Basic Approach. International Edition, . . McGraw-Hill Book Co. Singapore.

Patankar, S.V., V.S. Pratap, and D.B. Spalding. 1974. Prediction of lainar flow and heat transfer in helically coiled pipes. J. Fluid Mech. 62:539-551.

Patil, R.K., Shende, B.W., and P.K. Ghosh, 1982. Designing a helical-coil . heat exchanger. Chemical Engineering, December 1982: 85-88.

Perry, R. and Green, D. Perry's Chemical Engineers' Handbook, 6^{th} Edition. McGraw-Hill, Inc. New York, 1984.

Potter and Wiggert. 1991. Mechanics of Fluids. Printice Hall Inc. Publication. New Jersey.

Prandtl, L. and O. G. Tietjens. 1934. Applied Hydro- and Aeromechanics. Dover Publications, Inc. New York. 311 pp.

Prusa, J., and L.S. Yao. 1982. Numerical solution for fully developed flow in heated curved tubes. J. Fluid Mech. 123, 503-522.

Rogers, G.F.C. and Y.R. Mayhew. 1964. Heat transfer and pressure loss in helically coiled tubes with turbulent flow. Int. J. Heat Mass . Transfer:1207-1216.

Sandeep, K.P. and T.K. Palazoglu. 1999. Secondary flow I coiled tubes. . Paper No. 996148 presented at the ASAE annual International . meeting 1999 held at Toronto, July 18-22.

SAS User's Guide. 1988. Cary, NC: Statistical Analysis System Institute.. Inc

Schmidt, E.F. 1967. Warmenbergang and Drukverlust in Rohrschlangen . Chem. Ing. Tech 13:781-789

Seban, R. A. and E.F. Mc Laughlin. 1963. Heat transfer in tube coils with laminar and turbulent flow. Int. J Heat Mass Transfer. 6:387-395.

Shah, R.K. and S.D. Joshi. 1987. Convective heat transfer in curved ducts. In: Handbook of Single-Phase Convective Heat Transfer (eds. S. Kakac, R.K.Shah, W. Aung). Wiley Interscience. NY. Pp 5.1-5.46.

Sieder, E. N. and G.E. Tate. 1936. Heat transfer and Pressure drop of liquids in Tubes. Ind. Eng. Chem. 28:1429.

Singh R. P., and D. R. Heldman. 1993. Introduction to Food Engineering, Second Edition. Academic Press, Inc., San Diego, CA. 499 pp.

Taguchi, G. 1987. System of experimental design. Published by American Suppliers Inst. Inc. 1:472.

Tarbell, J.M., and M.R. Samuels. 1973. Momentum and heat transfer in . helical coils. The Chem. Eng. Journal. 5:117-127.

Tuttle, E.R.. 1990. Laminar flow in twisted pipes. J. Fluid Mech. 219:545-570.

Van Dyke, M. 1978. Extended Stokes series:laminar flow through a loosely coiled pipe. J. Fluid Mech 86:129-145.

Wang, C.Y. 1981. On the low Reynolds number flow in a helical pipe. J Fluid Mec. 108:185-194.

Wark, K. 1995. Thermodynamics. Fifth Edition. McGraw-Hill, Inc, New York. 954 pp.

Webster, D.R. and Humphery, J.H.C. 1993. Experimental Observation of Flow Instability in a Helical Coil. Journal of Fluids Engineering, 115(3): 436-443.

Wohl, M.H. 1968. Isothermal Laminar Flow of Non-Newtonian Fluids. Chemical Engineering. Apr. 8, 143-146.

Xin, R.C. and M.A. Ebadian, 1996. Natural convection heat transfer from helicoidal pipes. J. of Thermophysics and Heat Transfer 10(2): 297-302.

Yang, R. and S.F. Chang. 1994. Combined free forced convection for developed flow in curved pipes with finite curvature ration. Int. J. of Heat Fluid Flow. 15(6):470-476.

Yang, G. and M.A. Ebadian. 1996. Turbulent forced convection in a helicoidal pipe with substantial pitch. Int.J. of Heat and Mass Transfer. 39(10):2015-2022.

Zabielski, L. and A.J. Mestel. 1998. Steady flow in a helically symmetric pipe. J. Fluid Mech. 370. 297-320.